



# Design of a Heating System with Geothermal Energy and CO<sub>2</sub> capture

## **THESIS**

For the degree of: Master of Science in Sustainable Energy Technology

> Daniel Reyes Lastiri 4185285

November 2013

Faculty of Applied Sciences - Delft University of Technology

Members of the Graduation Committee

Dr. Karl-Heinz A.A. Wolf

Prof. dr. J.J.C. Geerlings

Prof. dr. J. Bruining

Cover photo: Strokkur geyser in Iceland,

by Hansueli Krapf

#### **Abstract**

Heating constitutes about 40% of the final energy consumption at TU Delft. In the present, the district heating system in campus obtains its energy from the combustion of natural gas in a combined heat and power plant. Although this plant produces heat and electricity with an efficiency over 80%, the dependance on a fossil fuel presents an opportunity for improvement by introducing a renewable energy source. In May 2013, the drilling for a geothermal plant in campus was approved.

The present heating system operates at high temperature (HT -  $130^{\circ}$ C) with 3-way valves. In the new heating system, a geothermal plant will provide part of the energy and some buildings will undergo renovations to work at medium temperature (MT -  $70^{\circ}$ C); they will be connected in series after HT buildings, constituting a cascade system.

In this study, steady state simulations of the heating system are performed using Cycle-Tempo. The results are then used for an exergy analysis of different configurations in the system.

The analysis of the ongoing transition in the present heating system from a 3-way to a 2-way valve configuration reveals that up to 180 kW of electricity from the grid used for pumping can be saved and replaced by heat produced locally at a higher efficiency, representing up to 36% in primary energy savings. Within the system boundaries, the exergy efficiency does not improve with the transition, but a reduction in the return temperature from 75-80°C to 50-75°C allows for geothermal energy utilisation.

For the new heating system, three configurations of the network are devised: a parallel network at high temperature, a cascade system renovating small buildings and a cascade system renovating large buildings. The exergy analysis reveals that the best option is to renovate the small buildings in campus. In this way, geothermal energy can provide 19% to 50% of the heat demand.

The suggested configuration for the new system can operate with an exergy efficiency 14% higher than the present system, reducing the primary energy consumption and the associated emission of  $CO_2$  by 47%.

Carbon capture and sequestration can decrease the emission of  $CO_2$  further by 51%. However, the capture process by means of the dominant technology, amine absorption, requires additional consumption of fossil fuels, which worsens the scarcity of these resources.

# Acknowledgements

This project is the culmination of my master studies, an experience that started thanks to the support of the DRI scholarship from TU Delft and the ESED scholarship. This funding and the attention provided by Tamara Bacsik, Patricia Carrion and Luis Calzado made it possible for me to go through this period without additional pressure from the outside world.

This study was performed within the framework of the Delft Aardwarmte Project (DAP) and the CATO-2 Programme work package 3.5.

Words of gratitude to the members of my graduation committee, Karl-Heinz Wolf, Hans Geerlings and Hans Bruining. Those seemingly simple talks with professor Wolf lit directions when the (3-) way seemed lost.

Special thanks to the people who gave a supporting hand in this project, providing answers to my endless questions and requests: Ad Winkels, Klaas Mester and Erik from FMVG, Andre and Jeroen from Van Beek, Theo Woudstra and Ali Eftekhari. Whether it was a constant flow of e-mails during the last months, or long discussion sessions (or both), I am truly grateful for your time and patience.

I would also like to thank Apolonio Juárez for the opportunity to continue working during my studies, and Emma Juárez for her support during that work and the extra lectures on equipment design, this time provided intercontinentally.

And thanks of course to my parents and sisters, whom I take with me wherever I go.

The experience of the last two and a half years cannot be related in all the space used for this thesis, but a word may help to start: grey. For the most enriching experience of a life can also be one of the biggest regrets in it. Grey in the irony of a virtual resource flowing into a useless institution, granted based on what was expected from an efficiency-driven, result-oriented individual that is no more. Grey in the strong disagreement with the introduction of the prevailing corporate model into the academic life, a model that desperately clings on the remnants of the collectivity that it obliterates and seduces into the idea that such is the form of development.

And it is amidst this chaos of monochromic faintness, that the people around becomes of outmost importance, keeping a few pieces of sanity safely inside this skin. To avoid yet another trite list, giving nouns and adjectives shall suffice: the chef, the warm and focused, the kite roommate, the ultimate kindness, the loud voice, the platonic love, the cheerful organizer, the philosophical soulmate, the fast traveller, the silent wisdom, the absent cuteness, the biking beauty, the ultimate cuteness and, out of the alphabetic order, the old beach boys and the unfulfilled commitment, present every single day. The time with you turns the grey into a colourful experience beyond the perception of a stomatopod. Thank you.

<sup>&</sup>quot;No black and white in the blue"

<sup>-</sup>Tim Jensen, Mai Yamane, Yoko Kanno.

# **Table of Contents**

Chapter 1	Introduction
1.1	Heating supply and demand at TU Delft
1.2	Heating system of TU Delft
1.3	Geothermal energy at TU Delft
1.4	Exergy
1.5	Research objective
1.6	Thesis outline
Chapter 2	Theoretical background
2.1	District heating systems (DHS)
2.2	Combined heat and power (CHP) plants
2.3	Geothermal energy
2.4	Exergy
2.5	Carbon capture and storage (CCS)
Chapter 3	System modules and their models
3.1	Borders and variables
3.2	Heating network
3.3	CHP plant, warmtekrachtcentrale (WKC)
3.4	Geothermal plant
3.5	Pressure and heat losses
3.6	General model configurations
Chapter 4	Present Heating System
4.1	Demand profile
4.2	Operation conditions
4.3	Simulation results
4.4	Energy balance
4.5	Exergy analysis
4.6	Conclusions for the present heating system
Chapter 5	New Heating System
5.1	New infrastructure
5.2	Network configurations
5.3	Operation conditions
5.4	Simulation results
5.5	Energy balance
5.6	Exergy analysis
5.7	Selected configuration
5.8	Conclusions for the new heating system
	$\sim$ .

Chapter 6	$CO_2$ c	apture and storage (CCS)	59
6.1	Desc	cription of the system	59
6.2	Resu	ılts	60
Chapter 7	Conclu	usions and recommendations	62
7.1	Con	clusions	62
7.2	Reco	ommendations for future work	63
References .			65
Appendices .			AP-1
Appe	endix A	Assumptions and inputs for the model of the network	AP-2
Appe	endix B	Assumptions and inputs for the model of the CHP plant	AP-5
Appe	endix C	Assumptions and inputs for the geothermal plant	AP-10
Appe	endix D	Demand of the DHS in TU Delft	AP-11
Appe	endix E	Simulation results	AP-15
Appe	endix F	Exergy cost of the new network infrastructure	AP-18
Appe	endix G	Exergy cost of the geothermal plant infrastructure	AP-21
Appe	endix H	New network configurations	AP-23
Appe	endix I	Error analysis	AP-28

# List of figures

Figure 1.1. Final yearly consumption by energy source at TU Delft	. 1
Figure 1.2. Yearly heat consumption and gas supply per unit area	. 2
Figure 1.3. Energy transformation at the power plant in TU Delft campus (WKC)	. 2
Figure 1.4. Configuration of the heating system in TU Delft	. 3
Figure 1.5. Delft Geothermal Project	. 4
Figure 2.1. Illustration of a district heating system (DHS).	. 7
Figure 2.2. Circuits of the heating network at TU Delft	. 9
Figure 2.3. Parallel connections and 3-way valve system in the current heating network at TU Delft. $\cdot$ . $\cdot$	. 9
Figure 2.4. Configuration of the heating system at TU Delft	10
Figure 2.5. Combined heat and power (CHP) versus conventional heat and electricity generation	11
Figure 2.6. Schematic of a basic CHP system	12
Figure 2.7. Illustration of a reciprocating piston-cylinder engine and its pressure-volume diagram	13
Figure 2.8. Illustration of a system for geothermal energy utilisation	15
Figure 2.9. Geothermal resources	15
Figure 2.10. Deep geothermal potential in the Netherlands	16
Figure 2.11. Illustration of the dead state.	17
Figure 2.12. Exergy destruction in a heat transfer process.	18
Figure 3.1. Modules defined for the simulation of the heating system at TU Delft	21
Figure 3.2. Map of the for blocks comprising the heating network.	23
Figure 3.3. Model diagram of a single heat exchanger branch in block N1	24
Figure 3.4. Diagram of the model for a gas engine	25
Figure 3.5. Diagram for the model of the boilers at WKC	26
Figure 3.6. Diagram of the model for the distribution pumps at WKC	27
Figure 3.7. Model of the geothermal plant	28
Figure 3.8. Illustration of the radii of the pipe and its insulation layer.	31
Figure 3.9. Flowchart of the model of the present heating system	33
Figure 3.10. Flowchart for the simulation of the new heating system.	33
Figure 4.1. Heat demand and environment temperature profiles for 2012	34
Figure 4.2. Frequency of the environment temperatures throughout the year	35
Figure 4.3. Overall exergy balance of the present heating system	38
Figure 4.4. Exergy balance of the network in the present heating system.	39
Figure 4.5. Exergy balance of the CHP plant in the present heating system.	41
Figure 5.1. General scheme of the cascade configuration for one block in the network	45
Figure 5.2. Exergy balance of the network in the proposed configurations of the new heating system	50
Figure 5.3. Exergy balance of the geothermal plant in the configurations of the new heating system	52
Figure 5.4. Exergy balance of the CHP plant in the proposed configurations of the new system	53
Figure 5.5. Exergy balance of the proposed configurations for the new heating system	54
Figure 5.6. Exergy balance of the present system versus the selected configuration for the new system	56
Figure 6.1. Prevented CO <sub>2</sub> emissions with carbon capture and storage (CCS) in the new heating system.	61

# List of tables

Table 1.1. Overview of the thesis	. 6
Table 2.1. Evolution of district heating systems (DHS)	. 8
Table 2.2. Operation conditions of the heating system in TU Delft during peak demand	. 8
Table 2.3. Advantages and disadvantages of the 3-way valve system	. 9
Table 2.4. Main groups of ${\rm CO}_2$ capture techniques	19
Table 2.5. Main reservoir options for geological storage of $CO_2$	20
Table 3.1. Characteristics of the distribution blocks in the heating network	22
Table 3.2. Head loss coefficients for the modelled accessories	30
Table 3.3. Relevance of friction losses for components in the main lines	30
Table 3.4. Relevance of friction losses for components in a branch	30
Table 3.5. Standard thickness of steel pipes.	32
Table 4.1. Average hourly demand for the steady state scenarios in the DHS of TU Delft	35
Table 4.2. Operations conditions of the present heating system	35
Table 4.3. Simulation results for the present heating system.	36
Table 4.4. Energy balance of the present heating system [kW].	37
Table 4.5. Exergy balance of the present heating system [kW]	38
Table 4.6. Exergy losses in the network of the present heating system [kW]	40
Table 4.7. Exergy losses in the CHP plant of the present heating system [kW]	41
Table 5.1. Exergy costs of the new infrastructure required in the network	44
Table 5.2. Exergy costs for the infrastructure of the geothermal plant	45
Table 5.3. Operations conditions of the new heating system.	46
Table 5.4. Operation conditions of the geothermal plant	47
Table 5.5. Simulation results for the new heating system	47
Table 5.6. Energy balance of the proposed configurations for the new heating system [kW]	48
Table 5.7. Exergy balance of the proposed configurations for the new heating system [kW]	49
Table 5.8. Exergy losses in the network of the proposed configurations for the new system [kW]	50
Table 5.9. Exergy losses in geothermal plant of the configurations for the new system [kW]	52
Table 5.10. Exergy losses in the CHP plant for the proposed configurations of the new system [kW]	54
Table 5.11. Comparison between the present system and the selected configuration for the new system.	56
Table 5.12. Start-up energy required to preheat the mixing vessels in the CHP plant	57
Table 6.1. Requirements for ${\rm CO_2}$ capture and storage and resulting emissions	61

# List of symbols and abbreviations

Symbol	Description	Unit
En	Energy flow	kW
Ex	Exergy	kW
ex	Specific exergy	kJ/kg
$Ex_D$	Exergy destruction	kW
P	Absolute pressure	bar
P (g)	Gauge presure	bar(g)
Q	Heat flow	kW
T	Temperature	°C
t	Time	S
$T_S$	Temperature of the soil	°C
U	Overall heat transfer coefficient	$kW/m^2 K$
V	Volume	$m^3$
$W_{el}$	Electrical power	kW
ε	Pipe roughness	mm
σ	Specific entropy	kJ/kg K
φ	Mass flow rate	kg/s

# **Subscripts Description**

th

1	Primary side of heat exchanger (heated fluid)
2	Secondary side of heat exchanger (fluid delivering heat)
des	Design
E	Entering a system component or module
el	Electrical
env	Environment
L	Leaving a system component or module
th	Thermal

Abbreviations Description

3mE Faculty of Mechanical, Maritime and Materials Engineering

(Maritieme Techniek en Technische Materiaalwetenschappen)

BK Faculty of Architecture (Bouwkunde)

CCS Carbon capture and storage
CHP Combined heat and power

CiTG Faculty of Civil Engineering and Geosciences

(Civiele Techniek en Geowetenschappen)

DAP Delft Geothermal Project (Delft Aardwarmte Project)

DHS District heating system

EWI Faculty of Electrical Engineering, Mathematics and Computer Science

(Electrotechniek, Wiskunde en Informatica)

FMVG Facility Management and Real Estate (Facilitair Management en Vastgoed)

HT High temperature (heat consumers)

HX Heat exchanger

IO Faculty of Industrial Design (Industrieel Ontwerpen)

LR Faculty of Aerospace Engineering

(Luchtvaart- en Ruimtevaarttechniek)

LT Low temperature (heat consumers)

MJA3 Meerjarenafspraken energie-efficiency (long term agreements on energy efficiency)

MT Medium temperature (heat consumers)

MTb Proposed system configuration for the new heating system, renovating big buildings
MTs Proposed system configuration for the new heating system, renovating small buildings

SC Sports center

TBM Faculty of Technology Policy and Management

(Techniek, Bestuur en Management)

TNW Faculty of Applied Sciences

(Technische Natuurwetenschappen)

WKC CHP plant at TU Delft (Waarmtekrachtcentrale)

# Introduction

The European Union adopted in 2009 a set of climate and energy policies known as the 20-20-20 targets. These policies, implemented by the Member States in December 2010, include the following goals for 2020 (EC, 2013a):

- 1) Reduce the greenhouse gas emission in the EU at least 20% below 1990 levels;
- 2) Achieve 20% of EU gross final energy consumption produced from renewable energy sources;
- 3) Reduce the in primary energy use by 20%, compared with projected levels.

The quantitative targets of the EU and each Member State are compiled in the *Directive 2009/28/EC on promotion of the use of energy from renewable energy sources*. In the Netherlands, the target regards the share of gross final energy consumption produced from renewable energy sources, consisting of an increase from 2.4% in 2005 to 14% in 2020 (European Parliament & Council of the European Union, 2009).

Under the MJA3 agreement (Meerjarenafspraaken energie-efficiency), the Dutch universities seek to improve their energy efficiency by 30% in 2020 with respect to 2005, i.e. an increase of 2% every year. It is within this context that TU Delft has set energy and environmental goals for 2020: the 30% energy efficiency increase set by the MJA3, 50% share of renewable energy and 100% CO<sub>2</sub> neutral operation (TU Delft, 2013).

Heating constitutes an important share of the energy demand at TU Delft, about 38% of the final energy consumption in 2012, as depicted in Figure 1.1. Renovations of the heating network in the campus are currently in the planning stages, along with the implementation of geothermal energy in the system.

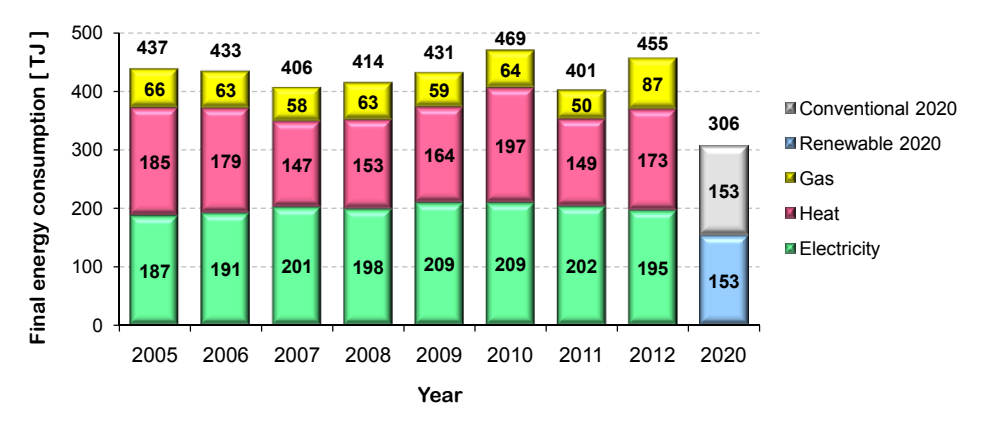


**Figure 1.1.** Final yearly consumption by energy source at TU Delft. Data provided by Facilitair, Management en Vastgoed (FMVG), TU Delft *Ceteris paribus*, the demand in 2020 must decrease to 306 TJ to meet the MJA3 goals. Following the TU Delft goal, 153 TJ must be produced from renewable energy.

# 1.1 Heating supply and demand at TU Delft

The heat at TU Delft is delivered by a power plant located in campus, the *warmtekrachtcentrale* (WKC). Currently, the water is heated up by combustion of natural gas in 3 boilers and 2 gas engines that also produce electricity. The production of electricity depends on the availability of return water from the heating system.

The total heat demand in 2012 was 173 TJ, with a monthly maximum of 33.147 TJ in February and a minimum of 0.168 TJ in July. The maximum hourly demand was 29.22 MWh (105.1 GJ).

The efficiency of heating is sometimes measured in terms of consumption per person. However, with a constant increase in the campus population, this parameter does not reflect any real effort to improve the energy utilisation.

Instead, the efficiency of the heating system can be measured in terms of fossil fuel supply per unit of gross floor area. As depicted in Figure 1.2, the efficiency is far from the 2020 goal as of 2012. Therefore, the heating system in campus presents an opportunity to reach the MJA3 goals.

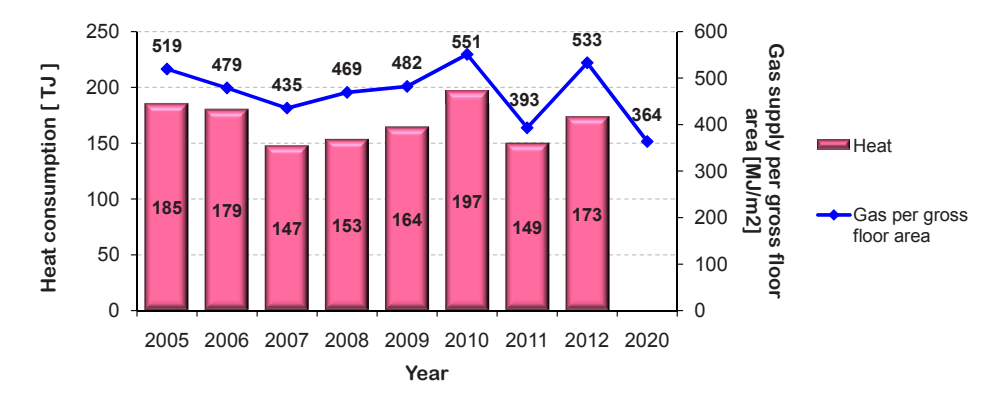
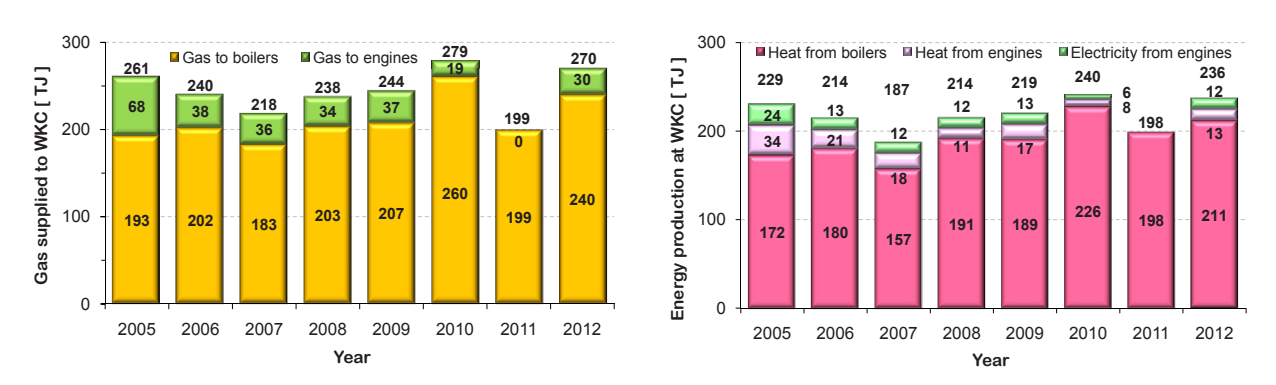


Figure 1.2. Yearly heat consumption and gas supply per unit area. The gross floor area in campus increased from 501,828 to 506,748 m $^2$  in 2008. Data provided by FMVG, TU Delft.

Following the MJA3 goal for heating alone, the gas supply per gross floor area must decrease to 364 MJ/m<sup>2</sup> by 2020.

The gas supplied to the power plant in campus and the secondary energy produced there over the past years is shown in Figure 1.3. Heat is delivered by the boilers and gas engines; the latter also produce electricity. New gas engines started operating in December 2012, after decommissioning of the old engines in 2010, improving the electrical efficiency in about 5%.



**Figure 1.3.** Energy transformation at the power plant in TU Delft campus (WKC). Yearly gas supply (left), and yearly heat and electricity production (right)

Data provided by FMVG, TU Delft.

# 1.2 Heating system of TU Delft

The present heating system in TU Delft is comprised of a heating network and a power plant.

The heating network is divided in 4 blocks, each with its own distribution pump, connected to a common reserve pump in case of failure. Two parallel pipelines run in each block transporting the supply and return water of the power plant. Branches of these pipelines carry the water to the buildings. At the end of the branches, sets of heat exchangers transfer the energy to the water in the buildings for its final consumption. All the branches are connected in parallel.

The energy is supplied by combustion of gas in the power plant. The heat delivered is used for space heating; the buildings have separate systems for hot tap water.

The system operates at high temperature and high pressure, 130/80°C (supply/return) and 13 bar during the peak demand. At partial loads, some of the supply water is bypassed directly to the return line by means of a 3-way valve system. This allows maintaining steady return temperatures throughout the year, facilitating control when following an increase in demand; but it also results in the loss of useful high temperature energy from the hot water (Figure 1.4).

In the long term, it is desired to utilise heating water at medium temperature ( $<100^{\circ}$ C) or low temperature ( $\le60^{\circ}$ C) circulating in a smart heating network.

As a transition step, several buildings will be renovated in order to make them suitable for medium temperature heating  $(70/40^{\circ}\text{C})$ . These medium temperature buildings (MT) will be connected to the high temperature consumers (HT) in series, constituting a cascade system. The 3-way valve bypass will be replaced by a 2-way valve system, thus reducing the waste of energy. Furthermore, geothermal energy will be implemented, granting the advantages of a local renewable energy source to the system (Figure 1.4).

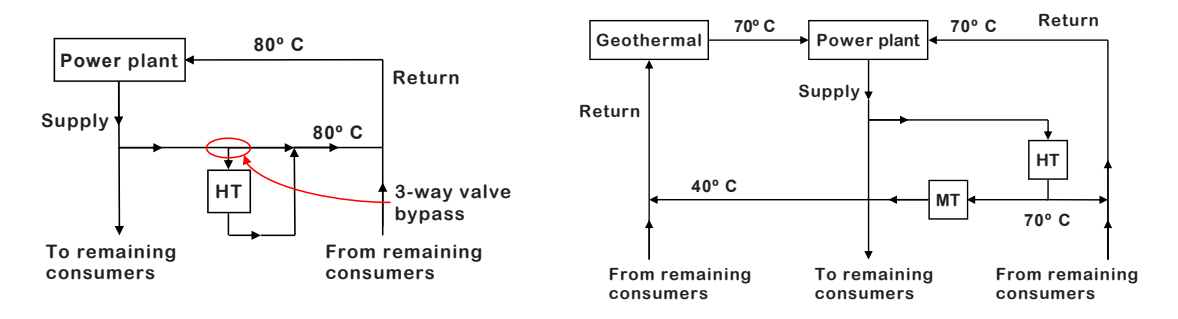


**Figure 1.4.** Configuration of the heating system in TU Delft.

Left: Present system with high temperature consumers (HT) and 3-way valve bypass to control heat supply. Right: New system with high temperature and medium temperature consumers (HT-MT) in a cascade configuration, without 3-way bypass.

There are two main options for the new configuration of the heating network, based on the selection of the buildings that will be renovated:

- 1) Renovate four large buildings,
- 2) Renovate several smaller buildings.

# 1.3 Geothermal energy at TU Delft

Geothermal power plants with capacities over 250 MW operate today in several parts of the world. When a high enthalpy resource is available, cogeneration of heat and electricity is possible. However, combined heat and electricity production from geothermal energy alone poses several challenges in the design and operation of the plant due to factors such as outputs below expectations, rapidly declining pressure and temperature leading to depletion of the heat source, scaling and corrosion.

The Delft Geothermal Project (DAP) was launched in 2007 aiming at providing TU Delft with sustainable energy for heating. Since 2009, TU Delft owns a concession for geothermal exploitation of 65 km² over a low enthalpy reservoir, which will help increasing the efficiency and sustainability of the heating system, while contributing with research and development in the areas of reservoir operation, drilling, production and district heating systems. Additionally, the DAP supports greenhouse farmers in the region with the development of their own geothermal initiatives and fulfils an advisory role on the topic with the municipality.

As part of the DAP, 6 geothermal wells are being realised in the Delft area for research, 2 by TU Delft and 4 by Ammerlaan BV. It is planned to drill at a depth of 2.5 km, where a reservoir shows a conservative potential of ca. 0.3 km<sup>3</sup>. The production is estimated to reach 150 m<sup>3</sup>/h at 75°C, with a total capacity of about 5 MW. Figure 1.5 shows the licensed area and the temperatures of the subsurface around the reservoir; the red lines represent production wells and the blue lines injection wells; the distance between production and injection well is about 2 km.

The estimated geothermal energy production may reduce the yearly consumption of natural gas at TU Delft by 30%; about  $3x10^6$  of gas associated with 5.6 kton of CO<sub>2</sub> (DAP, 2013; Wolf, 2009).

The geothermal reservoir also offers the possibility for CO<sub>2</sub> sequestration.

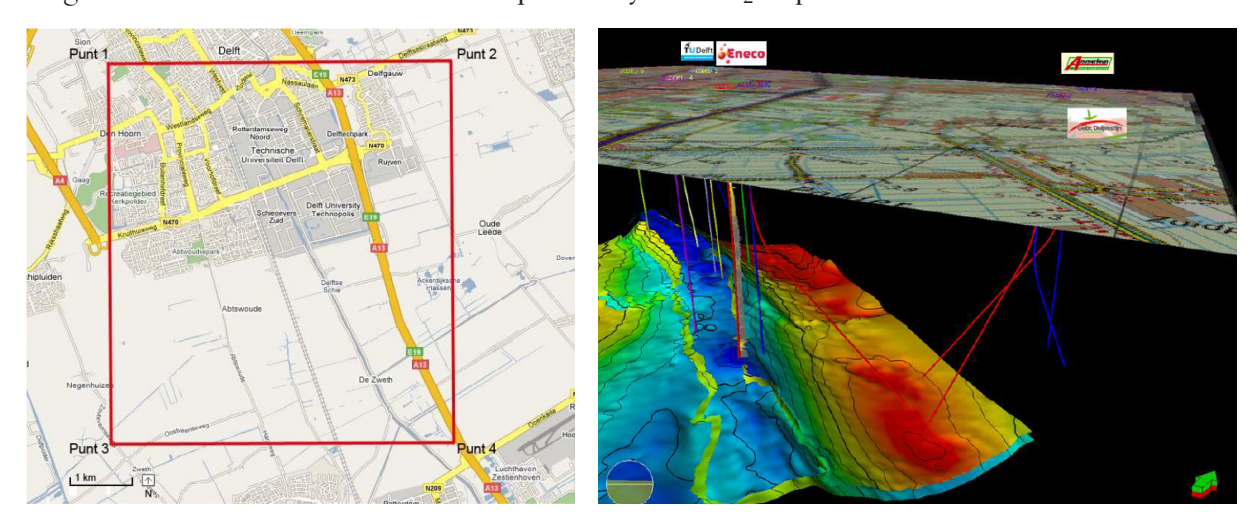


Figure 1.5. Delft Geothermal Project.

Left: Licensed area for geothermal exploitation in Delft, covering  $65 \text{ km}^2$  over a low enthalpy reservoir (T <  $100^{\circ}$ C). Right: Temperature map of Delft subsurface. The red lines indicate production wells (higher temperature) and the blue lines show the injection wells (lower temperature) (DAP, 2013).

# 1.4 Exergy

The exergy analysis is a method that combines the mass and energy conservation laws together with the second law of thermodynamics for the design and optimization of thermal systems.

Exergy can be defined as the maximum theoretical work that is possible to obtain when a system of interest interacts to equilibrium with a reference environment.

Exergy can be transferred to and from the environment but, unlike energy, exergy can also be destroyed by irreversibilities. Therefore, improving resource utilisation can be accomplished by reducing the exergy destruction within a system or its losses to the environment.

However, the limit of 100% exergy efficiency is not pursued as a practical objective. This theoretical limit can only be attained if there are no exergy losses or destruction, which would require extremely long times and complex devices that compromise the feasibility of the process. (Moran, 2010).

An exergy analysis is performed to evaluate quantitatively the causes of thermodynamic inefficiencies in the heating system of TU Delft, showing the possibilities for improvement. Hepbasli (2010) reports in a literature review of several projects, that most of the exergy losses in geothermal district heating occur in the reinjection and in the heat exchangers.

# 1.5 Research objective

In this study, an exergy analysis is performed for the present and new heating systems. The analysis includes the 3-way and 2-way valve systems, HT and MT consumers set in cascade and pre-heating by means of geothermal energy. The exergy required for the construction of new components will be taken into account. Additionally, the possibility to include carbon capture and sequestration will be discussed.

The research objective can be stated as follows:

Find a configuration of the heating network at TU Delft based on the planned renovations that will result in an exergy efficiency higher than that of the current system, taking into account the exergy costs for the construction of the new components required.

The specific objectives of this thesis are:

- 1) Model the present system with 3-way and 2-way valves and perform an exergy analysis.
- 2) Devise configurations for the new heating system with geothermal energy and perform an exergy analysis.
- 3) Discuss the implementation of CO<sub>2</sub> capture and sequestration.

The study is focused on the technical aspects of the system taking place at surface level.

# 1.6 Thesis outline

The table below provides a description of the contents in this thesis.

**Table 1.1.** Overview of the thesis.

Chapter	Content	
2.Theoretical background	Required knowledge to support the analysis and discussion of the project.	
3. System modules	Components of the heating system in TU Delft (module definition) Brief description of the models and additional calculations.	
4. Present heating system	Operation conditions Simulation results: 3-way vs. 2-way system Energy analysis and discussion Exergy analysis per module and discussion Conclusions on the present system	
Operation conditions. Simulation results: three different configurations Energy balance and discussion Exergy analysis per module and discussion Selected configuration Conclusions on the new system		
6. CO <sub>2</sub> capture and sequestration	Description of the system for carbon capture and sequestration Calculation of emissions prevented	
7. Conclusions and recommendations	Concluding ideas and suggestions for future work.	

# THEORETICAL BACKGROUND

In this chapter, the theoretical knowledge that supports the present project is provided. Relevant information is summarised in the topics of district heating, combined heat and power plants, geothermal energy, exergy analysis and CO<sub>2</sub> capture and storage.

# 2.1 District heating systems (DHS)

A district heating system is built to distribute heat generated at a central location to the consumers for the purpose of space and water heating. It is suitable for residential and commercial buildings and its application is spreading to comfort cooling.

The objective of district heating, as opposed to individual production, is to utilise surplus heat and to organise the heat production, achieving a higher efficiency. In order to reduce primary energy consumption and  $\rm CO_2$  emissions, district heating in Europe uses recycled heat from power generation, consuming fossil fuels to cover the peak demand and trying to implement renewable energy sources.

An additional advantage of district heating is the possibility to use a variety of local energy sources that, due to economics of scale, would be difficult or impossible to implement for individual applications, such as biomass fired boilers and deep geothermal energy. Also, by gathering exhaust gases from individual boilers in central chimneys, pollution prevention and control measures can be applied with higher effectiveness.

A DHS consists of 1) a production plant, 2) distribution and transmission network, and 3) consumer installations (Figure 2.1). Currently, in TU Delft the production is carried out in a combined heat and power plant that uses natural gas. The energy is distributed through insulated pipelines to the consumer buildings, where heat exchangers transmit the energy to the water circulating in their installations. The consumer installations include the piping, radiators and convectors in the buildings.

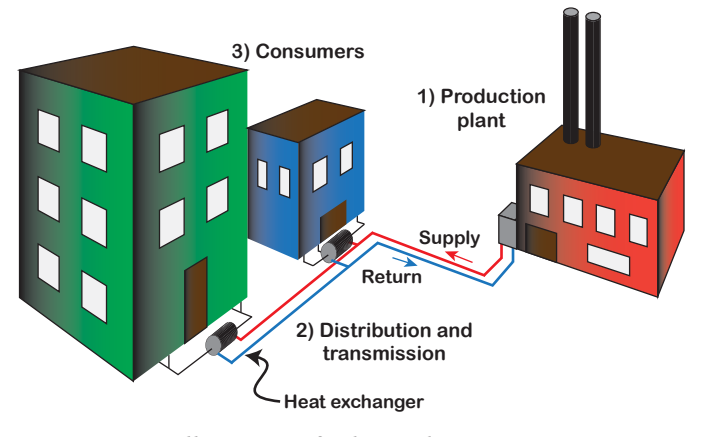


**Figure 2.1.** Illustration of a district heating system (DHS).

The hot water supplied by the plant transfers heat to the water in the buildings by means of heat exchangers.

Sizes of district heating range from small systems with capacities of 0.5 MW up to large systems of 500 MW supplying entire cities.

The evolution of district heating can be divided in 4 generations (Table 2.1). The first generation used steam as an energy carrier. The second generation uses pressurised hot water with supply temperatures over 100°C; these systems were introduced in the 1930s and dominated until the 1970s. The third generation became widespread in the 1980s; it uses pressurised water at supply temperatures below 100°C. The fourth generation, using water at low temperatures, is currently being tested in countries like Turkey and Denmark (DHC, 2012).

**Table 2.1.** Evolution of district heating systems (DHS). The system in TU Delft belongs to the second generation.

DHS Generation	Heat carrier	Supply temperature	Period
First generation	Steam	T > 120°C	1880s - 1930s
Second generation	Pressurised high temperature water	T > 100°C	1930s - 1970s
Third generation	Pressurised medium temperature water	$70^{\circ}\text{C} < \text{T} < 100^{\circ}\text{C}$	1970s – present
Fourth generation	Low temperature water	T < 60°C	Present (testing)

#### 2.1.1 District heating system of TU Delft

The DHS in TU Delft can be classified as medium sized, with an installed capacity of 92 MW in heat exchangers. It belongs to the second generation of district heating. The operation parameters during the peak demand are listed in Table 2.2. The supply temperature ranges from 85° to 130°C depending on the environment temperature ( $T_{env}$ ). The pressure required changes with demand, ranging from 10 to 13 bar.

Table 2.2. Operation conditions of the heating system in TU Delft during peak demand.

env 10 0:		
Parameter	Supply	Return
Pressure	13 bar	~11 bar
Temperature	130°C	80°C

The water is heated in a combined heat and power plant. The **heating network** is divided in **four blocks**. In each block, two parallel insulated pipelines transport the supply and return water. The transmission of energy takes place in heat exchangers located in the basement of the consumers, where the water that circulates in the buildings is heated.

It is possible to identify two circuits in the heating network. In the primary circuit, the energy carrier flows from the power plant to the buildings. The secondary circuits are those within the buildings, where the heat undergoes its final consumption (Figure 2.2). Under peak demand conditions, the heat exchangers operate at  $130/80^{\circ}$ C in the primary circuit and at  $70/90^{\circ}$ C in the secondary circuits (inlet/outlet).

The present heating network operates with two specific features: single parallel connections and a 3-way valve bypass system (Figure 2.3).

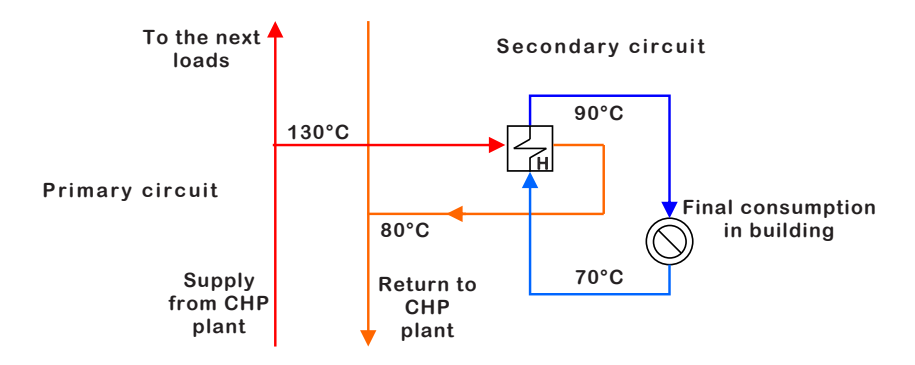
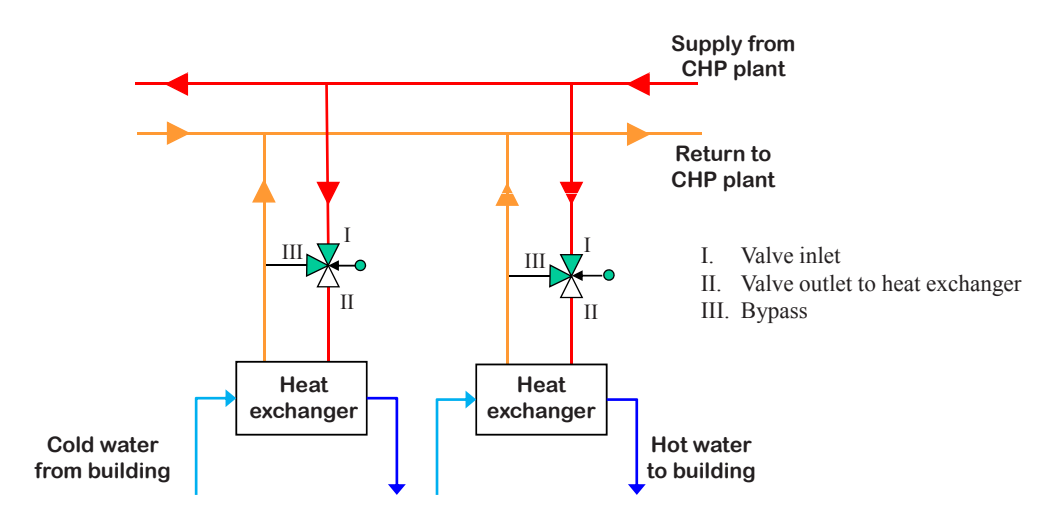


Figure 2.2. Circuits of the heating network at TU Delft.

In the primary circuit water is transported to and from the power plant (red). The secondary circuit consists of the heating infrastructure in the building (blue). The temperatures in the scheme correspond to the peak conditions ( $T_{env} \approx -10^{\circ}$ C)



**Figure 2.3.** Parallel connections and 3-way valve system in the current heating network at TU Delft. All sets of heat exchangers are connected to the primary circuit in parallel. The system has 99 heat exchangers. Under partial load, part of the flow is bypassed through the pipe III to the return line.

All sets of heat exchangers are connected to the primary circuit in parallel, receiving water at the same supply temperature. However, when operating at partial load, not all the energy from the supply water can be utilised, and only part of the flow is fed to the heat exchangers. The rest of the water is bypassed directly to the return line by means of a 3-way valve.

The present configuration, with parallel connections and a 3-way bypass, ensures a steady temperature throughout the year in the return water to the power plant (70 to 80°C), which improves the response to an increase in demand. Important drawbacks exist at partial loads, namely high electricity consumption for pumping and misuse of high temperature water in the bypass (exergy destruction) (Table 2.3).

**Table 2.3.** Advantages and disadvantages of the 3-way valve system.

Advantages	Drawbacks
Stable return temperature	High energy demand for pumping during partial loads
Low primary energy consumption required	Waste of useful energy from high temperature water in
to follow an increase in load	the bypass (exergy destruction)

#### 2.1.2 Transition of the heating system in TU Delft<sup>1</sup>

As part of the transition towards a smart heating system, several buildings will be renovated to make them suitable for medium temperature consumption, by preventing losses and improving the heat management. In this way, part of the DHS will have third generation characteristics.

The 3-way bypass system is being replaced by a 2-way system. Consequently, only the required water will flow in the primary circuit, saving energy for pumping and preventing exergy destruction due to mixing of streams at different temperatures.

The network will operate in a cascade system, with high temperature (HT) consumers followed in series by medium temperature (MT) consumers. During the peak demand, the HT consumers will operate at  $120/70^{\circ}$ C and part of the outlet water will be sent to the MT consumers operating at  $70/40^{\circ}$ C (inlet/outlet).

Furthermore, geothermal energy will be implemented, preheating the water that leaves the MT consumers from 40°C back to 70°C during the peak demand. The diagrams in Figure 2.4 illustrate the differences between the present and the new heating system.

Three main guidelines are followed in the present study:

- 1) Utilisation of the existing infrastructure,
- 2) Replace the 3-way by a 2-way valve system,
- 3) Transition from a parallel to a series/parallel (cascade) configuration.

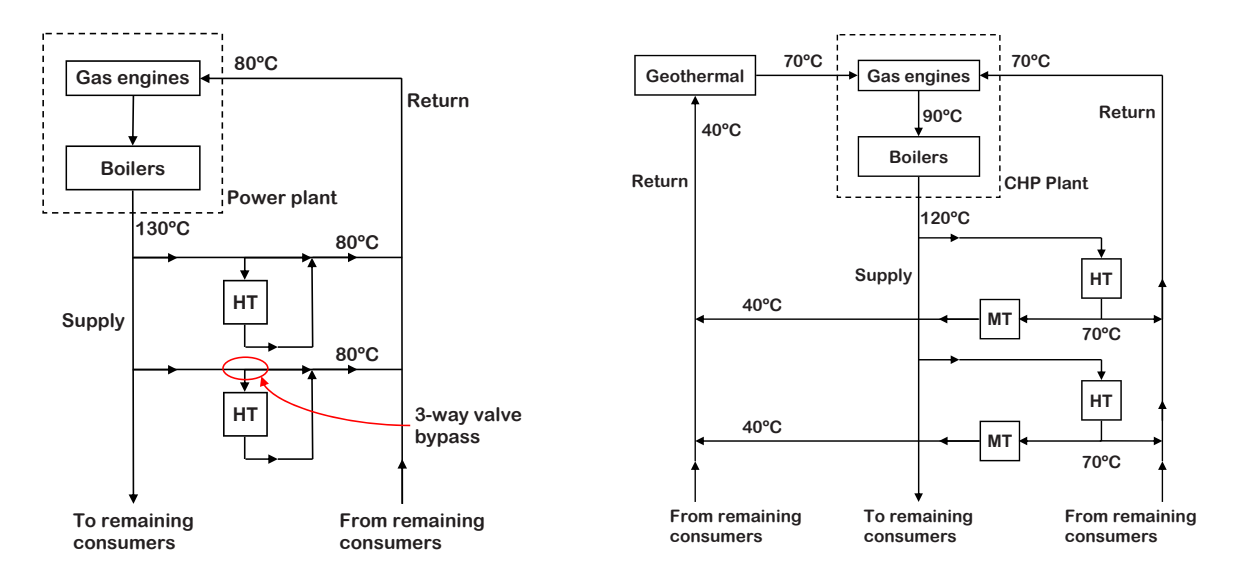


**Figure 2.4.** Configuration of the heating system at TU Delft.

Left: Present system with high temperature consumers (HT), parallel connections and 3-way valves. Right: New system with high and medium temperature consumers (HT, MT) in a cascade configuration.

There are two general options for the selection of buildings that will be renovated:

- 1) Renovate 4 large buildings, belonging to the faculties of:
  - Applied Sciences (TNW)
  - Architecture (BK)

<sup>1.</sup> The description given in this section corresponds to the renovation plans provided by FMVG as of April 2013

- Civil Engineering and Geosciences (CiTG)
- Electrical Engineering Mathematics and Computer Sciences (EWI).
- 2) Renovate the small buildings

# 2.2 Combined heat and power (CHP) plants

Combined heat and power, also known as cogeneration, consists of the simultaneous production of heat and power (typically electrical) from a single fuel source.

Conventional power plants produce electricity at about 35 % efficiency, which is further decreased by transmission losses. In contrast, on site CHP plants recover at least half of the exhaust heat, reaching overall efficiencies around 80%. The diagram in Figure 2.5 shows the comparison of fuel input and energy output between conventional and CHP systems.

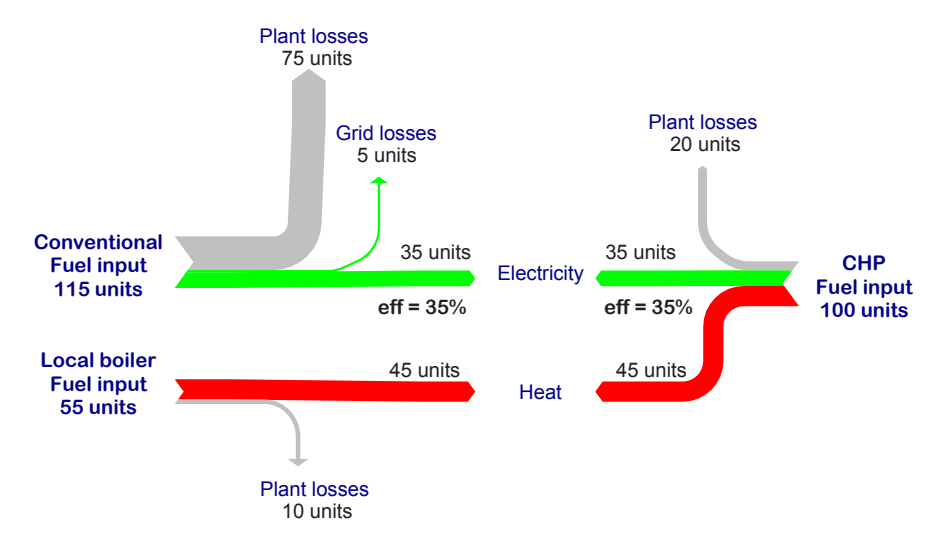


**Figure 2.5.** Combined heat and power (CHP) versus conventional heat and electricity generation. Conventional energy production has an efficiency below 50%, whereas CHP production can achieve 80% efficiency.

The CHP systems can be classified in two general categories:

- 1) Topping-cycle. The energy input is first used to produce electricity and some of the rejected heat is then used to provide thermal energy to facilities.
- 2) Bottoming-cycle. The energy input is first applied to produce thermal energy and some of the rejected heat is then used for electricity production.

A schematic of a basic CHP system is depicted in Figure 2.6. The key components are:

- Engine or prime mover (internal combustion engine, turbine or fuel cell)
- Generator
- Heat recovery
- Thermal uses
- Emission control

Pressurised systems additionally require an expansion tank to compensate the pressure increase occurring when the working fluid is heated up.

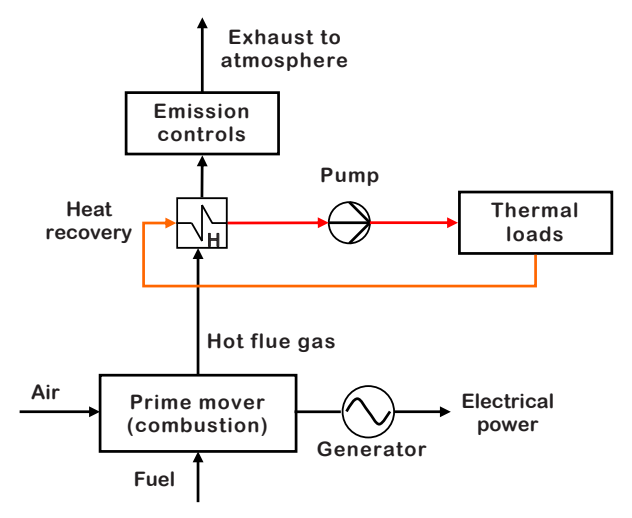


Figure 2.6. Schematic of a basic CHP system.

The process corresponds to a topping cycle, where the consumed heat is recovered after electricity production.

## 2.2.1 Internal combustion engines

Internal combustion engines are reciprocating machines, i.e. devices where the processes involved in power production occur within a piston-cylinder arrangement moving back and forth.

The two main types of internal combustion engines are spark-ignition and compression-ignition. In spark-ignited machines, the combustion is started by a spark plug. Compression-ignition works by compressing the air to a pressure and temperature high enough for the combustion to occur spontaneously when the fuel is injected. Spark-ignited machines are preferred for small scale applications, such as automobiles, due to their low weight and cost. Compression ignition is suitable for large amounts of power, such as locomotives and ships. In the middle range, both types can be used.

In a four-stroke engine, the piston executes four strokes for every two revolutions of the crankshaft. The process for spark-ignition type (Figure 2.7) occurs as follows:

- 1) With the valve open, the piston draws a fresh charge of fuel-air mix in the *intake stroke*.
- 2) With both valves closed, the piston undergoes a *compression stroke*. The piston executes work on the cylinder contents. Combustion is initiated near the end of compression by the spark plug, resulting in a high temperature and high pressure gas mixture.
- 3) The gas mixture expands executing the *power stroke*. The gas mixture exerts work on the piston.
- 4) The exhaust gases are purged from the cylinder through the open exhaust valve in the *exhaust stroke*.

Typical values for the distribution of input fuel energy for internal combustion engines are: 32% shaft power, 32% rejected in jacket water, 30% rejected into exhaust, 3% convection and radiation losses, 3% lube oil cooling.

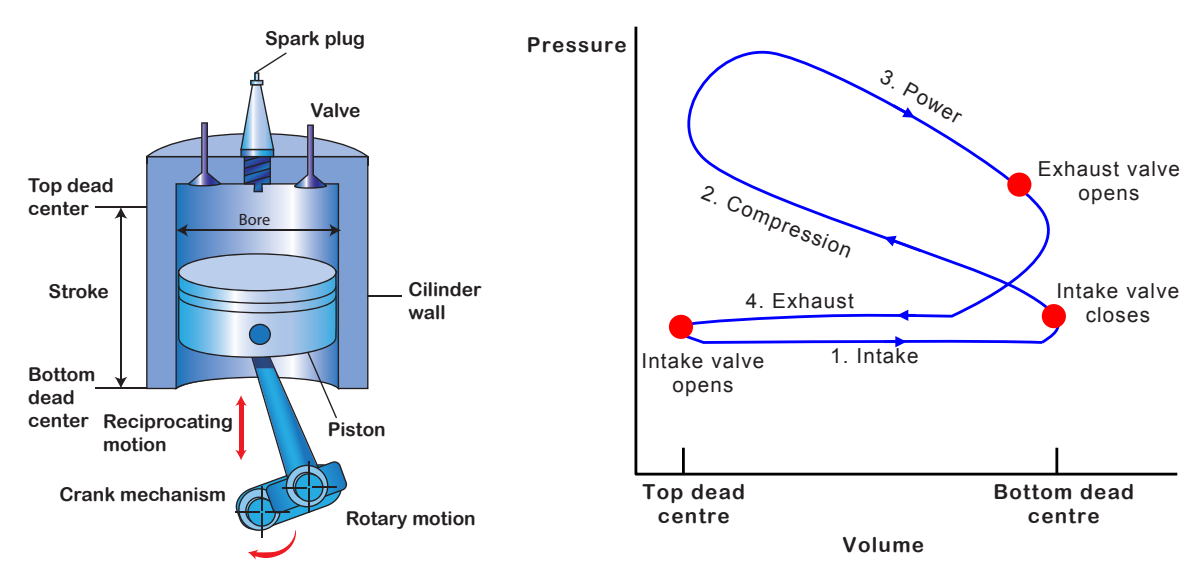


**Figure 2.7.** Illustration of a reciprocating piston-cylinder engine and its pressure-volume diagram. The process shown corresponds to a spark-ignited, four-stroke machine.

#### **2.2.2** Equivalence ratio, λ

The air to fuel ratio refers to the mass ratio during combustion. When the exact amount of air to completely burn all the fuel is present, the ratio is known as stoichiometric.

An important parameter to describe the combustion processes is the equivalence ratio  $\lambda$ , defined as the proportion of air to fuel ratios between the actual and the stoichiometric case:

$$\lambda = \frac{\text{actual air to fuel ratio}}{\text{stoichiometric air to fuel ratio}}$$

In the present, gas engines are operated with lean mixtures ( $\lambda > 1$ ), i.e. a concentration of oxygen higher than required for full combustion, which results in lower levels of atmospheric pollutants than rich mixtures ( $\lambda < 1$ ). However, part of the fuel energy is spent in heating the excess air.

#### 2.2.3 The CHP plant at TU Delft

The CHP system of TU Delft is a topping cycle operating with two gas engines of 2 MW each. The return water from the campus is partially heated by the recovery process in the engines, which also helps to cool down the equipment. The engines are spark-ignition and four-stroke type. The heating of water is completed by three gas boilers of 35, 30 and 15 MW.

The production of electricity depends on the availability of cooling water for the engines. This task is performed by the return water from the heating network.

The gas engines at TU Delft were installed in 2012 and commissioned on December the same year. They have a mechanical efficiency of 41% and a base thermal recovery of 23% with the option to recover additional heat from the flue gas up to 46%.

The previous gas engines had a mechanical efficiency of about 36% and a total thermal recovery of about 46%

# 2.3 Geothermal energy

Geothermal energy is the heat contained in the Earth and is the cause of geological phenomena on a planetary scale. Today, the term is used to indicate the part of the Earth's heat that could be recovered and exploited as an energy resource by man.

The first thermometer measurements reported in literature proving that the Earth's temperature increases with depth were performed in 1740 by De Gensanne. In the XX century, the Earth's heat balance and thermal history were accurately explained when the heat from the decay of radioactive isotopes of uranium (U<sup>238</sup>, U<sup>235</sup>), thorium (Th<sup>232</sup>) and potassium (K<sup>40</sup>) was taken into account. In the 1980s it was demonstrated that there is no thermal equilibrium between the radiogenic heat in Earth and the heat dissipated to space, concluding that the planet is slowly cooling down. According to recent estimates, the temperature of the mantle has decreased ca. 350° C in three billion years, remaining at about 4000° C at its base. Away from tectonic plate boundaries, the temperature gradient of the crust is about 30°C/km.

The total heat content of the Earth is estimated to be about  $13 \times 10^{18}$  TJ and that of the crust in the order of  $5 \times 10^{15}$  TJ. The thermal energy of the Earth is thus immense, but its utilisation is so far limited to areas in which the geological conditions permit liquid water or steam to transfer the heat from deep hot zones to the surface; such locations are the current geothermal resources. New techniques might allow the exploitation of other types of geothermal resources in the near future (IGA, 2013).

#### 2.3.1 Geothermal energy utilisation in the world

Evidence of practical uses of geothermal energy for bathing, washing and cooking purposes in ancient times has been found from Etruscans, Romans, Greeks, Indians, Chinese, Mexicans and Japanese. In the middle ages, Arabs and Turks developed and spread the traditional use of thermal baths, which lead to the development of the modern balneological industry (Hepbasli, 2010).

In 1904, electricity was generated for the first time from geothermal energy in the area now known as Larderello, Italy. The first geothermal district heating began operations in 1892 in Boise, Idaho (US). After 1910, the low pressure steam at Larderello started being used also for heating residential, industrial and greenhouses in the area (IGA, 2013).

From the plant in Larderello with 250  $\rm kW_e$ , geothermal energy utilisation has gown to an installed capacity of 60 GW in the world today.

In the present, geothermal energy systems consist of a production well, an injection well and a plant for the production of heat and/or electricity (Figure 2.8). Geothermal fields are typically operated at production rates that cause local declines in pressure and temperature, but the conditions can be restored when extraction ceases within a time scale of 100 years. The natural replenishment of heat in Earth and modern reservoir management techniques enable thus the sustainable use of geothermal energy as a low emission, renewable resource (Goldstein et al., 2011).

Geothermal resources can be classified as 1) convective or hydrothermal systems, 2) conductive systems and 3) deep aquifers.

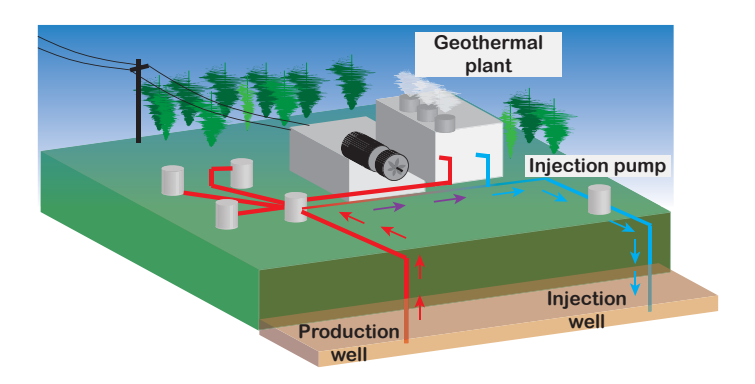
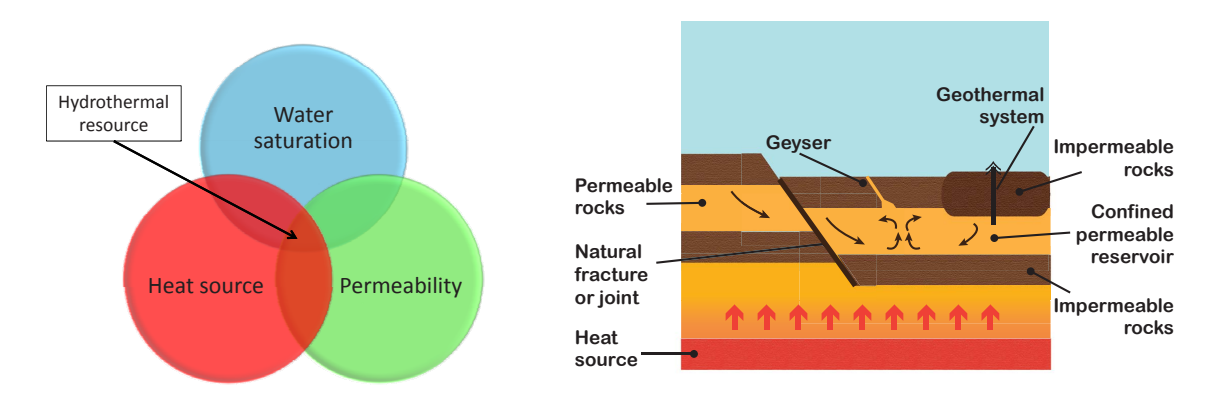


Figure 2.8. Illustration of a system for geothermal energy utilisation.

Geothermal water flows out from the reservoir through the production well. After utilisation at the geothermal plant, the water is injected back to reservoir to replenish the reservoir.

Hydrothermal systems are the main resource commercially available in the present. Their mean features are a large heat source, a permeable reservoir and a supply of water with a reliable recharge mechanism. These elements, illustrated in Figure 2.9, lie below a layer of impervious rock.

Enhanced or engineered geothermal systems enable the utilisation of other geothermal resources, such as hot dry rock (conductive) systems, characterised by low permeability and low porosity, and deep aquifer systems. This is accomplished by creating fluid connectivity through hydraulic stimulation and strategic well configurations.



**Figure 2.9.** Geothermal resources.

Left: Three conditions required for hydrothermal systems commercially available today. Right: Illustration of a hydrothermal system. Water is stored in the permeable reservoir.

In 2009, electricity was produced from a hydrothermal installed capacity of  $10.7~\rm GW_e$ , using  $2.4\times10^5~\rm TJ/yr$  of geothermal energy. The production contributed with only 0.3% to the world electricity supply. The top producer countries are US (3,094 MW<sub>e</sub>), Philippines (1,904 MW<sub>e</sub>) and Indonesia (1,197 MW<sub>e</sub>).

Regarding direct uses, the installed capacity at the end of 2009 was 50.6 GW<sub>th</sub>, generating  $4.4 \times 10^5$  TJ/h, 3.3% of the heat produced worldwide.

The global hydrothermal technical potential for the production of electricity has been estimated to be about 200 GW $_{\rm e}$ , equivalent to 5.7×10 $^{6}$ TJ/yr, 7.9% of the world electricity production in 2009. For geothermal direct uses, the potential of hydrothermal systems is estimated at about 4,400 GW $_{\rm th}$  from resources below 130 $^{\circ}$ C, equivalent to 41.6×10 $^{6}$ TJ/yr, 3.2 times the world heat production in 2009 (Goldstein et al., 2011; IEA, 2013).

#### 2.3.2 Geothermal energy in the Netherlands

In the Netherlands, water temperatures around 45°C are found between 1000 and 1200 m, and temperatures of 70°C or higher are found in aquifers deeper than 2000 m. The production of geothermal energy, including shallow systems, reached 316 TJ in 2011 (EC, 2013b).

A widely spread application in the country uses shallow sub-surface energy to deliver heat and cold to buildings. During summertime, cold water is extracted for air conditioning and the heated water is pumped back underground. During wintertime, hot water is extracted to provide heating and the cooled water is stored.

The country also has an important potential of deep geothermal energy. The geographical identification of the resource is depicted in Figure 2.10.

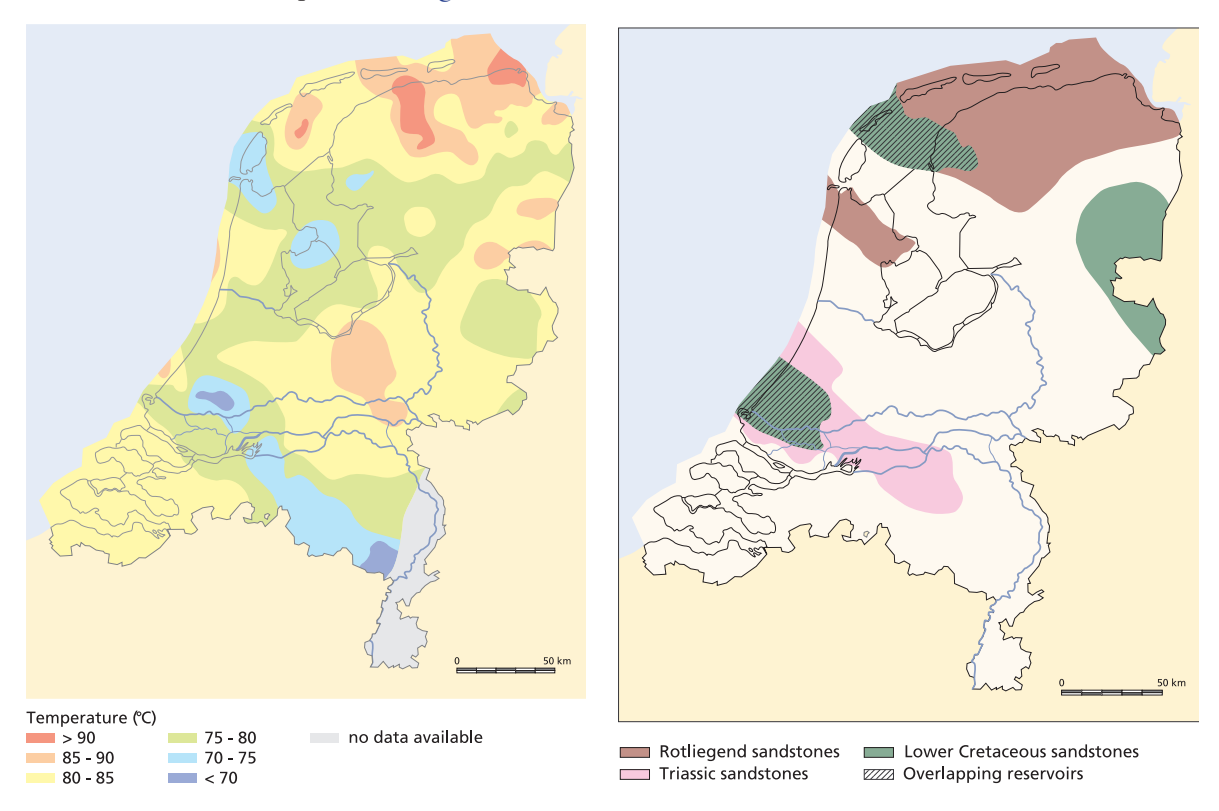


**Figure 2.10.** Deep geothermal potential in the Netherlands (Lokhorst & Wong, 2007). Left: temperatures at 2,000 m depth obtained from measurements in boreholes by NITG. Right: deep aquifers suitable for geothermal energy extraction (T>60°C and good transmissivity).

An exploration license was granted in 2009 to the foundation Delft Aardwarmte Project (DAP), which covers an area of 61 km<sup>2</sup> in the municipalities of Delft and Pijnacker-Nootdorp. The projects Ammerlaan and Duivestijn are located in this area.

The energy extracted in Ammerlaan is used for greenhouses and buildings; the water extracted from 2 km depth reaches a flow rate of  $100 \text{ m}^3/\text{h}$  at  $65^{\circ}\text{C}$ . The project Duivestijn started production in April 2012 at a flow rate of  $130 \text{ m}^3/\text{h}$  and a temperature of  $71^{\circ}\text{C}$  (Platform Geothermie, 2013).

In May 2012 an approval was granted for the drilling of a well to supply geothermal energy for the campus of TU Delft.

# 2.4 Exergy

When two systems at different states are brought into contact, work can be developed as they interact towards equilibrium.

When one of the two systems consists of the distant surroundings, it remains unaffected by any process involving the system of interest and its immediate surroundings, constituting thus an ideal exergy reference environment. This reference environment is known as the dead state (Figure 2.11).

Exergy is the maximum theoretical work that can be obtained when a system and the dead state interact to equilibrium. It is a measure of the quality of energy.

Exergy measures the departure of a system from the reference state. It is an attribute of system and environment together. Exergy can define the state of the system only if the dead state is specified.

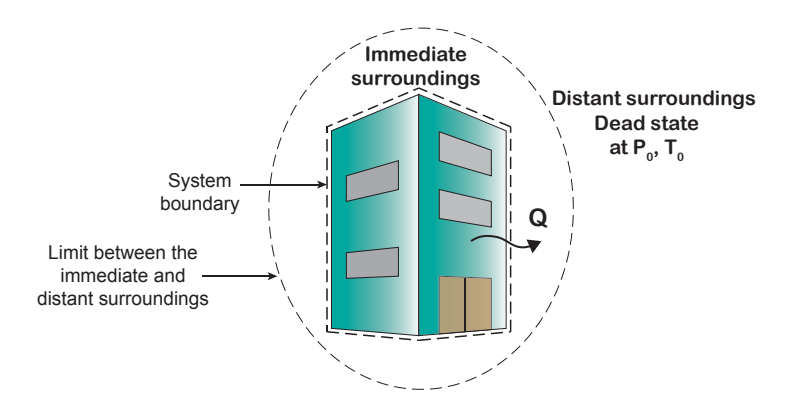


**Figure 2.11.** Illustration of the dead state.

The heat loss of the building (Q) only modifies the state of the immediate surroundings. The exergy of Q is the maximum amount of work that can be theoretically produced from it.

#### 2.4.1 Exergy balance

For an open system, the exergy rate balance can be written as follows:

$$\frac{dEx}{dt} = \sum_{j} \left( 1 - \frac{T_0}{T_j} \right) Q_j - \left( W - p_0 \frac{dV}{dt} \right) + \sum_{E} \phi_E ex_E - \sum_{L} \phi_L ex_L - Ex_D$$
 (2.1)

where  $dEx_T/dt$  is the rate of change in exergy of the system, the term  $(1 - T_0/T) Q_j$  represents the rate of exergy transfer accompanying heat at the location of the boundary at  $T_j$ , W is the exergy transfer by work,  $p_0 dV/dt$  is the exergy transfer by change of the system volume,  $\phi$  ex are the exergy flows entering and leaving the control volume, and  $Ex_D = T_0 \sigma$  is the exergy destruction. For the steady state, the change in exergy dEx/dt = 0.

#### 2.4.2 Exergy destruction

Exergy losses can accompany any mass or energy loss to the environment, such as the flue gas emitted in a power plant.

But, unlike energy, exergy losses can also occur **inside the boundaries of the system**; these losses are commonly referred as **exergy destruction**.

In a heating system, a typical example of exergy destruction occurs in the heat transfer process, as the one depicted in Figure 2.12. For *flow 2* heating *flow 1*, an infinitesimal heat transfer dQ takes place at  $T_1$  and  $T_2$ . The exergy transfer is shown graphically in a value diagram  $(1-T_0/T \text{ vs } Q)$ . The exergy gained by flow 1 is depicted by the area 1-2-3-4, and the exergy delivered by flow 2 corresponds to the area 1-2'-3'-4.

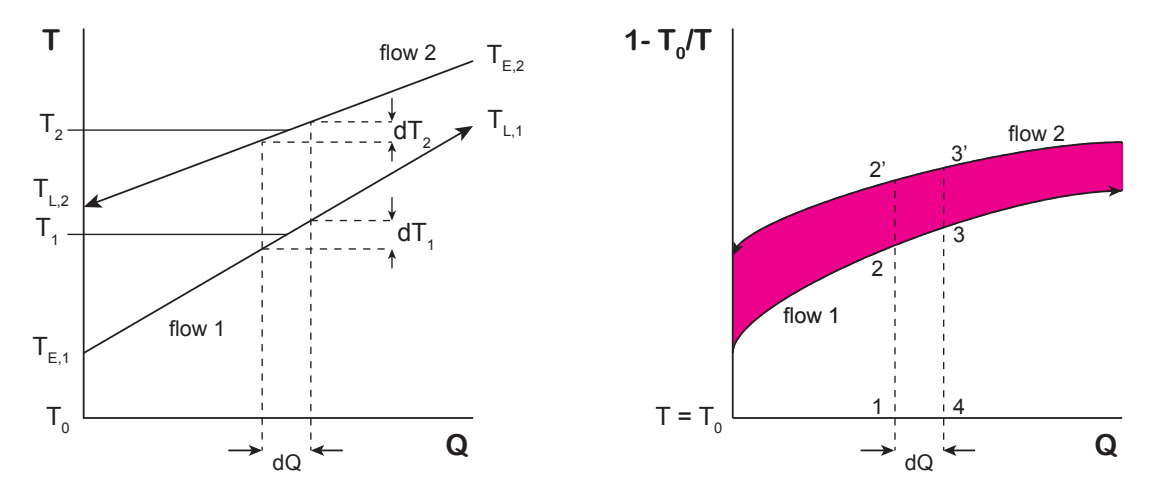


**Figure 2.12.** Exergy destruction in a heat transfer process. Left: Q-T diagram that represents *flow 2* heating *flow 1*. Right: Value diagram; the coloured area shows the exergy destruction.

The total exergy can be expressed by the heat transfer term of Eq. 2.1. The difference in the totals, shown as the coloured area in the value diagram, is the exergy destruction of the process.

$$Ex_{1} = \int_{T_{-1}}^{T_{L,1}} \left(1 - \frac{T_{0}}{T_{1}}\right) dQ \qquad Ex_{2} = \int_{T_{-2}}^{T_{L,2}} \left(1 - \frac{T_{0}}{T_{2}}\right) dQ \qquad Ex_{D} = Ex_{2} - Ex_{1}$$

#### 2.4.3 Chemical exergy

Chemical exergy is defined as the maximum amount of work that can be obtained when the system reacts to equilibrium with the environment (Sciubba, 2004).

This concept is useful to describe the exergy cost of materials, with the ocean or the Earth's crust taken as the reference environment.

#### 2.4.4 Simulation tool

The heating system is modelled using the software Cycle-Tempo, a program developed in TU Delft for the analysis of energy cycles.

Cycle-Tempo allows to define the dead state in terms of pressure, temperature and composition of the atmosphere. Additionally, it is possible to model several components for off design operation (partial loads).

As a first step in project engineering, the simulations are carried out for steady state, allowing to compare the performance of the systems of study at different conditions.

# 2.5 Carbon capture and storage (CCS)

Carbon capture and storage (CCS) is a set of technologies aimed at trapping  $CO_2$  produced from industrial and energy processes, compressing, transporting and injecting it into geological formations before it is emitted to the atmosphere.

 $\mathrm{CO}_2$  capture is not a new technology, it has been used for industrial processes and to increase oil or gas production. Nevertheless, capturing and storing  $\mathrm{CO}_2$  for climate change mitigation is new (CATO-2, 2013).

CCS technology can reduce the emission of  $CO_2$  by 85-90% in gas fired power plants. However, a power plant equipped with  $CO_2$  capture and compression consumes 10-40% more energy than an equivalent plant without it (IPCC, 2005).

The geothermal reservoir of the DAP can be used to store  $CO_2$ .

#### 2.5.1 CO<sub>2</sub> capture

In most energy processes,  $CO_2$  is present in a gas stream with other components, such as  $N_2$ ,  $H_2$ ,  $H_2O$ , CO and  $CH_4$ . In order to produce a pure  $CO_2$  stream required for transport and storage, it must be physically or chemically separated from the gas stream. The main capture techniques for energy processes are listed in Table 2.4 (Damen, 2007).

In post-combustion processes,  $CO_2$  is removed from flue gas produced in the combustion of fossil fuels or biomass. The leading technology is chemical absorption by means of an amine, already practiced in small scale to obtain high-purity  $CO_2$  for urea production and the beverage industry. The process can be applied to existing power plants.

Capture technique	Principle	Status
Post-combustion capture	$CO_2$ - $N_2$ separation	Applied on small scale
Pre-combustion capture	CO <sub>2</sub> - H <sub>2</sub> separation	Commercially applied in chemical industry
Oxyfuel combustion	$O2 - N_2$ separation (to prevent $N_2 - CO_2$ mixing)	Commercially applied in oxygen production

Table 2.4. Main groups of CO<sub>2</sub> capture techniques.

In the pre-combustion method, syngas  $(H_2, CO)$  undergoes a shift reaction producing  $CO_2$  and  $H_2$ . The former is captured and the latter is used as a fuel. This technique is applied in chemical industry, but it requires specialised equipment for power production from  $H_2$ , and thus it cannot be retrofitted in existing power plants operating on other fuels.

Oxyfuel combustion consists of burning the fuel in an oxygen atmosphere, resulting in a concentrated stream of  $\rm CO_2$  and  $\rm H_2O$  that can be easily separated by condensation. This scheme is in the demonstration phase.

#### 2.5.2 CO<sub>2</sub> transport

If the captured  $\mathrm{CO}_2$  is not located on top of the storage reservoir, it needs to be transported. For long distances on land, it is preferred to transport the  $\mathrm{CO}_2$  by pipeline after increasing the pressure over supercritical conditions (31°C and 74 bar) to prevent phase changes. In this way, large pipe diameters and high pressure drops are avoided.

# 2.5.3 CO<sub>2</sub> storage

The reservoirs for geological storage of CO<sub>2</sub> must meet the following requirements:

- Sufficient storage volume and permeability for planned injection.
- Depth below 800 m, at which CO<sub>2</sub> is in supercritical state, with a density that ensures
  optimal storage.
- The density of supercritical  $\mathrm{CO}_2$  is 50-80% of the reservoir water, therefore the  $\mathrm{CO}_2$  tends to rise due to buoyancy effects. The reservoir should be sealed with a low permeability cap rock to ensure retention times over 1000 years.

The main types of storage options are listed in the table below (Damen, 2007).

**Table 2.5.** Main reservoir options for geological storage of  $CO_2$ .

Storage option	Global capacity [Gt CO <sub>2</sub> ]	Status	
Discovered oil and gas fields	675 - 900	Proven in commercial projects	
Deep saline aquifers	$10^3 - 10^4$	Proven in a commercial project but uncertainty of seal	
Unminable coal seams	3 - 200	Demonstration phase	

Storage in deep saline aquifers, such as a geothermal reservoir, presents an enormous potential, although they have not been studied as extensively as hydrocarbon reservoirs.

# System modules and their models

In this chapter, the components of the system are grouped in modules that facilitate their simulation and analysis. The modules are modelled using Cycle-Tempo.

Section 3.1 comprises the delimitation of the modules. In subsequent sections each module is explained, including a brief description of the Cycle-Tempo models. In Section 3.5, the methods to calculate losses in pipelines are covered. Finally, in Section 3.6, a general description of the modelled scenarios is presented.

#### 3.1 Borders and variables

The present heating system is constituted by the combined heat and power (CHP) plant and the network infrastructure. Geothermal energy will be implemented in the new system.

For the study of the system, three main modules are delimited by boundaries at the points where mass or energy is exchanged with the environment or other modules. A simplified scheme of these modules is given in Figure 3.1.

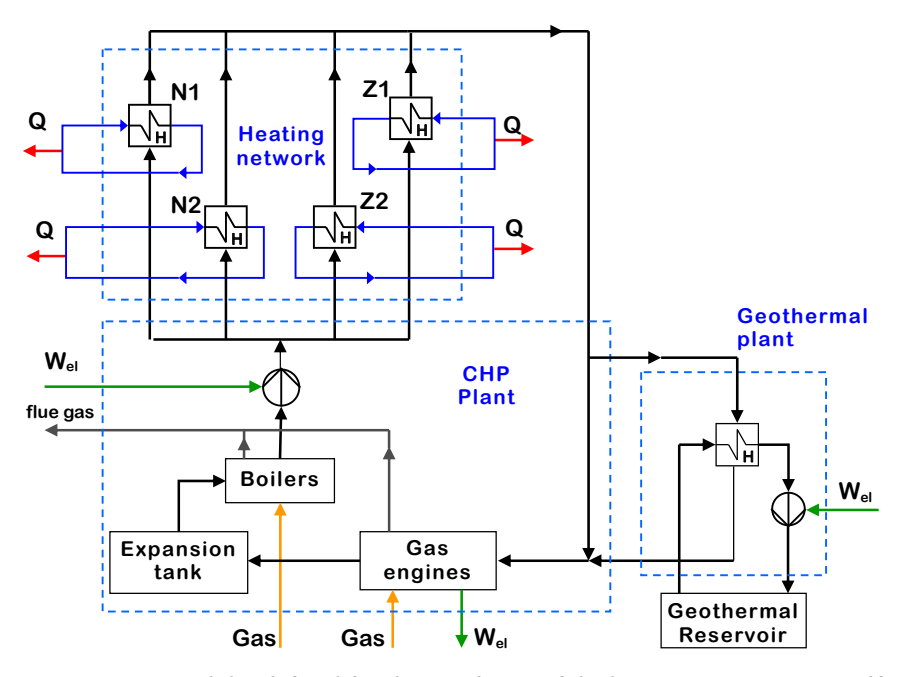


Figure 3.1. Modules defined for the simulation of the heating system at TU Delft.

The network is divided in four blocks: N1, N2, Z1 and Z2.

bined heat and power (CHP) plant provides energy by means of gas hollers and gas.

The combined heat and power (CHP) plant provides energy by means of gas boilers and gas engines. Geothermal energy will be introduced in the new system.

- 1) Heating network. It is divided in 4 blocks: North 1 (N1), North 2 (N2), South 1 (Z1) and South 2 (Z2). Underground insulated pipelines transport the water to the buildings. Heat exchangers located in the basements transfer the thermal energy (Q) from the hot water of the CHP plant to the water circulating in the pipelines and radiators of the buildings. Hot water from the CHP plant enters this module and exits at a lower temperature (primary circuit). Hot water is delivered to the buildings and returns to the module to be heated (secondary circuit). After the transition, part of the return water will be sent to the geothermal plant to be preheated
- 2) CHP Plant. It consists of gas engines, boilers, an expansion tank and pumps. Cold water enters the CHP plant from the return lines of the four blocks; natural gas is fed to the gas engines and to the boilers, which emit flue gas to the environment; the electricity produced by the gas engines is sold to a utility company; grid electricity is consumed to pump the hot water leaving the CHP plant. In the new system, part of the return water will be sent first to the geothermal plant.
- 3) Geothermal plant. It consists of heat exchangers that transfer thermal energy from the geothermal fluid to the return water of the network, and pumps that reinject the geothermal fluid back to the reservoir. The return water enters the geothermal plant to be preheated and returns to the CHP plant. Hot geothermal fluid enters the plant from the production well and exits at a colder temperature.

# 3.2 Heating network

The heating network is divided in four blocks that operate as individual distribution systems. These blocks are named after their geographical disposition. The map in Figure 3.2 displays the buildings serviced by the distribution lines; the zones corresponding to each of the four blocks are colour coded as follows:

**North 1 (orange)**: Building 31 (TBM), building 30 (OTB and O&S), building 12 (ChemE), building 8 (BK), building 20 (Aula), building 21 (Biliotheek) and building 22 (TNW); building 43 (WKC) is included also in this block.

North 2 (green): Building 31 (TBM), building 32 (IO) and building 34 (3mE)

**South 1 (pink):** Building 44, building 34 (3mE), building 35, building 36 (EWI), building 22 (TNW) and building 23 (CiTG)

**South 2 (yellow):** Building 45, building 46 (P&E), building 36 (EWI), building 23 (CiTG), building 37 (SC), building 66 (Fellowship), buildings 61-64 (LR) and building 65 (FMVG)

The main characteristics of each heating block are listed in Table 3.1.

**Table 3.1.** Characteristics of the distribution blocks in the heating network.

Block	North 1	North 2	South 1	South 2
Floor area supplied [m²]	137,000	80,000	109,000	162,000
Installed capacity (heat exchangers) [kW]	27,998	15,321	26,438	22,420
Flow rate [m³/h]	273	144	241	262
Total length [m]	4.35	1.99	2.80	6.14

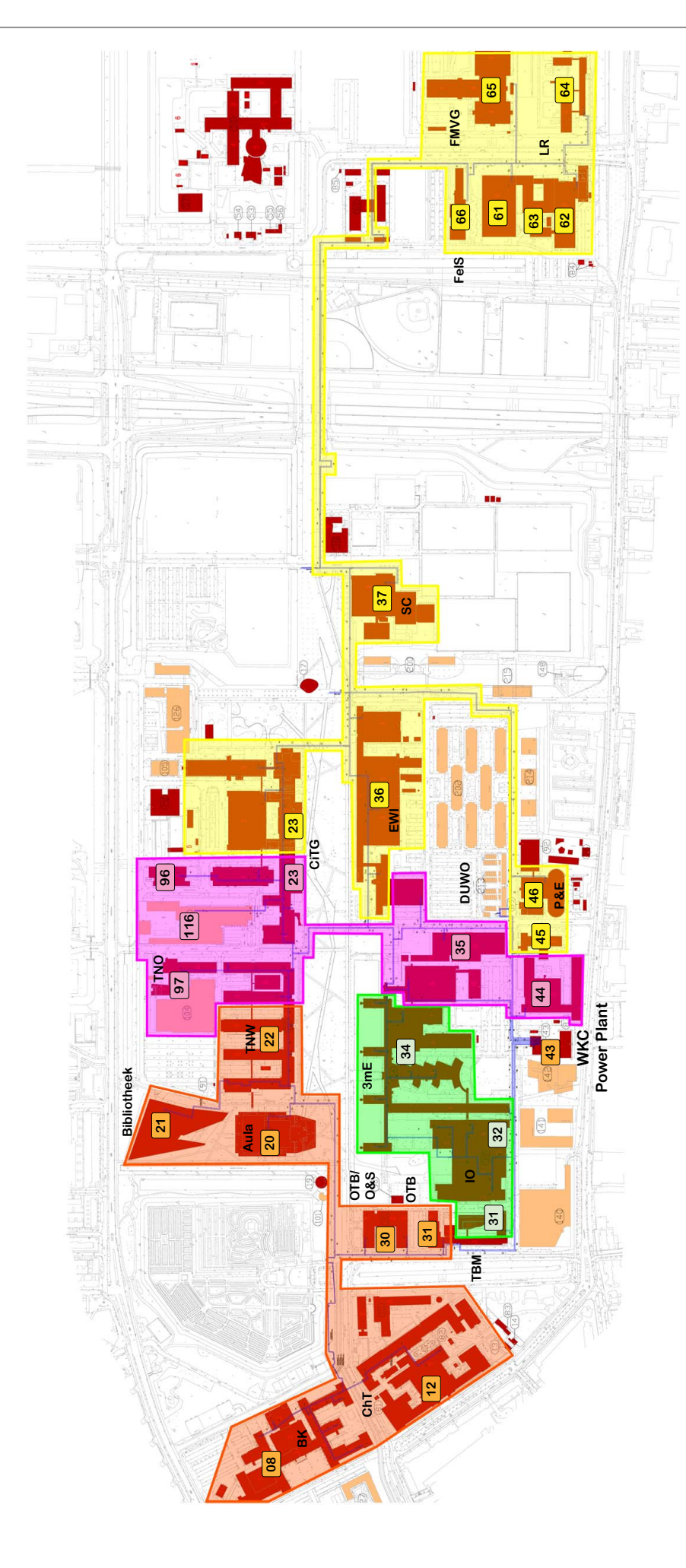


**Figure 3.2.** Map of the for blocks comprising the heating network. North 1 in orange, North 2 in green, South 1 in pink and South 2 in yellow.

#### 3.2.1 Model summary

The analysis developed in this project is focused on the primary circuit, providing a scientific basis for the selection of buildings to be renovated based on the performance of the system.

The supply and return pipelines run parallel to each other, with branches to the rooms in the buildings where the heat exchangers are located.

The diagram of an individual branch in block N1 is depicted in Figure 3.3 as an example .The block N1 has 15 of these branches. The list of assumptions and inputs for the model of the network is included in Appendix A.

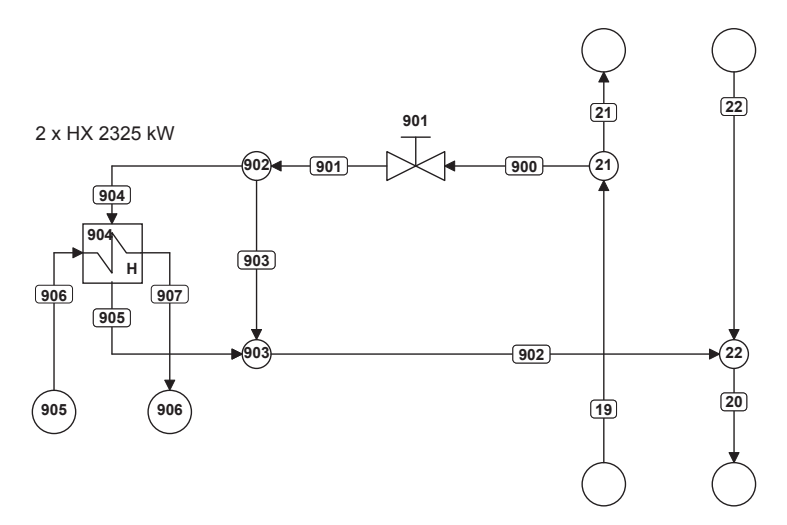


**Figure 3.3.** Model diagram of a single heat exchanger branch in block N1. The branch is connected in parallel to the main lines and includes a 3-way valve bypass, both features of the present configuration.

- **Pressure and heat losses in pipes** are specified for the main lines (19, 20, 21, 22) and the branch lines (900, 902). These losses include the pressure drop of bents.
- The **pressure drop in accessories** is included in splitters (21, 902) and valves (901).
- The **3-way bypass valve** is **modelled as a splitter/mixer** (902/903) that includes the pressure drop of a tee junction and a ball valve opened towards the heat exchangers.
- Parallel **heat exchangers (HX)** of the same size are modelled as a single unit (904).
- The flows of the **secondary circuit** are modelled as a source (905) and a sink (906). Cold water enters the heat exchanger and hot water leaves.

# 3.3 CHP plant, warmtekrachtcentrale (WKC)

The CHP plant at TU Delft (WKC) operates with 2 gas engines, 3 boilers and several pumps to move the water.

In this thesis, these components are modelled based on data from the design sheets provided by FMVG. The effect of the expansion tank is simulated as zero pressure changes due to heating and friction losses within the plant.

The full diagrams of the plant and the Cycle-Tempo model are provided in Appendix B, along with a comprehensive list of assumptions and inputs for the model.

#### 3.3.1 Gas engines

Four-stroke internal combustion engines of the spark-ignition type produce electricity from gas and preheat the water at the same time. There are 2 engines of 2 MW each.

Cooling water extracts heat from the engine. The hot water reaches a mixing vessel, where it preheats the network water. Electricity is produced by a generator and the exhaust gas leaves with the option for further heat recovery. No emission control is applied on the exhaust gas.

#### 3.3.1.1 Model summary

The diagram for a single gas engine is shown in the figure below.

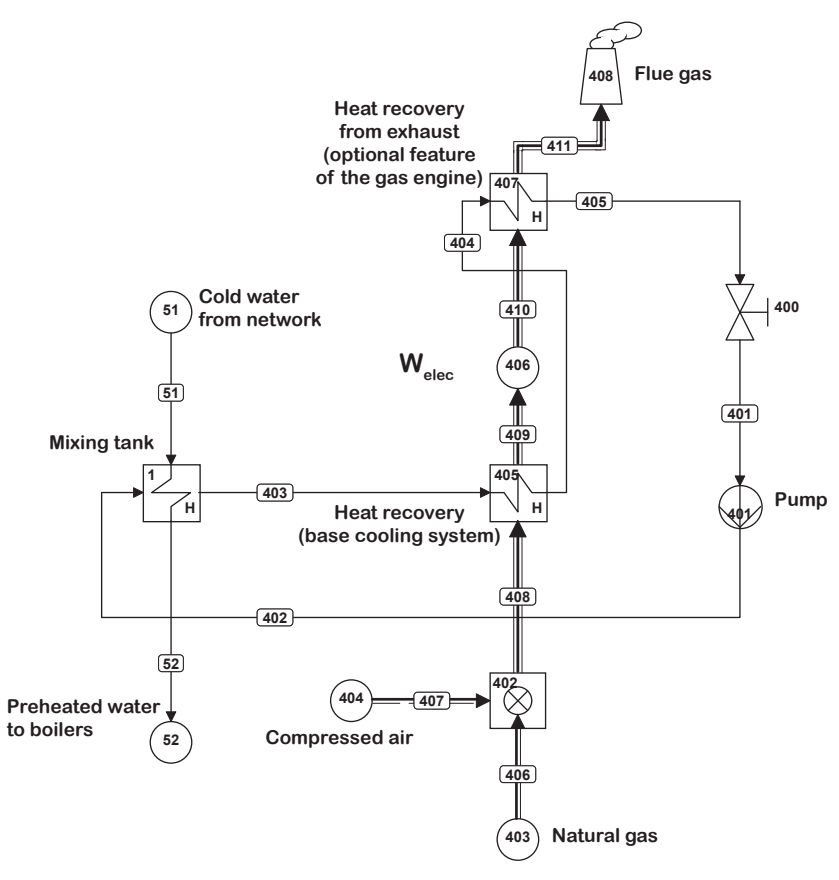


**Figure 3.4.** Diagram of the model for a gas engine. The power plant at TU Delft has two gas engines.

- The **mixing tank** is **modelled as a heat exchanger** (1) operating always on design conditions.
- The heat recovery (405) and the optional heating (407) are modelled as heat exchangers that can operate on design and off design.
- The *intake* and *compression* strokes of the gas engine are modelled as compressed air (404) entering a combustor (402). The energy taken from the piston for compression is thus simulated as the exergy cost of the pressurised air.
- The *power* and *exhaust* strokes are modelled as a pressure drop in the combustion gas (406). The exergy loss from the drop represents the electricity produced by the generator.

• The operation is modelled at **constant flow rate** specified in the **valve** (400).

#### 3.3.2 Boilers

Three boilers of 35, 30 and 15 MW complete the heating of the network water after the gas engines.

The water that is heated in the three boilers reaches one single mixing tank, where it in turn heats the network water. No emission control is applied in the flue gas.

Depending on the heat demand, part of the network water can be bypassed when no further heating is required.

#### 3.3.2.1 Model summary

The model scheme of the three boilers is shown in the figure below.

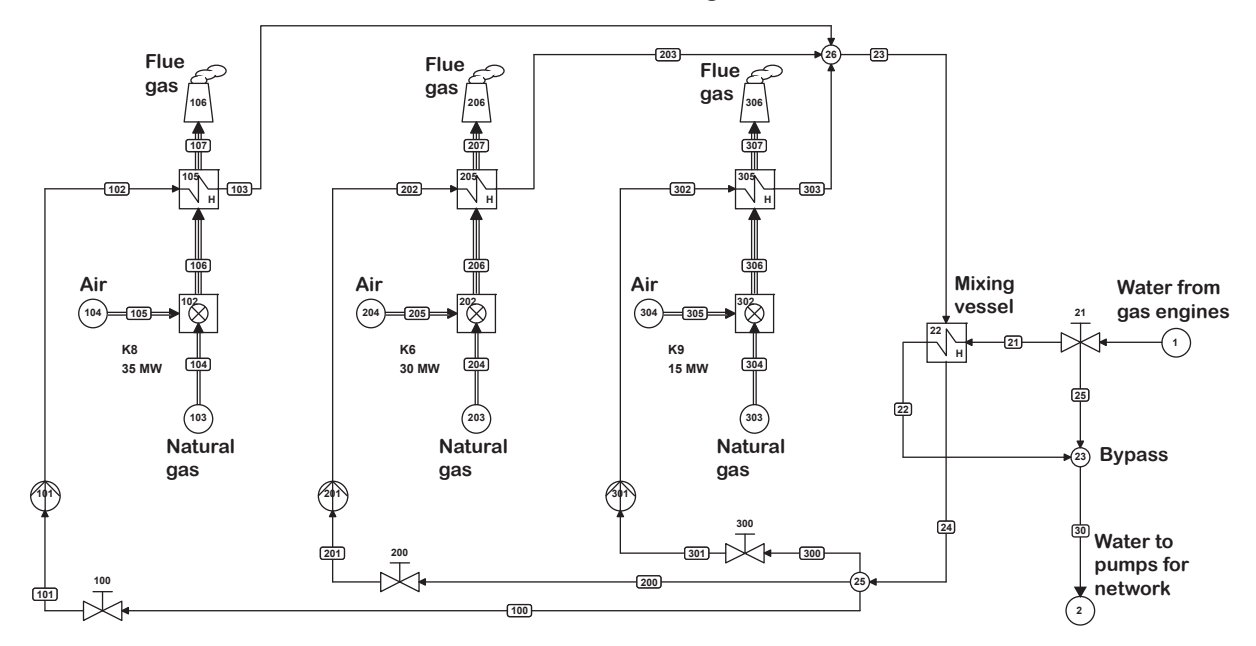


**Figure 3.5.** Diagram for the model of the boilers at WKC. The three boilers f the power plant in TU Delft are connected to a common mixing vessel.

- The boilers are modelled as combustors (102, 202, 302) followed by a heat exchanger (105, 205, 305) where the combustion gas transfers heat to the circulating water. The exchangers can operate both on design and off design.
- The **mixing vessel** is **modelled as a heat exchanger** (22) operating only on design conditions.
- One **pump** in each boiler moves the water between the boiler and the mixing (101, 201, 301).
- The operation of the boilers is modelled at **constant flow**, specified in the **valves** (100, 200, 300).
- The **bypass** is **modelled as a valve/mixer** (21/23). A ratio of bypassed flow is specified in the valve.

The hot network water is then transported to the distribution pumps that increase the pressure accordingly to the requirement of each block in the network.

#### 3.3.3 Distribution pumps

The water circulating in each block of the heating network is delivered by its own distribution pump. A backup pump exists in the CHP plant in case of failure. This pump is not included in the model. A new pump required to send the water to the geothermal plant is included in the model of the latter.

#### 3.3.3.1 Model summary

The model of the distribution pumps is depicted in the figure below.

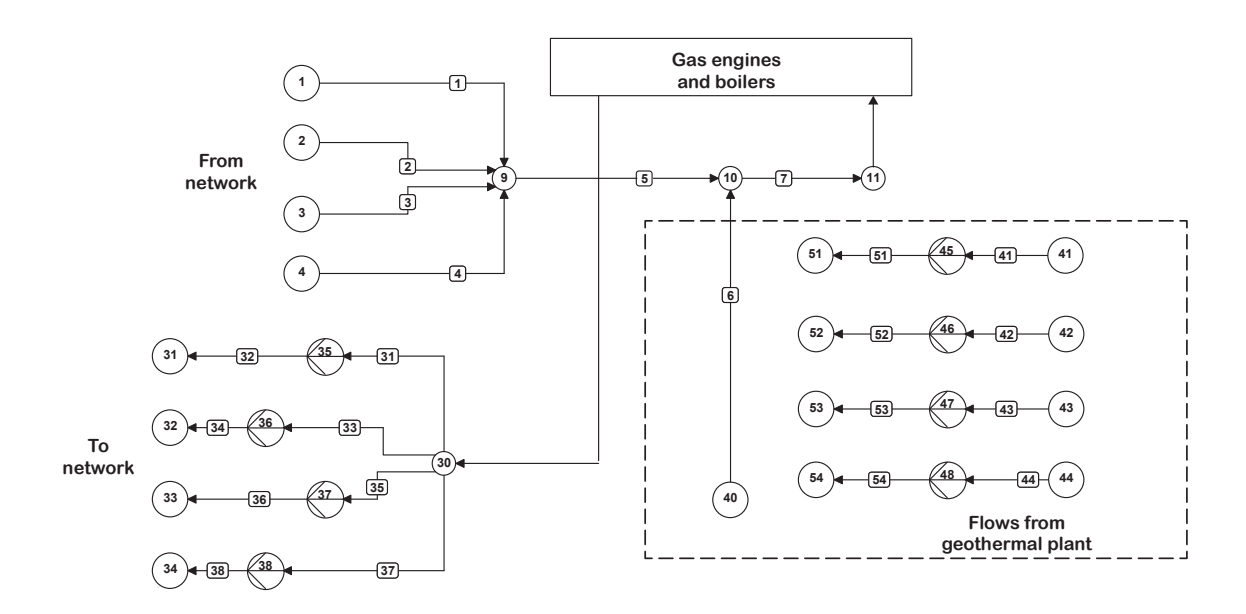


**Figure 3.6.** Diagram of the model for the distribution pumps at WKC.

- The **distribution pumps** (35-38) deliver **varying flow rates** depending on the demand.
- The preheated flow from the geothermal plant in the new system is modelled as a source (40).

For the new system with geothermal energy, in some scenarios, the temperature delivered by the geothermal plant can meet the demand of specific blocks in the network. To facilitate the analysis, these flows are specified separately (sources 41-44), although they are also fed to the distribution pumps.

## 3.4 Geothermal plant

The future geothermal plant will be constituted by a production and an injection well that transport the water from the reservoir to the surface and back. Heat exchangers will transfer the geothermal heat to the network water. Pumping power is required to reinject the geothermal fluid and to transport the network water from the CHP plant.

Matsamura (2012) reports an expected surface temperature in the production well of  $75.7^{\circ}$  C and a production rate of  $150\text{m}^3/\text{h}$ . The base thermal power is almost 5.1 MW. Oversized heat exchangers allow for further energy transfer. The geothermal plant expects to sell a minimum of 70,000 GJ/yr.

#### 3.4.1 Model summary

The model diagram for the geothermal plant is shown in Figure 3.7. The assumptions and inputs used in the model are included in Appendix C.

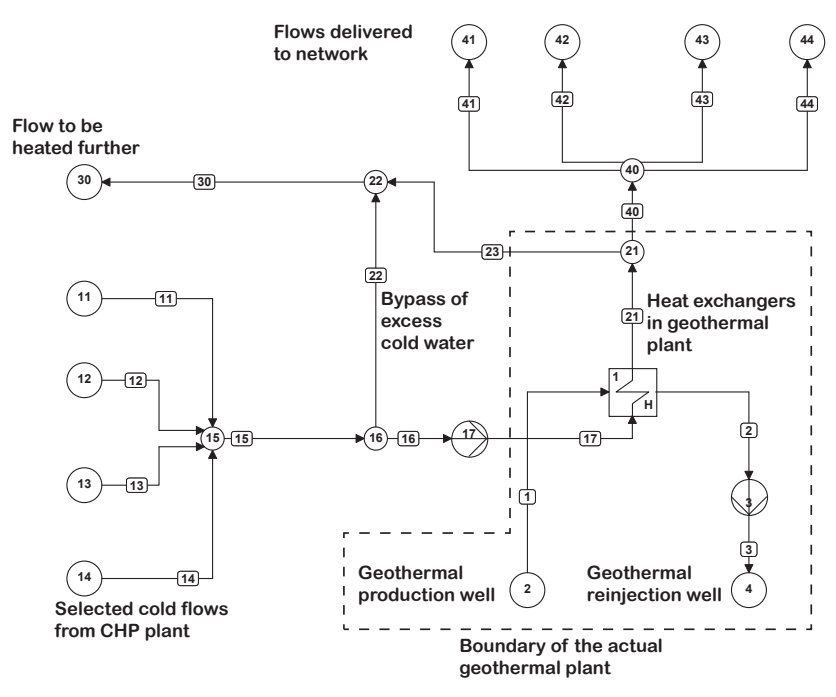


Figure 3.7. Model of the geothermal plant.

The processes outside of the boundary shown would physically take place in the CHP plant.

The model aims at maximising the utilisation of geothermal energy to achieve the requested minimum. Therefore, the expected geothermal flow rate  $(150 \text{ m}^3)$  is taken as constant throughout the year. However, pumping power constitutes the main exergy cost in a geothermal plant and maintaining a constant flow when it is not used can be inefficient. For future work, it is suggested to develop an adequate control strategy that maximises the exergy efficiency of the plant.

- The **production well** (at surface level) is **modelled as a source** of water at constant flow rate, pressure and temperature (2).
- The **reinjection well** (at surface level) is **modelled as a sink** (4). The pressure drop throughout the geothermal system (reservoir, pipes and heat exchangers) is overcome by an injection **pump**(3).
- The geothermal heat is transferred to the network water in **parallel heat exchangers** modelled as a single unit (1).
- When there is an **excess of cold water** from the network that cannot be heated by the available geothermal flow, it is **bypassed** and combined with the output of the geothermal plant (splitter 16 and mixer 22). The network water that can be heated is pumped to the geothermal plant (17).
- Pressure and heat losses are calculated separately. The losses are specified the inlet and outlet lines (pipes 17 and 21), representing the pipelines that will connect the CHP and geothermal plants.

In some scenarios, some blocks of the network present a return temperature hotter than others. Only the blocks of colder temperatures are fed to the geothermal plant. This is specified by individual sources per block (11-14).

For some scenarios, it is possible to cover the heating demand of specific blocks in the network with the temperature delivered by the geothermal plant. These cases are modelled as individual sinks (41-44). They represent water that goes back to the distribution pumps without further heating.

The water that returns to the CHP plant for further heating is modelled as a sink (30).

The latter three processes will physically take place in the CHP plant, but since they are necessary to harvest geothermal energy, they are included in this model.

#### 3.5 Pressure and heat losses

The pressure and heat losses are calculated separately and provided as inputs for the models of the network and the geothermal plant.

#### 3.5.1 Pressure drop

The friction losses in the pipes are calculated using the Darcy-Weisbach equation (Eq. 3.1), where  $\Delta P$  is the pressure drop due to friction, f is the Fanning friction factor, L is the length of the pipe segment,  $\rho$  is the density of water at the given pressure and temperature, and v is the velocity of the flow. The lengths and diameters are taken from the blueprints of the heating system provided by FMVG.

$$\Delta P = 4f \frac{L}{D} \frac{1}{2} \rho v^2 \tag{3.1}$$

The models tested at different conditions prove the prevalence of turbulent flow regime. Therefore, the Fanning friction factor f can be calculated using the Colebrook equation (Eq. 3.2), where d is the pipe internal diameter, Re is the Reynolds number and  $\varepsilon$  is the roughness of the pipe. Based on the models and field data, a roughness  $\varepsilon = 0.35$  mm is found; this value corresponds to moderately corroded carbon steel (Native Dynamics, 2012).

$$\frac{1}{\sqrt{f}} = -4.0\log_{10}\left(\frac{\varepsilon}{3.7d} + \frac{1.256}{\text{Re}\sqrt{f}}\right)$$
(3.2)

The **friction losses in accessories** are calculated from Eq. 3.4, where  $K_{w}$  is the corresponding head loss factor as listed in Table 3.2. The bents are assumed to be 90° and sharp.

$$\Delta P = K_w \frac{1}{2} \rho v^2 \tag{3.3}$$

In order to determine the relevance of the pressure drop for different components, the losses are calculated for the main line and for a single branch in block N1 at peak load in the current configuration. Contributions to the pressure drop lower than 1% are neglected.

**Table 3.2.** Head loss coefficients for the modelled accessories.

Component	Head loss coefficient $(K_{_{\mathrm{w}}})$					
90° sharp bent	1.3					
Tee junction	1.5 1.3 1.0 1.0					
Ball valve	0.29					
Sudden contraction	$0.45 \times (1 - A_2/A_1)$					
Sudden enlargement	$(1-A_1/A_2)^2$					

In the main lines, the losses due to **sudden contractions and enlargements** are **neglected** (Table 3.3).

As for the pressure drop in a branch, the losses in the **main valve** (ball valve) and the **3-way valve** are **neglected** (Table 3.4). The losses in the pipes are accounted for because the length can be considerably larger than the example (>10x).

**Table 3.3.** Relevance of friction losses for components in the main lines. The results correspond to the block N1 at peak operation.

Component	$\Delta P$ [bar]	Relevance	
Pipes	1.385	83.9%	Accounted for
Bents	0.268	9.4%	Accounted for
Tees	0.187	6.6%	Accounted for
Sudden contr./enl.	0.004	0.1%	Neglected

**Table 3.4.** Relevance of friction losses for components in a branch. The results correspond to TBM in block N1.

Component	ΔP [mbar]	Relevance	
Heat exchanger	500.00	99.906%	Accounted for
Pipes	0.41	0.082%	Accounted for
Supply valve	0.01	0.002%	Neglected
3-way valve	0.05	0.010%	Neglected

## 3.5.2 Heat losses in pipes

The energy balance for water in a pipe segment can be written as shown in Eq. 3.4, where  $\phi$  is the mass flow rate,  $C_P$  is the heat capacity and  $T_E$  and  $T_L$  are the temperatures entering and leaving the segment.  $T_E$  is assumed equal to the supply temperature from the CHP plant.  $C_P$  is evaluated at  $T_E$ .

$$Q_{loss} = \Delta H = \phi C_p \left( T_E - T_L \right)$$
(3.4)

The heat transfer through the pipe and insulation can be described by Eq. 3.5, where U is the overall heat transfer coefficient, A is the area of heat transfer evaluated at the internal diameter of the pipe and  $T_S$  is the temperature of the soil assumed constant at 5° C.

$$Q_{loss} = UA\Delta T_{lm} = UA \frac{(T_E - T_S) - (T_L - T_S)}{\ln\left(\frac{T_E - T_S}{T_L - T_S}\right)}$$
(3.5)

Equalling the previous two expressions and solving for  $T_L$ , Eq. 3.6 is obtained, where D is the internal diameter and L is the length of the pipe segment. Once  $T_L$  is calculated, it is substituted in Eq. 3.5 to obtain the heat losses.

$$T_{L} = \frac{T_{E} - T_{S}}{\exp\left(\frac{U\pi DL}{\phi C_{p}}\right)} + T_{S}$$
(3.6)

The overall heat transfer coefficient is calculated from Eq. 3.7, where  $h_c$  is the heat transfer coefficient of water, r are the radii and  $\lambda$  are the thermal conductivities of the pipe and the insulation. The pipe walls are composed of steel with  $\lambda_P = 43 \,\mathrm{W/m}$  K. The insulation consists of stone wool, with  $\lambda_{ins} = 0.045 \,\mathrm{W/m}$  K.

$$\frac{1}{U} = \frac{1}{h_c} + \frac{r_2 \ln\left(\frac{r_2}{r_1}\right)}{\lambda_p} + \frac{r_3 \ln\left(\frac{r_3}{r_2}\right)}{\lambda_{ins}}$$
(3.7)

The radii are represented in Figure 3.8. Standard thicknesses of steel pipes are listed in Table 3.5. The thickness of the insulation is assumed equal to 50 mm for internal pipe diameter  $D \le 100$  mm, and 100 mm for 100 mm  $\le D \le 200$  mm.

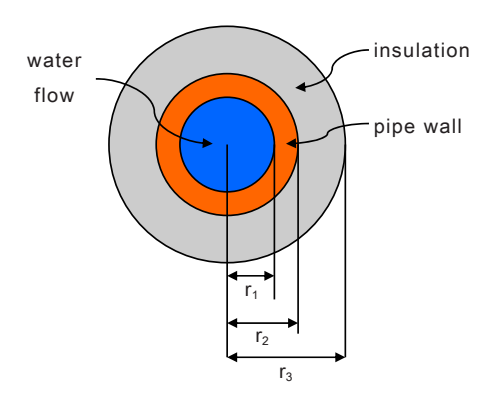


Figure 3.8. Illustration of the radii of the pipe and its insulation layer.

The construction is common to the pipelines transporting the water in the network of the heating system at TU Delft.

The heat transfer coefficient for water is calculated from the definition of the Nusselt number Nu (Eq. 3.8), where  $\lambda_w$  is the thermal conductivity of water evaluated at the inlet temperature  $T_E$ .

$$h_c = \langle Nu \rangle \frac{\lambda_w}{D} \tag{3.8}$$

Adapted from (Sayı	01, 2013).
Internal diameter D	Pipe thickness [mm]
20 mm ≤ D < 25 mm	2.87
$25 \text{ mm} \le D \le 40 \text{ mm}$	3.38
$40 \text{ mm} \le D \le 50 \text{ mm}$	3.70
$50 \text{ mm} \le D \le 80 \text{ mm}$	3.90
$80 \text{ mm} \le D \le 100 \text{ mm}$	5.50
$100 \text{ mm} \le D \le 125 \text{ mm}$	6.00
$125 \text{ mm} \le D \le 150 \text{ mm}$	6.60
$150 \text{ mm} \le D \le 200 \text{ mm}$	7.10
D = 200  mm	8.20

**Table 3.5.** Standard thickness of steel pipes. Adapted from (Saylor, 2013).

The Nusselt number Nu is determined from the expressions in Eq. 3.9, depending on the Reynolds Re, Prandtl Pr and Graetz Gz numbers. The properties for these numbers are evaluated at the inlet temperature  $T_E$ .

$$\langle Nu \rangle = \begin{cases} 0.027 \,\text{Re}^{0.8} \,\text{Pr}^{0.33} & \text{for Re} > 10^4; \text{Pr} \ge 0.7 \\ 1.62 \,\text{Gz}^{-1/3} & \text{for Re} < 10^4; \,\text{Gz} \le 0.05 \\ 3.66 & \text{for Re} \le 10^4; \,\text{Gz} > 0.05 \end{cases}$$
(3.9)

## 3.6 General model configurations

The present and future heating systems are modelled for different configurations, briefly explained in this section. In the next chapters, the operation conditions and results of each case are covered.

## 3.6.1 Present heating system

The present heating system is modelled for two different configurations:

- 1) System with 3-way valve bypass system.
- 2) System with 2-way valve system.

A flow chart describing the route of the working fluid is shown in Figure 3.9. For a 3-way valve system, the total amount of water calculated from an energy balance is fed to the buildings; in a 2-way valve system, only the required flow is fed to the buildings (1). The water flows through the heat exchanger (2) and back to the CHP plant. If the supply temperature  $T_{sup}$  is reached by the engines (3), no further heating is required, otherwise the boilers complete the process (4). The water is moved by the distribution pumps (5).

#### 3.6.2 New heating system

The new heating system will be integrated by the network, the geothermal plant and the CHP plant. Three different configurations are modelled for the future system:

- No renovations in the buildings
- 2) Renovations for MT operation of 4 large buildings.
- 3) Renovations for MT operation of several small buildings.

It is important to point out that in several cases there is a deficit or an excess of energy in a particular stream. The solution proposed herein is to **maintain a 3-way valve system** and add other bypasses whenever this energy mismatch occurs. Such cases and their repercussions are analysed in Chapter 5.

A general flowchart describing the route of the working fluid is shown in Figure 3.10. Hot water reaches the HT consumers (1). At the outlet, the water may carry an excess or a deficit of energy for the MT buildings (2), resulting in a bypass. The water returns to the CHP plant where only the streams with low temperature ( $T < 70^{\circ}C$ ) are sent to the geothermal plant (3); if there is an excess it stays in the CHP plant. All the streams are then mixed and reach the engines and the boilers if further heating is needed. The water is then pumped back to the consumers (5). In some cases, the outlet of the CHP plant can be used to supply a block in the network.

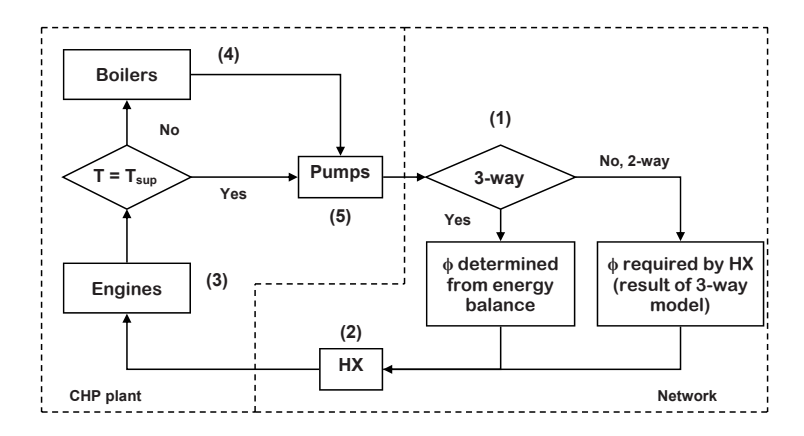


**Figure 3.9.** Flowchart of the model of the present heating system. The model shows the route of the working fluid.

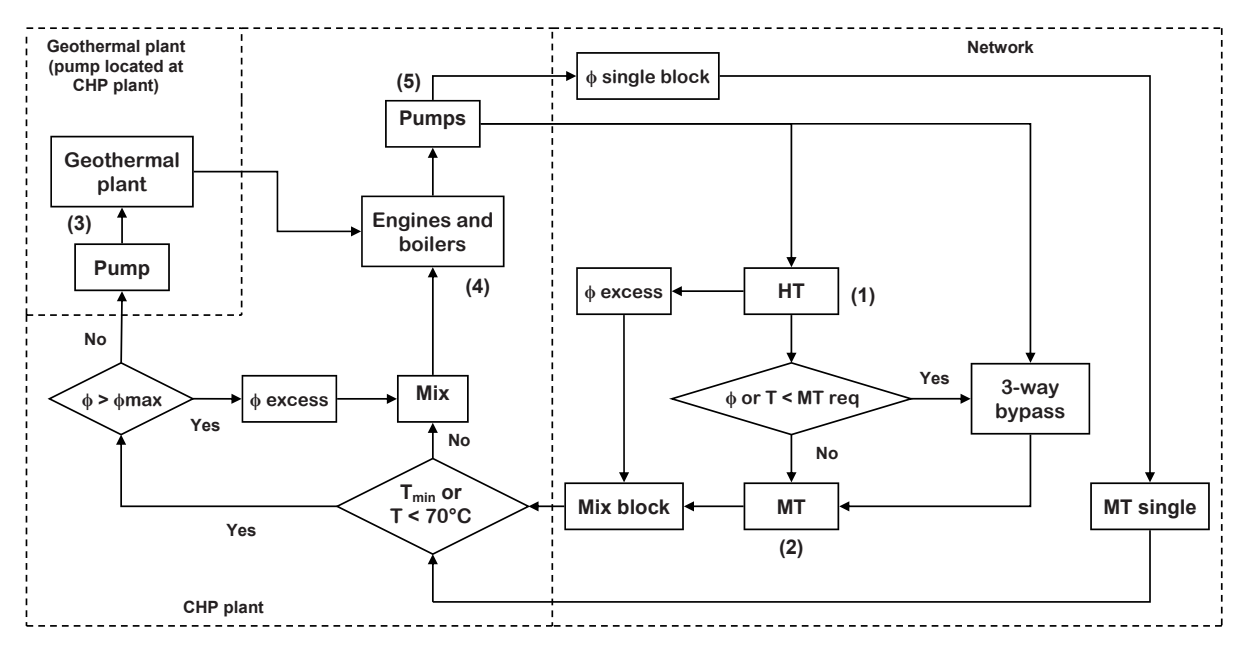


**Figure 3.10.** Flowchart for the simulation of the new heating system. The model shows the route of the working fluid.

## PRESENT HEATING SYSTEM

In this chapter, an exergy analysis of the current heating system at TU Delft is performed. Two system configurations are evaluated:

- 1) With 3-way valve bypasses
- 2) With 2-way valves.

These configurations do not include geothermal energy.

## 4.1 Demand profile

The analysis is based on the loads measured in 2012 by the Facilitair Management & Vastgoed (FMVG) of TU Delft and the company Van Beek. Hourly data for the energy flow at specific points in the network was provided by personnel from Van Beek; the load profile is shown in Figure 4.1 for illustration purposes<sup>1</sup>. Hourly environment temperature  $T_{env}$  data provided by the meteorological station Weer Delft is included in the same figure.

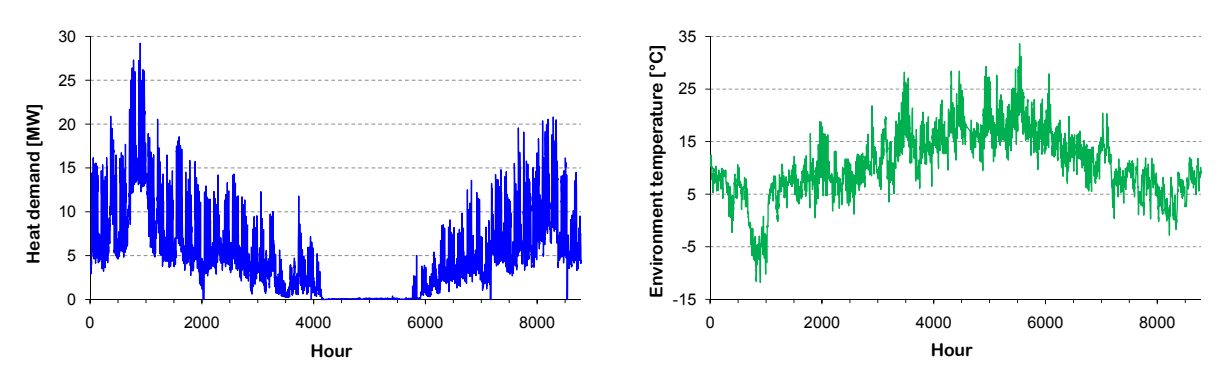


**Figure 4.1.** Heat demand and environment temperature profiles for 2012. Left: Heat demand at TU Delft (data provided by Van Beek). Right: Environment temperature in Delft (data provided by Weer Delft).

The graphs show a dependence between the heat demand and the environment temperature. Therefore, the scenarios for the analysis are based on  $T_{env}$  itself.

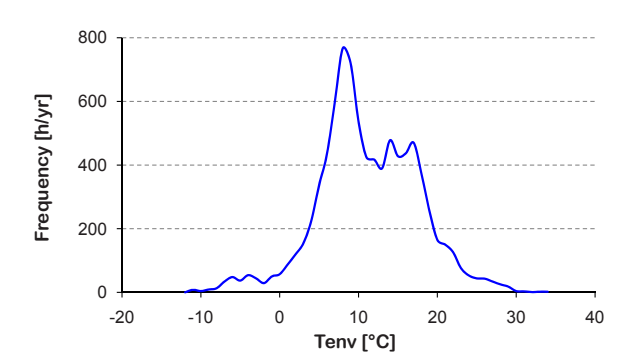
Three hourly load scenarios are selected for the simulation of the system:  $T_{env} = -10^{\circ}\text{C}$ ,  $0^{\circ}\text{C}$  and  $10^{\circ}\text{C}$  with a margin of  $\pm 1^{\circ}\text{C}$ . Average demands for each scenario are calculated for working days of the university calendar during the day (7:00 to 18:00 h). The demands for each block in the network are listed in Table 4.1 (including the estimated demand for the buildings that are not monitored yet). A complete list of the measured demand per installed meter and the estimated demand per branch is provided in Appendix D.

<sup>1.</sup> The heat demand in some buildings of the network is not being monitored as of today. Therefore, the real demand is a little bit higher than shown in the profile. Averages for the missing data are estimated for single steady state scenarios in Appendix D.

<b>Table 4.1.</b> Average hourly demand for the steady state scenarios in the DHS of TU Delft.
The values are calculated for day hours in working days of 2012.

Block	$T_{env} = -10 \pm 1$ °C	$T_{env} = 0 \pm 1$ °C	$T_{env} = 10 \pm 1$ °C
N1	8977.5 kW	6711.0 kW	3134.0 kW
N2	4025.0 kW	2948.0 kW	1209.0  kW
<b>Z</b> 1	9623.0 kW	6715.0 kW	3107.0  kW
<b>Z</b> 2	8325.0 kW	5733.5 kW	2541.4 kW
Total	30950.5 kW	22107.5 kW	9991.4 kW

Scenarios at higher  $T_{\rm env}$  could not be simulated due to inconsistencies in the field data gathered for those conditions. However, the operation up to 11°C constitutes 87% of the cumulative heat demand (Figure 4.2), therefore it can be argued that the selected scenarios are representative of the system operation.



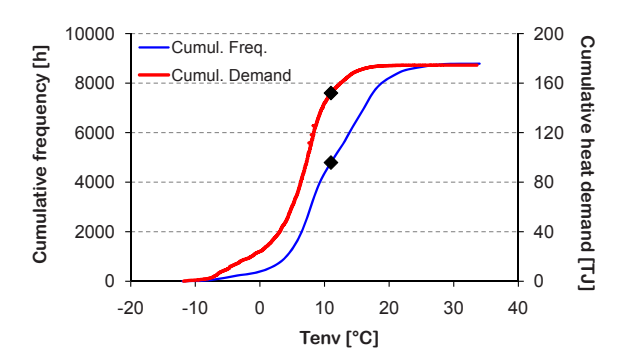


**Figure 4.2.** Frequency of the environment temperatures throughout the year. Left: Frequency of  $T_{env}$  in Delft, 2012.

Right: Cumulative frequency of  $T_{env}$  and cumulative heat demand with respect to  $T_{env}$ , 2012. The demand up to 10+1°C constitutes 87% of the total yearly heat consumption in 2012

## 4.2 Operation conditions

Table 4.2 summarises the main operation parameters of the heating system. These conditions are determined based on the design values, monitoring data provided by FMVG and field measurements. A comprehensive list of the variables used in the simulation is provided in Appendix A to Appendix C.

**Table 4.2.** Operations conditions of the present heating system. Determined from design values, monitoring data and field measurements.

<b>V</b> 7	Scenario				
Variable	-10°C	0°C	10°C		
Primary circuit					
$P_{E}(g)$ [bar]	13	12	11		
$T_{E}$ [°C]	130	104.8	85.3		
Secondary circuits					
P <sub>E</sub> [bar]	3	3	3		
$T_{E}$ [°C]	70	60	50		
$T_L$ [°C]	90	73.3	56.7		
Heat exchangers					
ΔP [bar]	0.5	0.375	0.25		

The values for P are gauge pressures.  $P_{atm} = 1.01325$  bar is added for the model inputs.

#### 4.3 Simulation results

The table below lists the main results of the models for the network and the CHP plant. A comprehensive list is provided in Appendix E.

Vanialda		Scenarios 3-way		Scen	way		
Variable		-10° C	0° C	10° C	-10° C	0° C	10° C
Network	:						
$\phi_{\text{E}}$	[kg/s]	146.9	208.5	231.2	136.6	126.5	68.8
CHP plan	nt						
$T_{E}$	[°C]	79.6	79.4	74.9	75.8	62.8	49.9
$\varphi_{gas}$	[kg/s]	1.004	0.748	0.400	1.014	0.751	0.405
Q	[kW]	31244	22216	10025	31253	22318	10187
$W_{el,pump}$	[kW]	120	208	255	111	104	75
W <sub>el,delivere</sub>	d [kW]	3881	3874	3886	3881	3876	3872
$\phi_{\mathrm{CO2}}$	[kg/s]	2.140	1.597	0.851	2.162	1.599	0.864

**Table 4.3.** Simulation results for the present heating system.

The 3-way system requires higher flow rates of water for partial loads. Implementing a 2-way system can reduce the flow rate by 70% at  $T_{env} = 10$ °C.

Eliminating the water bypass also reduces the pressure drop considerably for the partial loads, which is translated into less energy required for pumping  $(W_{el,pump})$ .

The 2-way valve system also allows for lower return temperatures at partial loads ( $T_E$  at CHP plant), which is necessary for the implementation of geothermal energy. However, even with a 2-way valve system, during high loads the return temperature is too high for geothermal energy harnessing. Temperatures below 60°C are desired to meet the minimum energy purchase required by the geothermal plant in the new system.

In all three scenarios modelled herein, the gas engines can operate at full load (generating the maximum electrical output at almost 3.9 MW). Thus, their gas consumption and heat recovery is the same for every scenario.

## 4.4 Energy balance

The inputs, losses and outputs of the heating system for the simulated scenarios are presented in the energy balance of Table 4.4, constituting hourly operation.

## 4.4.1 Discussion on the energy balance

In all tree scenarios, the 2-way system requires less electricity for pumping than the 3-way system, saving 10 kW at -10°C and 180 kW at 10°C. Those savings in electricity are compensated by a higher gas consumption to meet the heating demand, which results in higher losses in the flue gas. Therefore, within the boundaries of the system, there is no efficiency improvement resulting from the implementation of the 2-way valve system alone.

**Table 4.4.** Energy balance of the present heating system [kW].

D	Tenv = -	-10° C	Tenv =	$Tenv = 0^{\circ} C$		Tenv = $10^{\circ}$ C	
Process	3 way	2 way	3 way	2 way	3 way	2 way	
Gas	42961.6	43334.8	31796.9	31899.6	16802.6	16994.6	
Electricity to pumps	120.2	110.7	207.1	103.0	253.5	73.7	
Supply	43081.8	43445.5	32004.0	32002.6	17056.1	17068.3	
Loss flue gas	7772.3	8135.8	5634.9	5634.9	2831.1	2861.7	
Loss generator	118.7	119.1	126.1	123.6	128.1	128.1	
Loss pumps	20.1	18.8	30.5	18.0	34.6	13.7	
Loss friction at WKC	0.8	0.9	0.8	0.9	0.3	0.3	
Losses CHP plant	7911.9	8274.5	5792.4	5777.3	2994.0	3003.7	
Losses network	264.3	264.7	229.2	239.8	197.1	200.7	
<b>Total losses</b>	8176.3	8539.2	6021.6	6017.1	3191.1	3204.4	
Electricity delivered	3881.3	3880.9	3873.9	3876.4	3871.9	3871.9	
Heat delivered	31024.3	31024.3	22107.5	22107.5	9991.4	9991.4	
Delivered energy	34905.6	34905.3	25981.4	25983.9	13863.2	13863.2	
Statistical difference	-0.1	1.1	1.0	1.7	1.7	0.7	
Overall efficiency	81.0%	80.3%	81.2%	81.2%	81.3%	81.2%	

In a broader sense, the power for pumping comes from the national grid, supplied mainly by fossil fuels with an efficiency of 44% (Taylor et al., 2008). Thus,  $180~\rm kW_e$  for pumping require 409 kW in primary energy for the grid. On the other hand, the heat that replaces the power is produced locally from gas with 59% efficiency (305 kW primary energy), along with power at 23% efficiency (70 kW<sub>e</sub>), saving 159 kW extra of primary energy in the grid. Overall, up to 263 kW of primary energy can be saved, (a reduction of 36%).

The total energy supply at  $T_{env} = -10^{\circ}\text{C}$  is higher in the 2-way system by 400 kW, which can be explained by two reasons: 1) a small increase of heat loss in the pipelines resulting from the lower flow rates (the water has more time to cool down) and 2) the temperature of the return water in the 3-way system (80°C) is higher than the design temperature of the cooling system in the gas engines (78°C), but it still allows their operation at full load. Therefore, the water leaves the engines at a higher temperature than the 2-way system (86°C vs. 82°C), requiring less energy from the boilers. This however, is an exceptional case.

## 4.5 Exergy analysis

The overall exergy balance is shown in Table 4.5 and Figure 4.3. Like the energy balance shows, there is no efficiency improvement from the 3-way to the 2-way valve systems.

It is important to notice that the exergy efficiencies of the system (26-30%) are considerably lower than the energy efficiencies ( $\sim$ 80%). This is due to the fact that the combustion of natural gas takes place at very high temperatures (above 1000°C), i.e. it is an energy source with a very high exergy content. On the other hand, the energy demand happens at low exergy levels.

<b>Table 4.5.</b> Exergy balance of the present heating system
--

¥7 1-1 -	Tenv = -	-10° C	Tenv =	$Tenv = 0^{\circ} C$		10° C
Variable	3 way	2 way	3 way	2 way	3 way	2 way
Gas supply	39776.9	40122.4	29666.3	29762.9	15903.6	16082.8
Air supply	1051.0	1060.5	1066.6	1077.8	1111.2	1111.2
Electricity to pumps	120.2	110.7	207.1	103.0	253.5	73.7
Total supply	40948.0	41293.6	30940.0	30943.8	17268.3	17267.6
Losses CHP plant	27568.4	28033.6	21385.0	21830.4	11288.5	11676.1
% Loss CHP plant	94.5%	94.9%	94.0%	96.0%	93.5%	96.7%
Losses network	1611.9	1492.2	1365.5	921.3	789.1	401.2
% Loss network	5.5%	5.1%	6.0%	4.0%	6.5%	3.3%
Total losses	29180.3	29525.8	22750.5	22751.7	12077.6	12077.3
Heat delivered	7886.6	7886.6	4315.4	4315.4	1318.4	1318.4
Electricity delivered	3881.3	3880.9	3873.9	3876.4	3871.9	3871.9
Total delivered	11767.9	11767.5	8189.3	8191.7	5190.3	5190.3
Statistical difference	-0.2	0.2	0.2	0.3	0.4	0.1
Overall efficiency	28.7%	28.5%	26.5%	26.5%	30.1%	30.1%

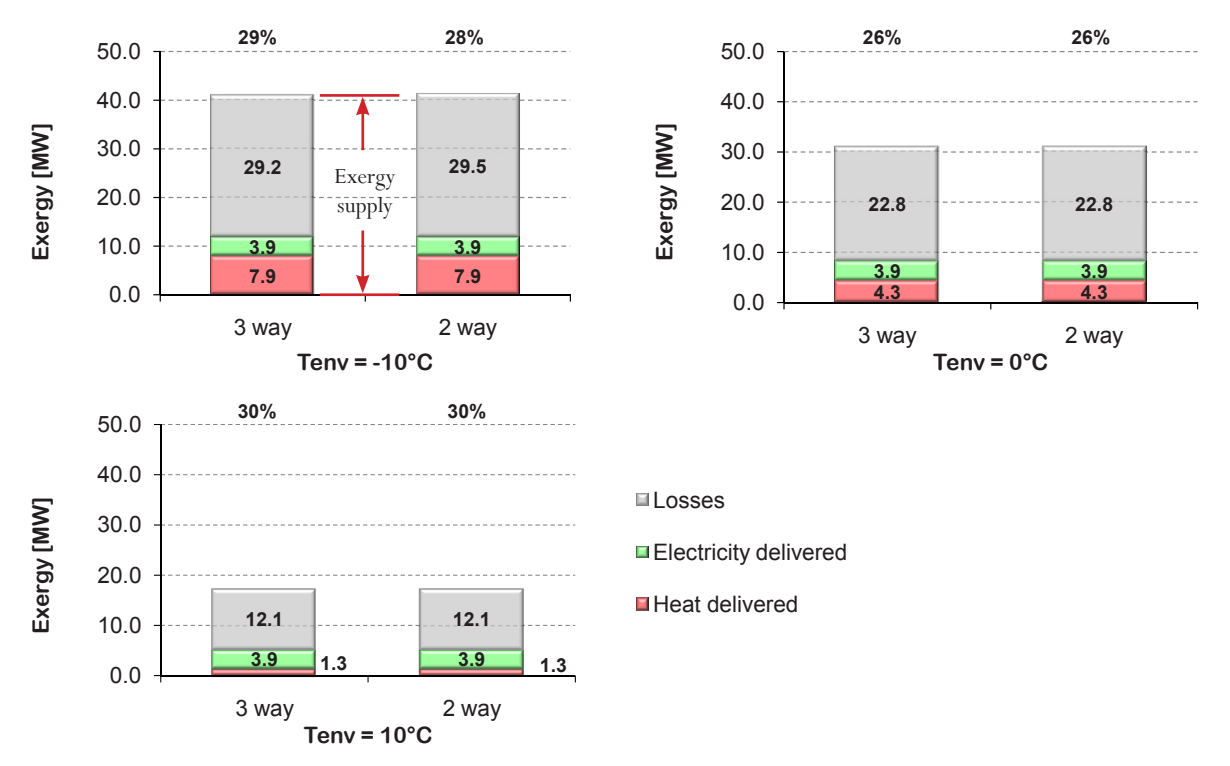


**Figure 4.3.** Overall exergy balance of the present heating system. The height of the columns represents the total exergy supply (gas and electricity). The efficiency shown on top is calculated as <code>exergy delivered/exergy supply</code>.

The energy balance suggests that a slightly higher energy supply is required in the 2-way system due to increased heat losses in the network. However, the exergy analysis reveals that the losses are larger for the 2-way system only in the CHP plant, not in the network. These results are discussed in detail by breaking down the analysis in modules.

#### 4.5.1 Exergy of the heating network

The difference between the 3-way and 2-way valve systems can be clearly appreciated in terms of exergy (Figure 4.4). The height of the columns in the figure represents the total exergy entering the network as hot water. The 2-way system requires less exergy to meet the demand; with respect to the 3-way system, it decreases by 7% at -10°C and by 70% at 10°C.

The difference lies in the exergy content of the water that returns to the CHP plant. In the 2-way system, most of the exergy entering the network is delivered as heat and the water leaves colder than in the 3-way system. This also means that the network in the 2-way system has a higher exergy efficiency, which increases slightly with  $T_{env}$  from 49% at -10°C to 52% at 10°C, as opposed to the 3-way system in which the exergy efficiency decreases from 46% at -10°C to 16% at 10°C.

The losses in the network constitute a small fraction of the exergy processes in it: 9% for the 3-way system, and varying from 9-16% in the 2-way system. The specific losses and their shares are detailed in Table 4.6.

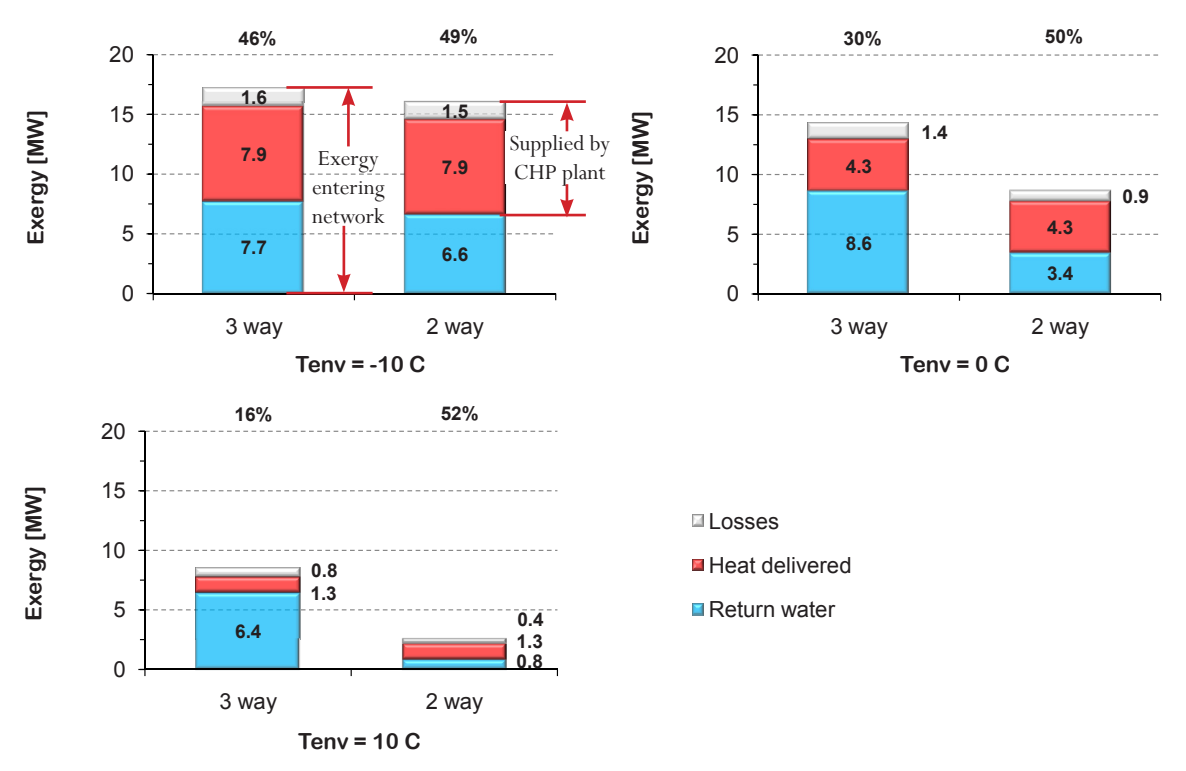


Figure 4.4. Exergy balance of the network in the present heating system.

The height of the columns represents the exergy entering the network.

The top two bars in each column correspond to the exergy supplied by the CHP plant.

The efficiency shown on top is calculated as exergy delivered/exergy input.

## 4.5.1.1 Discussion on the exergy of the network

As mentioned before, the exergy analysis 'contradicts' the energy balance by showing that the 2-way system has lower losses in the network than the 3-way system. Although the energy loss in the pipelines might be higher for the 2-way system, these losses occur at lower water temperatures in the return lines, i.e. the energy lost has a lower quality.

	0,		1	C	, ,		
Losses	$Tenv = -10^{\circ} C$		Tenv =	$Tenv = 0^{\circ} C$		Tenv = $10^{\circ}$ C	
	3 way	2 way	3 way	2 way	3 way	2 way	
Loss HX	1395.5	1395.1	853.9	851.6	368.2	364.8	
Loss mixing pipes	115.8	0.0	398.3	0.0	299.8	0.0	
Loss pipes & acc.	100.6	97.0	113.4	69.7	121.1	36.5	
Losses network	1611.9	1492.2	1365.5	921.3	789.1	401.2	
% Loss HX	87%	93%	63%	92%	47%	91%	
% Loss mixing pipes	7%	0%	29%	0%	38%	0%	
% Loss pipes & acc.	6%	7%	8%	8%	15%	9%	

**Table 4.6.** Exergy losses in the network of the present heating system [kW].

The largest thermodynamic inefficiency prevented by the 2-way system is the exergy destruction due to mixing of streams at different temperatures. In the 3-way system, these losses can be higher than the total heat and friction losses in the network (>100 kW).

The latter improvements in the network from the 2-way system do not imply a better efficiency for the heating system as a whole, but they bring an opportunity for alternative energy sources. A lower exergy content in the return water (colder return temperatures) allows for utilisation of energy sources with low exergy, such as geothermal energy.

The reduction in the exergy content of the return water increases at partial loads. Compared to the 3-way system, it decreases by 14% at  $T_{env} = -10^{\circ}$ C and by 87% at  $T_{env} = 10^{\circ}$ C.

## 4.5.2 Exergy of the CHP plant

The exergy processes occurring in the CHP plant are depicted in Figure 4.5. The exergy supplied to the plant is represented by the columns starting at the exergy level of the return water.

The main difference between the 2-way and 3-way systems lies in the exergy delivered to the network, represented by the sum of the return water and the heat added to it. As previously discussed, this exergy is smaller for the 2-way system due to the lower exergy content of the return water.

The exergy losses in the CHP plant are listed in Table 4.7. These losses are much higher than the ones in the network mainly due to the exergy lost in the combustion process, which takes place at very high temperatures ( $\sim 1500$ °C). In other words, the energy lost in these conditions has a very high quality.

Most of the exergy supplied to the power plant is lost, 65-69% in the 3-way system and 68-70% in the 2 way system. In all three scenarios the losses are bigger for the 2-way system and its efficiency is lower.

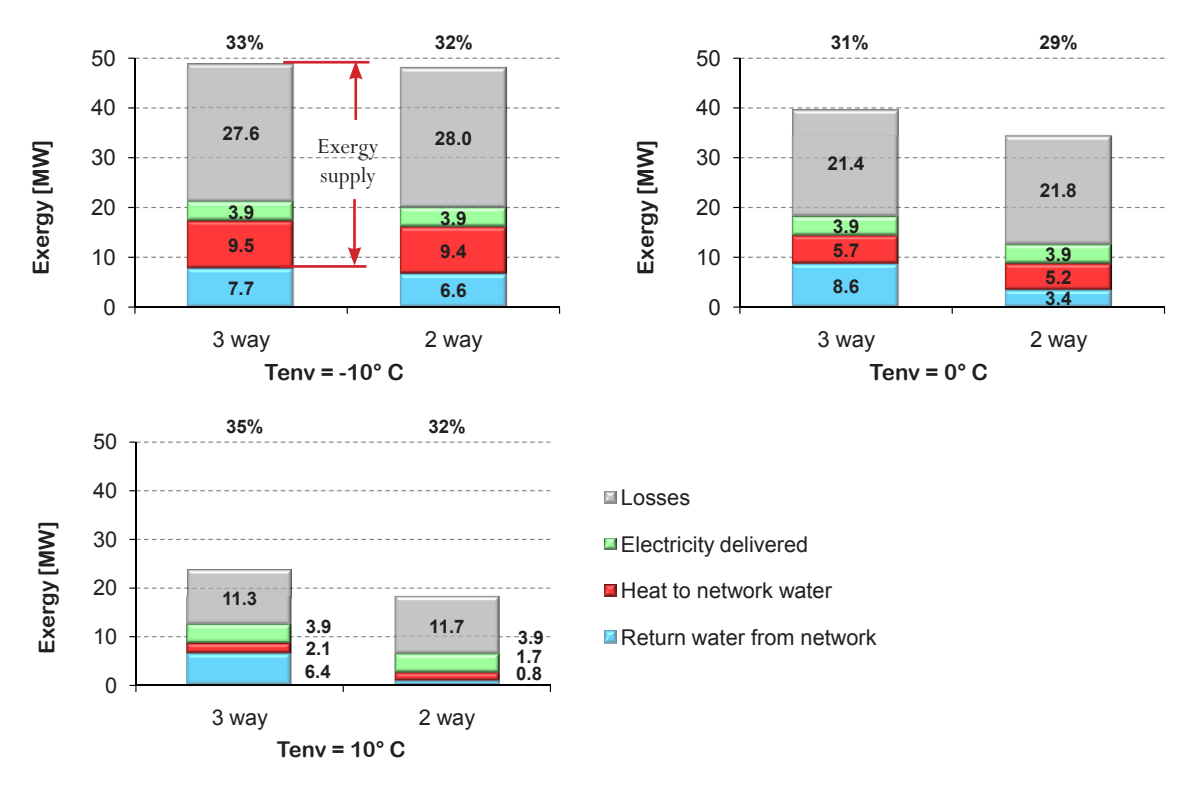


Figure 4.5. Exergy balance of the CHP plant in the present heating system. The three top bars in each column correspond to the total exergy supply (gas and electricity).

The bottom two bars constitute the exergy fed to the network.

The efficiency shown on top is calculated as exergy of heat transferred/exergy supply.

**Table 4.7.** Exergy losses in the CHP plant of the present heating system [kW]. The 2-way system helps to prevent losses due to pumping but it presents higher losses due to heat transfer in heat exchangers and mixing vessels.

T	Tenv = 0	-10° C	Tenv =	0° C	Tenv =	10° C
Losses	3 way	2 way	3 way	2 way	3 way	2 way
Loss combustion	12095.7	12189.6	9644.9	9669.3	5728.4	5785.0
Loss HX	11011.2	11136.7	8838.4	8893.7	4392.5	4465.0
Loss mixing vessels	2471.0	2580.9	1566.4	1967.4	541.5	858.2
Loss flue gas	1957.7	2096.4	1269.3	1269.1	540.1	546.7
Loss pumps	29.8	27.6	49.4	26.9	60.1	20.4
Loss mix pipes	3.1	2.3	16.6	4.1	25.9	0.7
Losses CHP plant	27568.4	28033.6	21385.0	21830.4	11288.5	11676.1
% loss combustion	43.9%	43.5%	45.1%	44.3%	50.7%	49.5%
% loss HX	39.9%	39.7%	41.3%	40.7%	38.9%	38.2%
% loss mixing vessels	9.0%	9.2%	7.3%	9.0%	4.8%	7.4%
% loss flue gas	7.1%	7.5%	5.9%	5.8%	4.8%	4.7%
% loss pumps	0.1%	0.1%	0.2%	0.1%	0.5%	0.2%
% loss mix in pipes	0.0%	0.0%	0.1%	0.0%	0.2%	0.0%

## 4.5.2.1 Discussion on the exergy of the CHP plant

Implementing a 2-way system results in lower electricity consumption for pumping, and thus in lesser exergy losses associated to it. This however, is a very small improvement when compared to the magnitude of the other losses. In all the simulated scenarios, pump losses are less than 1% of the total losses in the plant.

Since the water returning from the network in the 2-way system is colder, the gas engines preheat it to a lower temperature than in the 3-way system. The remainder heating is covered by the boilers. A larger energy transfer process occurs in the boilers, which results in a higher exergy destruction for the scenarios at  $-10^{\circ}$ C and  $0^{\circ}$ C.

For the same reason, the exergy destruction happening in the mixing vessel of the boilers is higher for the 2-way system by 110-400~kW. This is the specific thermodynamic inefficiency that causes a slightly higher energy and exergy supply in the 2-way system.

## 4.6 Conclusions for the present heating system

Implementing a 2-way valve system can decrease the electricity consumption for pumping, specially at partial loads. Up to 180 kW can be saved at  $T_{env} = 10^{\circ}$ C. This energy is substituted by heat, and therefore the efficiency of the system does not improve.

However, seen from a broader context, the pumping power is supplied by a 44% efficient grid in The Netherlands (409 kW primary energy) and is substituted by gas in the local plant. Overall, the primary energy consumption can decrease by 36%.

A slightly higher energy supply is required in the 2-way system. The exergy analysis allows to identify the specific process where the main thermodynamic inefficiency occurs, namely the mixing vessel of the boilers, which constitutes an intermediate heat transfer process. The exergy destruction due to this mixing is higher in the 2-way system by up to 400 kW. Therefore, the control strategy applied to the 2-way system must pay special attention to this process.

The main exergy losses occur in the CHP plant, constituting 94-97% of the total exergy supply in both systems. The highest share are the combustion losses, ranging from 12.2 MW at  $-10^{\circ}$ C to 5.8 MW at  $10^{\circ}$ C, representing 43-51% of the losses in the plant.

The 2-way system decreases the amount of hot water required and it is used with less thermodynamic inefficiencies. The main loss prevented is the exergy destruction due to mixing, which can be higher than the friction and heat losses in the pipes when operating with 3-way valves ( $\geq$ 100 kW).

The return water in the 2-way system has a lower temperature (50°C at  $T_{env} = 10$ °C), presenting an opportunity for utilisation of energy sources with a lower exergy content. Such is the case of geothermal energy.

However, the return temperature at  $T_{env} = -10^{\circ}\text{C}$  and  $0^{\circ}\text{C}$  (76 and  $63^{\circ}\text{C}$ ) is still too high to match the conditions expected from the geothermal plant (T<50°C are preferred). Lower temperatures of operation are thus required. New operation conditions are defined in the next chapter.

## **NEW HEATING SYSTEM**

This chapter presents an exergy analysis of possible configurations for the new heating system in TU Delft. The same hourly load scenarios evaluated in the previous chapter are modelled here ( $T_{env} = -10^{\circ}\text{C}$ ,  $0^{\circ}\text{C}$  and  $10^{\circ}\text{C}$ ).

The buildings in the campus will be renovated in order to make them suitable for medium temperature heating. But, due to financial limitations, it is only possible to renovate some of the buildings. Thus, a cascade system that includes high temperature (HT) and medium temperature (MT) consumers will be a transition step towards a full MT heating system.

Three possible network configurations with geothermal energy are studied:

- 1) Present parallel configuration with new operation conditions (**New HT**).
- 2) Renovating several small buildings for a cascade configuration (MTs).
- Renovating 4 big buildings for a cascade configuration (**MTb**), namely part of Electrical Engineering (EWI), and Civil Engineering (CiTG), as well as Architecture (BK) and Applied Sciences (TNW).

The cascade configurations sometimes require new MT consumers. This can be interpreted as a potential to provide heat to new buildings. But it is also a constraint for the new configurations, that would rely on the availability of these additional connections.

At the end of this chapter, one configuration is selected and compared with the present system.

#### 5.1 New infrastructure

The new system requires additional infrastructure, which is accounted for as exergy costs added to the exergy supply. New components are mainly required in two modules: the network and the geothermal plant.

#### 5.1.1 Network

New heat exchangers and additions to the distribution pipelines are required. The exergy cost of new accessories is neglected.

The new pipe segments with stone wool insulation are required to connect the consumers in a cascade system configuration, while preventing mixing of streams at different temperatures.

The heat exchangers existing in campus today cannot operate under the design conditions for MT consumers. A preliminary design of new heat exchangers is performed based on the Kern method and the following criteria:

- Sizing to 200% of the peak demand. Although the cost for oversized equipment is higher, it allows for a future increase in the demand and for operation in a low temperature (LT) system.
- Sizing for operation conditions at  $35/75^{\circ}$ C in the primary circuit and  $80/40^{\circ}$ C in the secondary circuit. These conditions include a margin in case of a heat deficit when operating on peak conditions ( $35/65^{\circ}$ C and  $70/40^{\circ}$ C).
- Maximum length  $L \le 3$  m. This limit is based on the space available in some of the rooms in the system.
- Heat exchangers in a room connected in parallel to prevent increasing the pressure drop and to facilitate maintenance (as opposed to a connection in series)

The design yields results on the sizes of pipes and shells, which allows for an estimation of the total exergy cost. However, there are two main limitations in the method used:

- A single set of parameters was used for all the heat exchangers in the system. Better
  performances can be achieved with specific design parameters for each heat exchanger,
  which may result in higher or lower individual exergy costs.
- The velocities are kept below 1 m/s to prevent erosion, but due to the generalised design method, velocities can be as low as 0.05 m/s, which may cause fouling problems.

Therefore, it is important to point out that the results of the heat exchangers design are not meant for its implementation, but only to estimate the exergy costs.

The exergy of the new infrastructure required for the network is summarised in the table below. Additional infrastructure is not required for the configuration New HT.

Further details on the heat exchanger design and the exergy calculations can be found in Appendix F.

**Table 5.1.** Exergy costs of the new infrastructure required in the network. Includes the cost of steel heat exchangers, steel pipe segments and their stone wool insulation.

Exergy cost	Heat exchangers [GJ]	Pipes [GJ]	Insulation [GJ]	Total [GJ]	Hourly cost [kW]
MTs	21660	679	58	22397	23.6
MTb	23974	823	81	24878	26.2

The hourly cost is calculated based on a 30 year lifetime and 8784 h for 2012.

## 5.1.2 Geothermal plant

The exergy cost of the geothermal plant is calculated for the wells, heat exchangers and insulated pipelines. Costs for the pumps, valves and accessories are neglected.

De Mooij (2010) estimates an exergy cost of 47,837 GJ for the construction of the geothermal doublet (production and injection wells). This cost includes the exergy used for drilling the boreholes and for the production of steel and concrete.

For the pipelines, steel pipe schedule 40 with D=250~mm is considered, which transports the network water from the CHP plant to and in the geothermal plant. Supply and return lines are added, for an assumed total of 1000 m.

A preliminary design for the heat exchangers is performed based on the Kern method and the following design criteria:

- Sizing to 150% of the maximum heat transfer for 150 m<sup>3</sup>/h at 75.7/45.7° C (production/reinjection). A total of 7.65 MW.
- Heat exchangers connected in parallel.
- Length smaller or equal to 6 m ( $L \le 6$  m).

The result is a total of 8 heat exchangers of 956.25 kW each, with L = 6 m.

The costs of the infrastructure for the plant are listed in the table below. They are the same for the three proposed configurations. Further details on these calculations are provided in Appendix G.

**Table 5.2.** Exergy costs for the infrastructure of the geothermal plant. Includes cost of the geothermal wells, steel heat exchangers and insulated pipelines.

Exergy cost	Wells [GJ]	Heat exchangers [GJ]	Pipes [GJ]	Insulation [GJ]	Total [GJ]	Hourly cost [kW]
Geothermal plant	47,837	7,869	3,473	405	59,584	62.8

The hourly cost is calculated based on a 30 year lifetime and 8784 h for 2012.

## 5.2 Network configurations

For the configuration **New HT**, no renovations take place in the network. All the consumers are HT and connected in parallel. Only the operation conditions differ from the present network.

In configurations MTs and MTb, the network undergoes renovations. HT-MT consumers are connected in series. A simplified scheme of the cascade system is shown in Figure 5.1. With the existing infrastructure, sometimes it is not possible to connect the outlet of a HT building to a MT consumer. This results in mixing of streams at different temperatures (exergy destruction). Furthermore, the outlet of HT buildings may carry an excess or deficit of energy to supply a MT consumer, particularly at partial loads; a bypass is proposed in this study for such cases, which also results in exergy destruction. Details on the network configurations devised in this study for each block are provided in Appendix H.

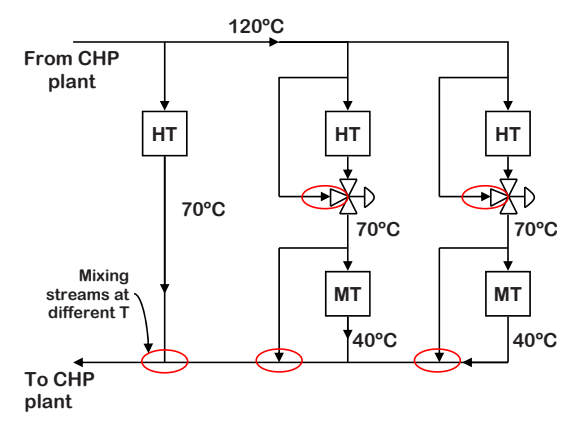


**Figure 5.1.** General scheme of the cascade configuration for one block in the network. 3-way valve bypasses are suggested to compensate energy mismatch between HT and MT consumers. Some HT buildings cannot be connected in series with the existing infrastructure.

## 5.3 Operation conditions

As mentioned in the previous section, under partial loads, the outlet of HT consumers may not carry enough energy for the MT consumers. Two possible solutions are considered:

- 1) Increase the temperature supplied to the HT consumers.
- 2) Increase the water flow rate and operate the HT consumers of a cascade element in a 3-way valve system configuration.

In terms of energy, there is no difference between the suggested solutions; both require roughly the same extra consumption of gas. However, if the exergy is accounted for, it is preferred to increase the flow rate than increasing the temperature.

The latter can be explained by the heat transfer term of the exergy balance (Eq. 2.1), Ex =  $Q(1-T_0/T)$ . For the same heat transfer, a higher temperature T means that a higher exergy supply is required. Furthermore, increasing the temperature of all the circulating water to satisfy the deficit of specific consumers, implies exergy inefficiencies.

However, increasing the flow rate over a certain limit may result in damages on the network infrastructure due to erosion. A velocity limit of 2 m/s is generalised for the network pipelines.

Taking into account the aforementioned constrains, the operation parameters shown below are selected.

W:-1-1-	Н	Consum	ers	MT consumers			
Variable	-10° C	0° C	10° C	-10° C	0° C	10° C	
Primary circuit							
$P_{E}(g)[bar]$	13	12	11	12	11.5	11	
$T_{E}$ [°C]	130	104.8	85.3	120	95.2	87	
Secondary circuits							
$P_{E}(g)[bar]$	3	3	3	3	3	3	
$T_{E}$ [°C]	70	60	50	35	37	39	
$T_L$ [°C]	90	73.3	56.7	65	63	61	
Heat exchangers							
ΔP [bar]	0.5	0.375	0.25	0.5	0.375	0.25	

**Table 5.3.** Operations conditions of the new heating system.

The values for *P* are gauge pressures.  $P_{atm} = 1.01325$  bar is added for the model inputs.

As mentioned in Section 3.4, the model of the geothermal plant aims at maximising the energy utilisation from it. Thus, the production of geothermal fluid and its properties are considered constant throughout the year. The reinjection pressure is assumed at 30 bar to allow for a pressure drop of 25 bar in the subsoil and 1 bar in the pipes and heat exchangers at the surface of the plant (Table 5.4).

A comprehensive list of the assumptions and input variables in the models is provided in Appendix A to Appendix C.

**Table 5.4.** Operation conditions of the geothermal plant.

	φ [kg/s]		ΔP HX [bar]	P <sub>INJ,2</sub> [bar]	T <sub>E,2</sub> [°C]	T <sub>L,1</sub> [°C]
Operation conditions	150	5	1	30	75.7	70

The values of *P* are absolute pressure.

Fluids 1 and 2 (in the subscripts) refer to the primary and secondary side of the heat exchangers. The fluid in the primary side receives heat. The fluid in the secondary side provides heat.

#### 5.4 Simulation results

The main results of the simulations for the three proposed configurations are listed in Table 5.5.

In the previous chapter, it was shown that the implementation of a 2-way valve system decreases the required flow rate with increasing  $T_{env}$ ; however, the operation conditions of New HT require a constant flow rate up to 0°C.

Due to the addition and cancellation of buildings, there are slight differences in the demand between each configuration. Therefore, in the energy and exergy balances it is important to give special attention to the efficiencies.

The MTs configuration presents an advantage on geothermal energy utilisation, with a heat transfer *Q* close to or higher than 5 MW in all three scenarios. Furthermore, the outlet of the geothermal plant can meet the demand of block N2, constituted entirely by MT consumers in this configuration.

The MTb configuration covers a higher demand with lower flow rates. However, this advantage over the other configurations decreases at low partial loads ( $T_{env} = 10^{\circ}$ C)

**Table 5.5.** Simulation results for the new heating system.

Variable	Ter	nv = -10	°C	Te	$env = 0^{\circ}$	С	Te	$nv = 10^{\circ}$	C
Variable	NHT	MTs	MTb	N HT	MTs	MTb	N HT	MTs	MTb
Network		,							
Q delivered [kW]	30950	29435	31258	22108	20989	22334	9991	9453	10079
φ <sub>E</sub> total [kg/s]	136.6	120.8	104.3	138.6	122.0	117.7	60.1	57.3	95.3
Geothermal plant									
$T_{E}$ [°C]	65.8	40.8	40.1	56.9	44.8	40.7	46.6	47.1	58.7
φ <sub>E</sub> [kg/s]	96.0	47.8	47.6	58.5	49.3	47.8	50.1	50.3	61.3
Q [kW]	1666	5820	5932	3186	5179	5836	4891	4815	2895
$\phi_L$ to N2 [kg/s]	0.0	29.3	0.0	0.0	23.9	0.0	0.0	0.0	0.0
CHP plant									
$T_{E}$ [°C]	68.8	58.3	61.8	62.4	56.5	61.8	66.1	67.2	68.6
$\phi_{gas} [kg/s]$	0.958	0.796	0.847	0.656	0.568	0.583	0.267	0.253	0.325
Q [kW]	29443	23718	25512	19025	15898	16464	5248	4742	7334
W <sub>el,in</sub> [kW]	114	146	124	111	124	105	79	82	97
$\phi_{\text{CO2}} [\text{kg/s}]$	2.038	1.693	1.804	1.397	1.209	1.241	0.568	0.536	0.692

## 5.5 Energy balance

The energy inputs, losses and outputs of the proposed configurations for the new heating system are listed in the energy balance of Table 5.6 (hourly operation). The costs of new infrastructure are not included. The power required for reinjection at the geothermal plant is not included in the balance because it is the same for all three configurations.

D.	Ten	$v = -10^{\circ}$	C	Te	$nv = 0^{\circ}$	С	Ter	$nv = 10^{\circ}$	C
Process	N HT	MTs	MTb	N HT	MTs	MTb	N HT	MTs	MTb
Gas supply	40936	33964	36131	27821	24063	24893	11102	10500	13573
Geothermal heat	1666	5820	5932	3186	5179	5836	4891	4815	2895
Electricity to pumps	174	161	134	149	139	121	92	98	108
Total supply	42776	39945	42197	31156	29382	30866	16084	15412	16576
Losses CHP plant	7680	6443	6835	4992	4363	4477	2020	1955	2438
Losses network	242	173	217	169	141	166	159	131	167
Losses geo. plant	15	7	10	9	8	9	10	8	19
Losses	7937	6624	7062	5170	4512	4652	2189	2094	2624
Heat delivered	30950	29435	31258	22108	20989	22334	9991	9453	10079
Electricity delivered	3881	3881	3881	3876	3876	3876	3895	3872	3872
Delivered energy	34831	33316	35139	25984	24865	26210	13887	13325	13951
Statistical difference	7.0	5.1	-3.7	2.0	4.8	-11.0	8.8	-6.5	0.8
Overall efficiency	81.4%	83.4%	83.3%	83.4%	84.6%	84.9%	86.3%	86.5%	84.2%

Table 5.6. Energy balance of the proposed configurations for the new heating system [kW].

## 5.5.1 Discussion on the energy balance

Slight improvements in the energy efficiency can be appreciated with cascade systems (1-2%). However, the efficiency of the MTb configuration falls behind the others at  $T_{env} = 10^{\circ}$ C. The causes are identified next in the exergy analysis of each module.

The statistical difference is larger than in the analysis of the present heating system. This figure is the total difference in the balance due to rounding of partial results, unit conversion and other possible errors. An error analysis of the models is provided in Appendix I.

## 5.5.2 Geothermal energy utilisation

The geothermal plant fixes a minimum delivery of 70,000 GJ/yr. Assuming an even distribution throughout the year, (8784 h in 2012), a minimum hourly geothermal utilisation of 2214 kW must be met.

The MTs configuration surpasses this minimum by a factor larger than 2x in all three scenarios. The amount of hours with  $T_{env}$  up to  $10^{\circ}$ C ( $+1^{\circ}$ C) constitute 54% of the total in 2012. Thus, during half of the year, this configuration may use twice the minimum of geothermal energy. Therefore, based on year 2012, it is possible to argue that the MTs configuration is able to meet the requirement of the geothermal plant.

The latter cannot be said from configurations New HT and MTb. Nonetheless, a dynamic model of the system is needed to prove with certainty whether the yearly minimum of 70,000 GJ is covered.

#### 5.6 Exergy analysis

The main processes involved in the exergy of the proposed configurations are shown in the balance of Table 5.7.

The exergy costs of new infrastructure constitute less than 1% of the total exergy supply to the system.

The higher losses take place in the CHP plant. The introduction of the geothermal plant does not cause large losses in the system; however the numbers do not include the pressure drop in the subsurface.

Before providing an exergy analysis of the system as a whole, it is necessary to separate the system by modules, showing their individual costs, inputs and outputs.

	Ten	$v = -10^{\circ}$	C	Te	$nv = 0^{\circ}$	~	Тот	$nv = 10^{\circ}$	
Process	N HT	MTs	MTb	N HT	MTs	MTb	N HT	MTs	MTb
Gas supply	37912	31488	33503	25984	22502	23157	10586	10023	12891
Air supply	1059	1056	1057	1078	1078	1078	1134	1113	1112
Geothermal supply	394	1203	1221	624	938	1028	752	743	489
Electricity to pumps	174	161	134	149	139	121	92	98	108
Infrastructure	63	86	89	63	86	89	63	86	89
Total supply	39603	33994	36005	27898	24743	25473	12626	12062	14689
Losses CHP plant	26839	22328	23764	19018	16351	16771	6897	6426	8790
% Loss CHP plant	94.1%	94.1%	93.4%	94.8%	94.6%	94.0%	92.0%	91.4%	91.8%
Losses network	1555	1205	1557	889	751	938	461	459	644
% Loss Network	5.5%	5.1%	6.1%	4.4%	4.3%	5.3%	6.2%	6.5%	6.7%
Loss geo plant	130	188	131	153	178	141	139	142	141
% Loss geo plant	0.5%	0.8%	0.5%	0.8%	1.0%	0.8%	1.9%	2.0%	1.5%
<b>Total losses</b>	28525	23721	25452	20060	17280	17851	7498	7027	9575
Heat to buildings	7195	6389	6657	3960	3587	3765	1228	1163	1240
Electricity to grid	3881	3881	3881	3876	3876	3876	3895	3872	3872
Total delivered	11076	10270	10538	7837	7463	7642	5124	5035	5112
Statistical difference	2.4	3.6	14.3	1.2	0.7	-19.2	4.5	0.3	1.6

**Table 5.7.** Exergy balance of the proposed configurations for the new heating system [kW]

#### 5.6.1 Exergy of the heating network

The efficiency in the utilisation of heating water is depicted in Figure 5.2. The losses and their contribution to the total are listed in Table 5.8.

As the demand decreases (increasing  $T_{env}$ ), the exergy required by the New HT configuration decreases considerably. Due to the 2-way valves, the hot water transfers more of its energy to the buildings and it returns to the CHP plant with a lower exergy content.

The cascade configuration MTs represents an improvement in the efficiency of the network over the parallel system New HT, particularly during high loads, where the efficiency is 5 to 9% larger. Renovating the big buildings (MTb) constitutes an even better improvement during high demands. However, its efficiency largely decreases at low partial loads, from 62% at -10°C to 34% at 10°C.

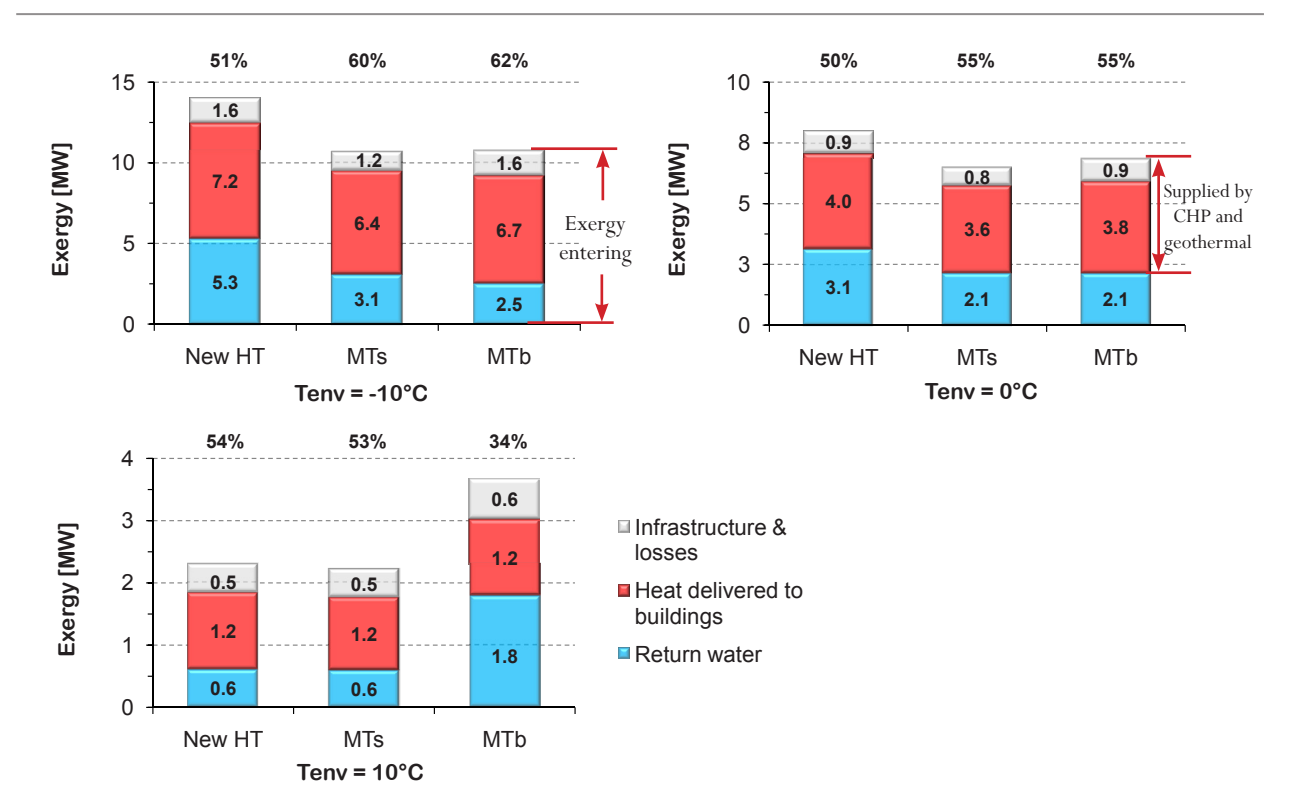


**Figure 5.2.** Exergy balance of the network in the proposed configurations of the new heating system. The height of the columns represent the total amount of exergy entering the distribution network. The top two bars (red and grey) correspond to the exergy supplied by the CHP and geothermal plants, including the cost of new infrastructure.

**Table 5.8.** Exergy losses in the network of the proposed configurations for the new system [kW]. The costs for the new infrastructure are included as losses.

T	Tei	$nv = -10^{\circ}$	°C	Te	$env = 0^{\circ}$	C	Te	$nv = 10^{\circ}$	C
Losses	N HT	MTs	MTb	N HT	MTs	MTb	N HT	MTs	MTb
Loss HX	1469	1040	1170	832	591	619	430	309	329
Loss pipes	83	56	69	53	41	48	30	25	39
Loss mixing pipes	3	85	291	4	95	245	0	102	250
Loss infrastructure	0	24	26	0	24	26	0	24	26
Losses network	1555	1205	1557	889	751	938	461	459	644
% Loss HX	94%	86%	75%	94%	79%	66%	93%	67%	51%
% Loss pipes	5%	5%	4%	6%	5%	5%	7%	5%	6%
% Loss mixing pipes	0%	7%	19%	0%	13%	26%	0%	22%	39%
% Loss infrastructure	0%	2%	2%	0%	3%	3%	0%	5%	4%

#### 5.6.1.1 Discussion on the exergy of the network

Compared to the system in parallel, a cascade system can decrease the required exergy supply by 24% during high demands. This is due to the fact that part of the water leaving the HT buildings feeds the MT consumers without needing additional hot water pumped from the CHP plant.

Although small, the exergy of new infrastructure is comparable to the losses in the pipes (2-5% of the losses), a magnitude that can help deciding between configurations.

Under partial loads, this benefit is less significant. The MTs configuration requires 5% less flow than the New HT configuration at  $T_{env} = 10$ °C. And the MTb configuration uses an exergy supply higher than the parallel system by 59%.

The latter inefficiencies can be explained as follows: In a 2-way system at partial loads, the water leaves the HT buildings at temperatures as low as 45°C. The MT buildings require temperatures above 55°C to operate at these conditions. Therefore, a bypass is necessary to reheat the outlet of the HT consumers with hot water from the CHP plant. The proposed solution in this study is to keep the 3-way valves in the HT buildings for that purpose (against the renovation guidelines). The result is a higher exergy losses due to mixing in the cascade systems.

When an MT consumer has a demand much higher than the preceding HT building, even the water corresponding to a 3-way system is not enough for its demand, and a large bypass is necessary. This is the case of several connections in the MTb configuration. As a result, the water leaving the HT buildings is reheated at temperatures above  $70^{\circ}$ C, and it leaves the MT buildings hotter than in a parallel 2-way system (47°C vs. 39°C). Additionally, since it is preferred to pump more water than to increase the supply temperature, excess water is supplied to the network and bypassed also at the MT consumers, resulting in return temperatures as high as  $76^{\circ}$ C. This is shown graphically as the high exergy content of the return water in the MTb configuration at  $T_{env} = 10^{\circ}$ C.

Although the MTs configuration does not have the higher efficiencies in all scenarios, its performance is not negatively affected with a change in demand under the conditions evaluated.

#### 5.6.2 Exergy of the geothermal plant

The exergy flows in the geothermal plant are depicted in Figure 5.3. In this particular case, the exergy costs are lower than the exergy obtained in the form of hot geothermal fluid. These costs are shown as negative values in the columns. The losses in the plant and their shares in the total are detailed in Table 5.9.

#### 5.6.2.1 Discussion on the exergy of the geothermal plant

The graphs show that the exergy costs of the geothermal plant are low when compared to the total circulating exergy (negative section vs. positive section of the columns), ranging from 12 to 23%. However, an important share of the electricity supply is lost as mechanical exergy in the reinjection, required to overcome the pressure losses in the wells and the reservoir. The reinjection constitutes ca. 35% of the total exergy in the plant when the geothermal consumption is close to 5 MW, and it increases up to 75% when the geothermal consumption is lower.

The parallel system (New HT) extracts a small amount of geothermal exergy during high heat demand (387 kW at  $T_{env} = -10^{\circ}$ C), due to the relatively high return temperature from the network (66°C). The performance of this configuration improves at partial loads, from 20% to 60% efficiency, when the return temperature decreases to 47°C due to the 2-way valves.

The MTb configuration behaves in the opposite way, utilising more geothermal exergy during high heat demand (1.16 MW at  $T_{env} = -10^{\circ}$ C), and decreasing its efficiency from 60 to 30% at low partial loads. This is also due to the high return temperatures (66°C) that occur due to the bypass explained in the previous section (exergy of the network).

The MTs configuration does not have the best performance at each condition, but it maintains good geothermal exergy utilisation in all three scenarios (55-60% of the exergy in the plant). As mentioned in the energy balance, it is possible to argue that this configuration meets the minimum utilisation of 70,000 GJ/yr (energy) required by the geothermal plant.

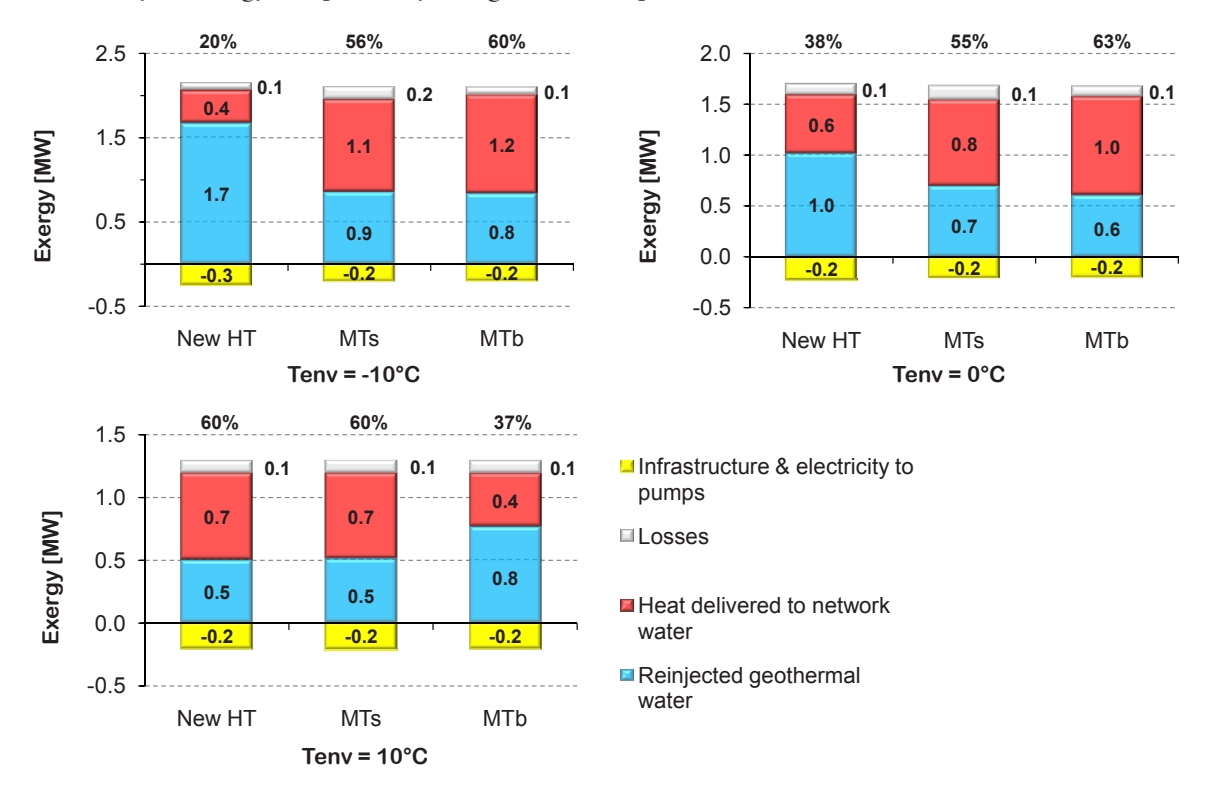


Figure 5.3. Exergy balance of the geothermal plant in the proposed configurations of the new heating system. The bottom negative bars (yellow) correspond to the exergy cost and supply of the plant. The positive side of the columns represent the total exergy flowing in the plant (geothermal and network water). The efficiency shown on top of the columns is calculated as <code>exergy</code> of heat transferred/exergy flowing in the plant.

**Table 5.9.** Exergy losses in geothermal plant of the configurations for the new system [kW]. The pressure losses in the reservoir are treated as the exergy of the reinjection water.

7	Teı	nv = -10	° C	Te	$e_{nv} = 0^{\circ}$	C	Te	$nv = 10^{\circ}$	, C
Losses	N HT	MTs	MTb	N HT	MTs	MTb	N HT	MTs	MTb
Loss pumps	13	4	3	9	4	3	3	4	3
Loss HX	21	51	52	30	46	53	45	44	29
Loss pipes	29	6	4	19	6	3	4	6	4
Loss mix	4	65	10	33	60	19	24	25	42
Loss infrastructure	63	63	63	63	63	63	63	63	63
Losses geo. plant	130	188	131	153	178	141	139	142	141
% Loss pumps	10%	2%	2%	6%	2%	2%	2%	3%	2%
% Loss HX	16%	27%	40%	19%	26%	37%	32%	31%	20%
% Loss pipes	22%	3%	3%	12%	3%	2%	3%	4%	3%
% Loss mix	3%	35%	8%	22%	34%	14%	18%	18%	30%
% Loss infrastructure	48%	33%	48%	41%	35%	44%	45%	44%	45%

#### 5.6.3 Exergy of the CHP plant

The exergy flows in the CHP plant are shown in Figure 5.4. There are no large differences in the efficiencies of the three proposed configurations. The losses in the plant are broken down in Table 5.10.

## 5.6.3.1 Discussion on the exergy of the CHP plant

In the cascade configurations at  $T_{env} = -10^{\circ}\text{C}$  and  $0^{\circ}\text{C}$ , a lower amount of exergy is transferred from the CHP plant to the working fluid, due to the lower requirements in the network and to the larger contribution of geothermal energy. A reduction of 9-13% can be accomplished with the cascade systems (in kW of exergy transferred to the water per kW of exergy delivered to the buildings).

However, at  $T_{env} = 10^{\circ}$ C, the efficiency of the MTb configuration drops. The cause is located at the mixing vessels (namely, the one from the boilers), which can be explained as follows: although the water enters the plant at the same temperature as the other configurations (ca. 68°C), the MTb configuration presents a higher flow rate; the gas engines preheat the water at a temperature lower than in the other two configurations (77°C vs. 82°C). Thus, a higher heat transfer from the boilers is required, which results in exergy destruction in the mixing vessel of those units.

The MTs configuration presents a slight improvement in efficiency with respect to the parallel New HT configuration. Both configurations maintain their performance under the evaluated  $T_{env}$ .

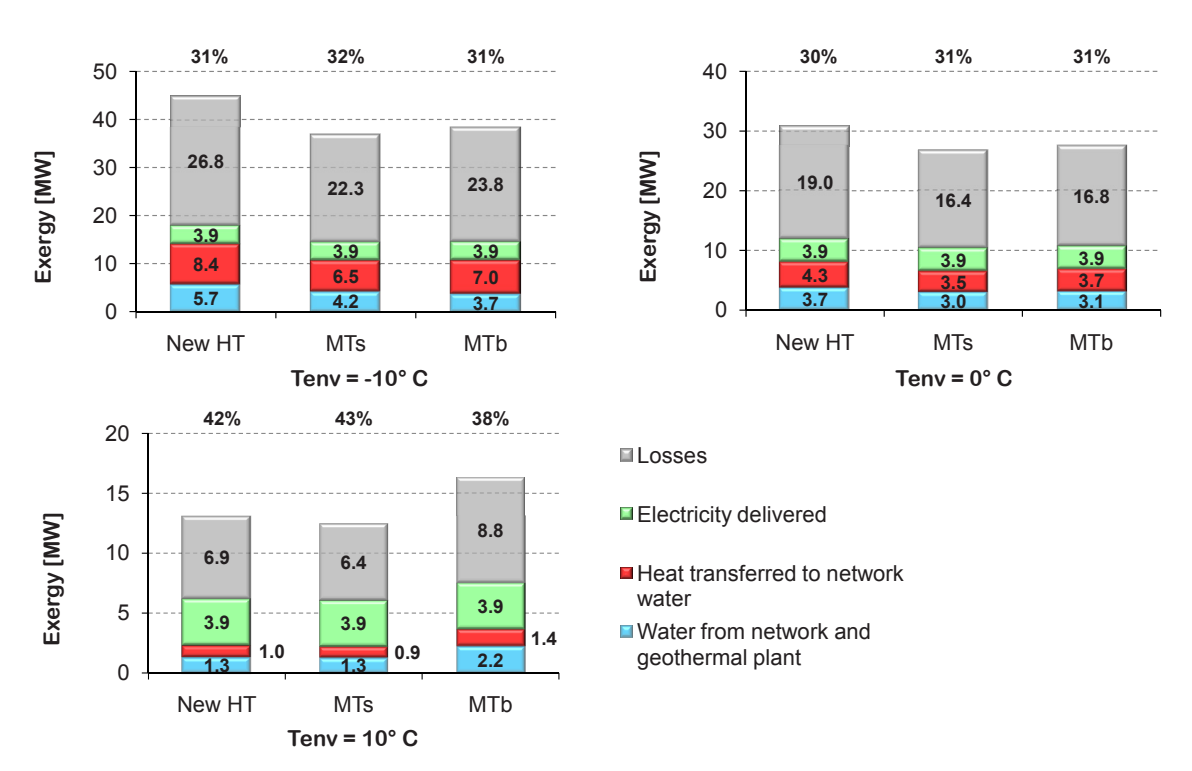


Figure 5.4. Exergy balance of the CHP plant in the proposed configurations of the new system.

The height of the columns represents the total exergy flowing in the plant.

The top three bars correspond to the exergy supply to the plant (gas and electricity).

The exergy delivered by the plant is constituted by the heat transferred to the network and the electricity produced (red and green bars)

The efficiency shown on top is calculated as exergy delivered/exergy supply.

% Loss mix

% Loss pumps

T	Ten	$v = -10^{\circ}$	C	Te	nv = 0°	С	Ter	$n_{\rm V} = 10^{\circ}$	C
Losses	N HT	MTs	MTb	N HT	MTs	MTb	N HT	MTs	MTb
Loss combustion	11556	9712	10291	8530	7480	7670	4050	3872	4777
Loss HX	10806	8692	9351	7792	6497	6731	2286	2050	3249
Loss mixing vessels	2532	2265	2357	1596	1413	1370	202	162	314
Loss flue gas	1919	1592	1695	1072	924	951	340	320	422
Loss mix	0	32	38	0	6	18	0	0	2
Loss pumps	27	36	32	28	31	32	20	22	26
Losses CHP plant	26839	22328	23764	19018	16351	16771	6897	6426	8790
% Loss combustion	43.1%	43.5%	43.3%	44.9%	45.7%	45.7%	58.7%	60.3%	54.3%
% Loss HX	40.3%	38.9%	39.4%	41.0%	39.7%	40.1%	33.1%	31.9%	37.0%
% Loss mixing vessels	9.4%	10.1%	9.9%	8.4%	8.6%	8.2%	2.9%	2.5%	3.6%
% Loss flue gas	7.1%	7.1%	7.1%	5.6%	5.7%	5.7%	4.9%	5.0%	4.8%

**Table 5.10.** Exergy losses in the CHP plant for the proposed configurations of the new system [kW].

#### 5.6.4 Exergy of the overall heating system

0.0%

0.1%

0.1%

0.2%

0.2%

0.1%

The exergy analysis per module helps to identify the actual exergy costs of the proposed configurations for the new system. These costs are shown as the total height of the columns in Figure 5.5. They include the new infrastructure, gas and electricity. The exergy provided by the geothermal water is 'free'.

0.0%

0.1%

0.0%

0.2%

0.1%

0.2%

0.0%

0.3%

0.0%

0.3%

0.0%

0.3%

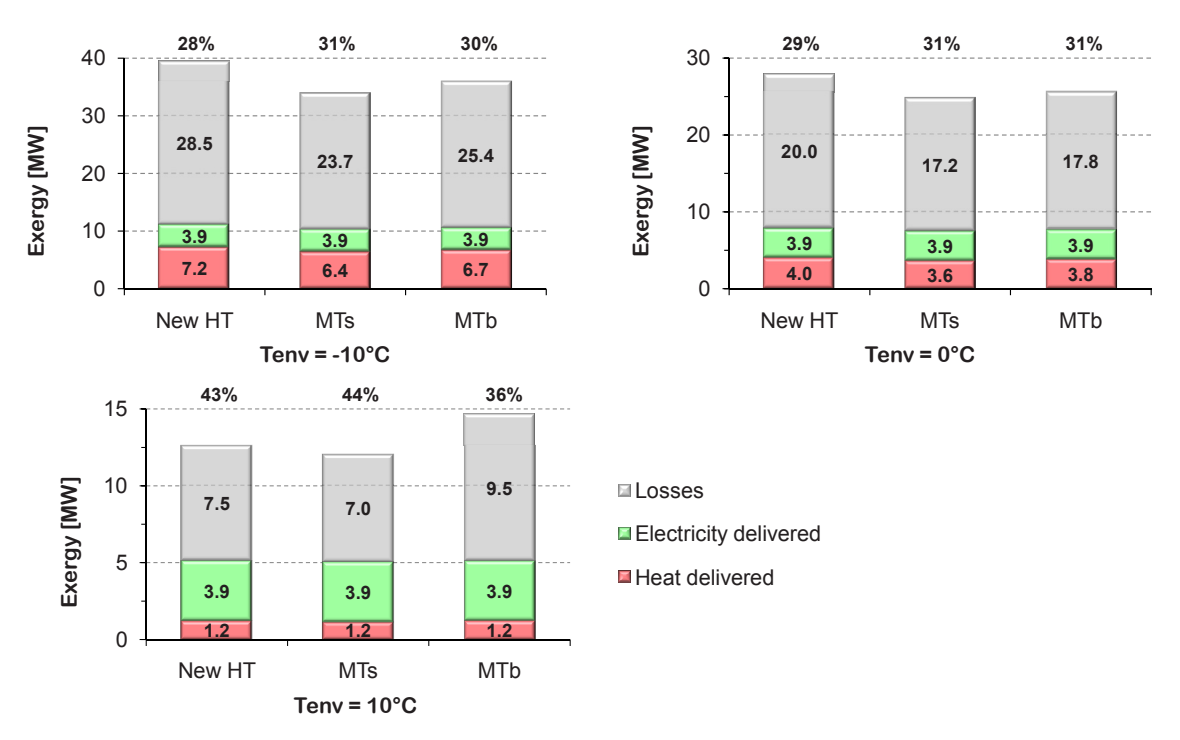


Figure 5.5. Exergy balance of the proposed configurations for the new heating system. The height of the columns represents the total exergy cost and supply of the system.

The exergy of the geothermal heat does not constitute a cost.

The efficiency on top of the columns is calculated as exergy delivered/total exergy cost.

The difference in the exergy costs between configurations in each scenario are mainly due to the difference in heat demand ( $Q_{NewHT} > Q_{MTb} > Q_{MTs}$ ). However, there are also differences in the overall efficiencies which help to compare the configurations.

The exergy efficiency of the New HT configuration is 3% lower than the cascade configurations at -10°C and 0°C.

The overall efficiencies of the cascade configurations are similar at -10°C and 0°C. But at 10°C, the performance of MTb drops 8% below the MTs configuration (even lower than the New HT configuration).

The MTs configuration has an efficiency up to 3% higher than the second best option in the scenarios evaluated.

## 5.7 Selected configuration

The exergy analysis reveals that there are no large differences in the overall efficiencies of the proposed configurations for the new heating system.

However, the New HT configuration has higher thermodynamic inefficiencies under high demands, and the MTb configuration has a significant drop of efficiency at low partial loads. Both situations result in lower geothermal energy utilisation.

On the other hand, the efficiency of the MTs configuration is not negatively affected by changes in the demand. Furthermore, the simulated scenarios make it possible to argue that this configuration meets the minimum geothermal energy consumption (70,000 GJ/yr).

# Therefore, a cascade system with renovations of small buildings is the suggested configuration for the new system (MTs).

There are additional advantages and disadvantages to take into consideration:

#### Advantages

 The possibility to operate block N2 individually at MT conditions. The geothermal plant alone can provide the heat required by the entire block, reducing its dependance on a preceding HT consumer.

#### Drawbacks

- Block N1 relies on the availability of a new MT consumer connected to the outlet of the faculty of architecture (BK).
- The efficiency of block Z2 decreases considerably at low partial loads due to a surplus flow rate from the HT buildings that is bypassed around the MT consumers. The configuration thus relies on a connection with block N2, reducing the bypass and covering the demand of the entire block.

#### 5.7.1 Present configuration vs. new configuration

The comparison of between the present system with a 3-way valve configuration and the selected cascade configuration for the new system MTs is shown in Figure 5.6. and Table 5.11.

Given the fact that the heat demand is slightly different between systems, values per kW of heat delivered to the buildings are presented in the table (energy). The consumption of electricity for pumping is higher in the new system due to the consumption in the geothermal plant. However, even when considering a 44% efficiency of the grid, the primary energy consumption per kW of heat delivered decreases by 18% at 10°C and by 47% at 10°C with the new system.

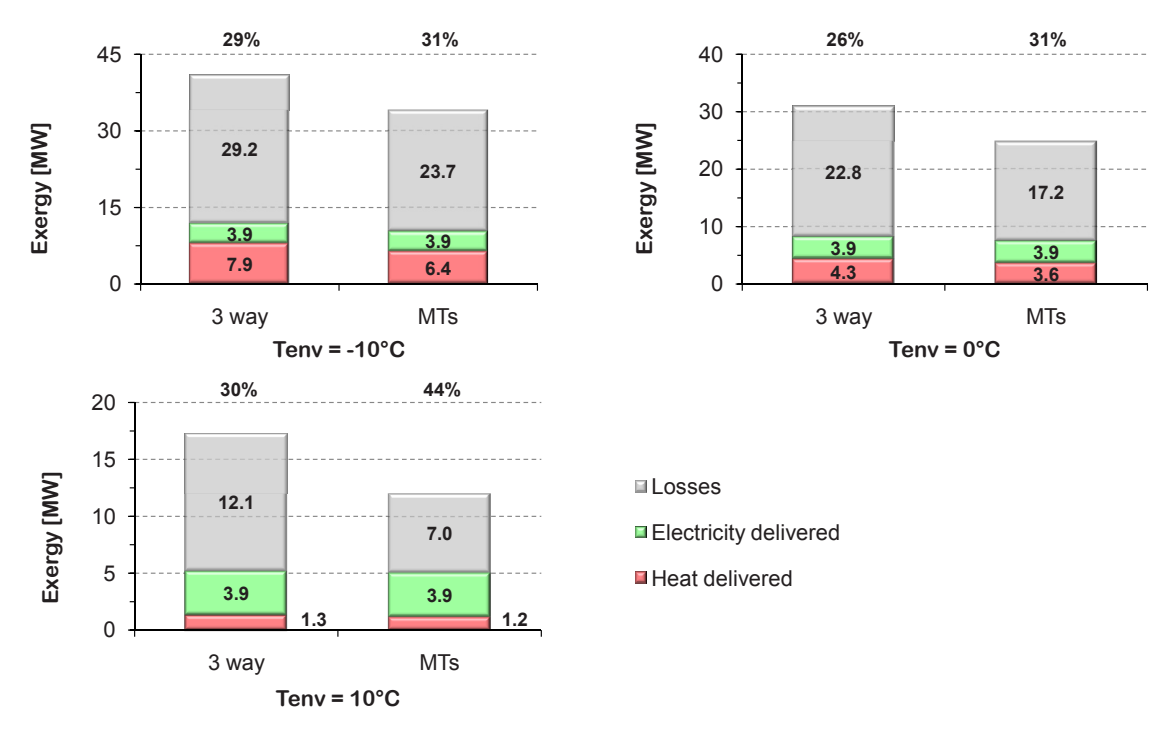


**Figure 5.6.** Exergy balance of the present system versus the selected configuration for the new system. The height of the columns represents the exergy cost and supply to the system. The efficiency shown on top of each column is calculated as *exergy delivered/exergy supply*.

**Table 5.11.** Comparison between the present system and the selected configuration for the new system. Since the heat demand is slightly different between systems, the values per kW of heat delivered are provided.

Variable	Tenv =	-10°C	Tenv =	= 0°C	Tenv =	: 10°C
variable	3-way	MTs	3-way	MTs	3-way	MTs
φ [kg/s]	146.9	120.8	208.5	122.0	231.2	57.3
$\phi_{gas}$ [kg/s]	1.004	0.796	0.748	0.568	0.400	0.253
Q <sub>gas</sub> [kW]	31244	23718	22216	15898	10025	4742
$\phi_{\text{CO}2}$ [kg/s]	2.140	1.693	1.597	1.209	0.851	0.536
W <sub>el,E</sub> [kW]	120	296	208	274	255	233
Q <sub>geo</sub> [kW]	0	5820	0	5179	0	4815
Q delivered [kW]	31024	29435	22107	20989	9991	9453
W <sub>el</sub> delivered [kW]	3881	3881	3874	3876	3886	3872
$Q_{gas}/Q$ [kW/kW]	1.007	0.806	1.005	0.757	1.003	0.502
$\frac{\text{W}_{\text{el,in}}}{\text{Q}}$ [kW/kW]	0.004	0.010	0.009	0.013	0.026	0.025
En <sub>primary</sub> /Q [kW/kW]	1.016	0.829	1.026	0.787	1.061	0.558

#### 5.7.2 Operation under no heat demand

As a safety measure in geothermal plants, it is recommended to have the possibility for utilisation at all times. Therefore, the utilisation of geothermal energy at zero heat demand is evaluated herein.

It is possible to preheat the water of the mixing vessels from the boilers and gas engines. The vessel of the boilers has a volume of 2500 L and each of the two gas engines has a mixing vessel of 310 L, for a total water volume of  $3.12 m^3$ .

It is assumed that the water in the vessels is heated from 15 to 60°C as part of the plant start-up, with water fed from the geothermal plant at 70°C. Four heating times are simulated to determine whether slow of fast heating times are better. The results are shown in Table 5.12.

Increasing the heating time slightly increases the total electricity consumption for pumping. Therefore it is suggested to heat the mixing vessels in short times.

However, this application constitutes only a small fraction of the expected geothermal flow rate  $\phi_{geo}$  (40.6 kg/s). Additional applications must be evaluated in future work, such as heating tap water.

Heating time [h]	Q required [kW]	φ required (70/60°C) [kg/s]	W <sub>el</sub> pump to plant [kW]	W <sub>el</sub> pump injection [kW]	φ <sub>geo</sub> [kg/s]	Energy to pumps [kWh]
1	163.2	3.894	0.780	9.520	2.464	10.3
2	81.6	1.947	0.390	5.060	1.243	10.9
3	54.4	1.298	0.260	3.450	0.827	11.1
8	20.4	0.487	0.100	1.610	0.31	13.7

**Table 5.12.** Start-up energy required to preheat the mixing vessels in the CHP plant. The losses in the pipelines are neglected in the calculation of the pump energy.

## 5.8 Conclusions for the new heating system

In this chapter, the new heating system was simulated and analysed for three network configurations: 1) a parallel configuration with no MT consumers (New HT), 2) a cascade system with renovations in small buildings (MTs) and 3) a cascade system with renovations of big buildings (MTb). One configuration was selected and compared to the present system.

The introduction of MT consumers in the system requires new heat exchangers. If oversized, the new heat exchangers may allow for future increase in heat demand and operation under LT conditions. Heat exchangers were designed for 200% of the current peak demand.

The cascade configurations require additional flows, particularly at partial loads, in order to increase the temperature of the water leaving the HT buildings to the levels required by MT consumers (from 47 to 64°C at  $T_{env} = 10$ °C). The proposed solution is to maintain the operation of 3-way valves in the HT buildings.

The New HT configuration presents lower geothermal utilisation than the other configurations during high heat demand (1.7 MW vs. 5.9 MW), due to relatively high return temperatures from the network when compared to cascade systems ( $63^{\circ}$ C vs.  $43^{\circ}$ C).

The MTb configuration presents thermodynamic inefficiencies and lower geothermal utilisation at low partial loads (2.9 MW vs 4.9 MW), caused by the bypass flows required to match the demand of MT consumers with the outlet of HT buildings.

As a general guideline based on the results of this project: from an exergy point of view, it is not recommended to connect large MT consumers in series after small HT consumers

The MTs configuration maintains good geothermal utilisation in the scenarios evaluated (close to or higher than 5 MW). Although a 3-way bypass is also required at partial loads, the overall exergy efficiency is slightly higher than in the parallel New HT configuration (1%-3%). This improvement however, is within to the error margin of the simulations.

Nevertheless, due to the steady efficiency and the improved performance of the network, it is suggested to implement a cascade system by renovating the small buildings for MT operation.

Two important limitations for the MTs network must be taken into consideration: 1) Block N1 relies on the availability of an MT consumer fed from the outlet of architecture. 2) Block Z1 requires a connection to block N2 that sends the excess hot water not needed by the small MT consumers.

The new heating can decrease the primary energy supply by 18-47% with respect to the present system.

# CO<sub>2</sub> CAPTURE AND STORAGE (CCS)

In this chapter, the possibility to implement  $CO_2$  capture and sequestration in the new heating system is briefly discussed.

This part of the present thesis project became secondary in relevance when the geothermal drilling in campus was approved and the evaluation of the transition in the heating network took priority. Additionally, the political discussion on carbon storage, made it necessary to avoid the topic when discussing the project. Therefore, the analysis presented here consists mainly on the application of general figures reported in literature.

The total prevented emissions are calculated taking into account the additional emissions that result from the implementation of the CO<sub>2</sub> capture and sequestration system.

## 6.1 Description of the system

The suggested technologies for each step of CCS are explained in this section.

#### 6.1.1 Capture

The predominant technology for  $\mathrm{CO}_2$  capture is the chemical absorption with an aqueous solution of MEA (monoethanolamine). The system consists of a combination of absorber and stripper. In the absorber, the  $\mathrm{CO}_2$  in the flue gas is dissolved in the amine. The  $\mathrm{CO}_2$  rich amine enters then the stripper where countercurrent steam takes the  $\mathrm{CO}_2$  from the amine. 85% of the  $\mathrm{CO}_2$  in the flue gas can be captured.

Additional energy is required in the stripper, operating typically at 130°C. An average energy cost of 5400 kJ/kg CO<sub>2</sub> is assumed, from which 90% is heat and the remainder is electricity (Undrum, 2000). The emissions resulting from this additional energy requirement are based on the performance of the boilers at the CHP plant, (0.218 kg CO<sub>2</sub>/kWh) and the average emission factor for electricity in The Netherlands (0.566 kg CO<sub>2</sub>/kWh) (Harmelink, 2012).

#### **6.1.2 Sequestration**

For the carbon sequestration, the injection of a solution  $CO_2$ -water is considered. This idea, although still on a conceptual level, is expected to save energy required for the compression of  $CO_2$  to the supercritical conditions. Additional advantages of mixed injection are the prevention of salt precipitation, enhancement of  $CO_2$  residual trapping<sup>1</sup>, enhancement of spreading and a decrease in the risk of leaking (Den Boer et al, 2012).

Two options for the sequestration in the geothermal reservoir are evaluated:

For the mechanisms of CO<sub>2</sub> trapping see: http://www.co2captureproject.org/co2\_trapping.html

- 1) Maximising the total  $CO_2$  capture and exergy extraction from geothermal resource.
- 2) Minimising the energy required for compression.

For the first option, the work of Salimi et al. (2011) is considered. Based on simulations of the reservoir in the Delft area, the authors conclude that injecting a rich solution of  $CO_2$  at  $20^{\circ}C$  may result in the formation of heterogeneous zones in the reservoir, which would have a lower negative impact in its heat production and would increase the total  $CO_2$  capture. A 0.03 mole fraction (1.66 mol  $CO_2$ /kg  $H_2O$ ) is suggested. However, at the proposed injection pressure in the previous chapter (30 bar), the solubility of  $CO_2$  in water is only 0.9 mol  $CO_2$ /kg  $H_2O$  (Duan et al., 2006). This value is used to calculate the required geothermal water for the mixed injection. Additional energy is thus required to compress the  $CO_2$  to 30 bar.

Regarding the second option, an aqueous solution at low concentration of CO<sub>2</sub> is evaluated. At 20°C and 10 bar, the solubility is ca. **0.35 mol CO<sub>2</sub>/kg H<sub>2</sub>O**. However, low concentrations of CO<sub>2</sub>, may decrease the heat recovery by half and the total storage capacity would be severely reduced (Salimi et al, 2011). Additional energy is required to compress the CO<sub>2</sub> to 10 bar.

The compression for both cases is simulated in Cycle-Tempo with an inlet at 20°C and 1 bar(g). In the first case, a four stage compression is considered, with cooling between compressors to 20°C and outlet pressures of 3, 7, 15, 20 bar. For the second case, a two-stage compression is used, with 4, 10 bar as outlet pressures.

In both cases, the  $CO_2$  can be dissolved in water using an additional absorption column. No additional energy is required for pumping, since this power is part of the electricity used for reinjection.

#### 6.2 Results

The resulting emissions from the new heating system with CCS are presented in Table 6.1. The comparison between heating systems with and without CCS is depicted grapically in Figure 6.1.

Given the fact that both options have a lower concentration than the optimum suggested in literature, an additional well exclusive for  $CO_2$  transport may be required; the  $CO_2$  impact of this well is included in the calculations. Based on the work of De Mooij (2012), a total of **2955 ton CO\_2** result from the construction of one well, including drilling, production of steel and production of cement. The resulting emissions are lower than those deriving from capture and sequestration.

The higher emissions deriving from  ${\rm CO}_2$  capture and storage occur due to the capture process, constituting around 90% of the total.

Decreasing the pressure for the solution of  $CO_2$  in water from 30 bar to 10 bar can only decrease the electricity consumption and derived emissions by 2-4%. At 10 bar, the geothermal fluid required to dissolve all the  $CO_2$  is higher than the expected production at the geothermal plant (40.646 kg/s), except for low partial loads of the heating system ( $T_{env} = 10^{\circ}$ C). Therefore, the **preferred option** for sequestration is dissolving the  $CO_2$  in water at the injection pressure of **30 bar**.

In total, carbon capture and sequestration can reduce the emissions by 51%. For every kg of CO<sub>2</sub> captured and stored, approximately 0.4 kg CO<sub>2</sub> are additionally produced from combustion. The additional fossil fuel usage does not contribute to an adequate management of these scarce resources.

Evaluating other options for  $CO_2$  capture with lower energy demand, such as alternative solvents for absorption at lower temperatures, is suggested for future work. This could also be performed by means of an exergy analysis.

 $\label{eq:table 6.1.} \textbf{ Requirements for CO}_2 \ \text{capture and storage and resulting emissions}.$  The numbers in blue are the CO $_2$  emitted as a result of the proposed capture and storage process.

Process	-10°C	0°C	10°C
$\phi_{\rm CO2}$ emitted by the new heating system (MTs) [kg/s]	1.693	1.209	0.536
$\phi_{\rm CO2}$ captured [kg/s]	1.439	1.028	0.455
Capture requirements			
Heat required [kW]	6995	4994	2213
Electricity required [kW]	777	555	246
$\varphi_{\rm CO2}$ resulting from capture [kg/s]	0.524	0.374	0.166
Additional well			
$\varphi_{\rm CO2}$ resulting from well construction [kg/s]	0.003	0.003	0.003
Sequestration requirements (1) P = 30 bar			
Electricity for compression [kW]	329	296	137
$\varphi_{\rm CO2}$ resulting from sequestration [kg/s]	0.042	0.038	0.018
$\phi_{\rm geo}$ required to dissolve ${\rm CO}_2$ [kg/s]	36.348	25.949	11.501
Sequestration requirements (2) P = 10 bar			
W <sub>el</sub> compression [kW]	250	182	85
$\phi_{\rm CO2}$ from sequestration [kg/s]	0.032	0.023	0.011
$\phi_{geo}$ required [kg/s]	93.467	66.725	29.573

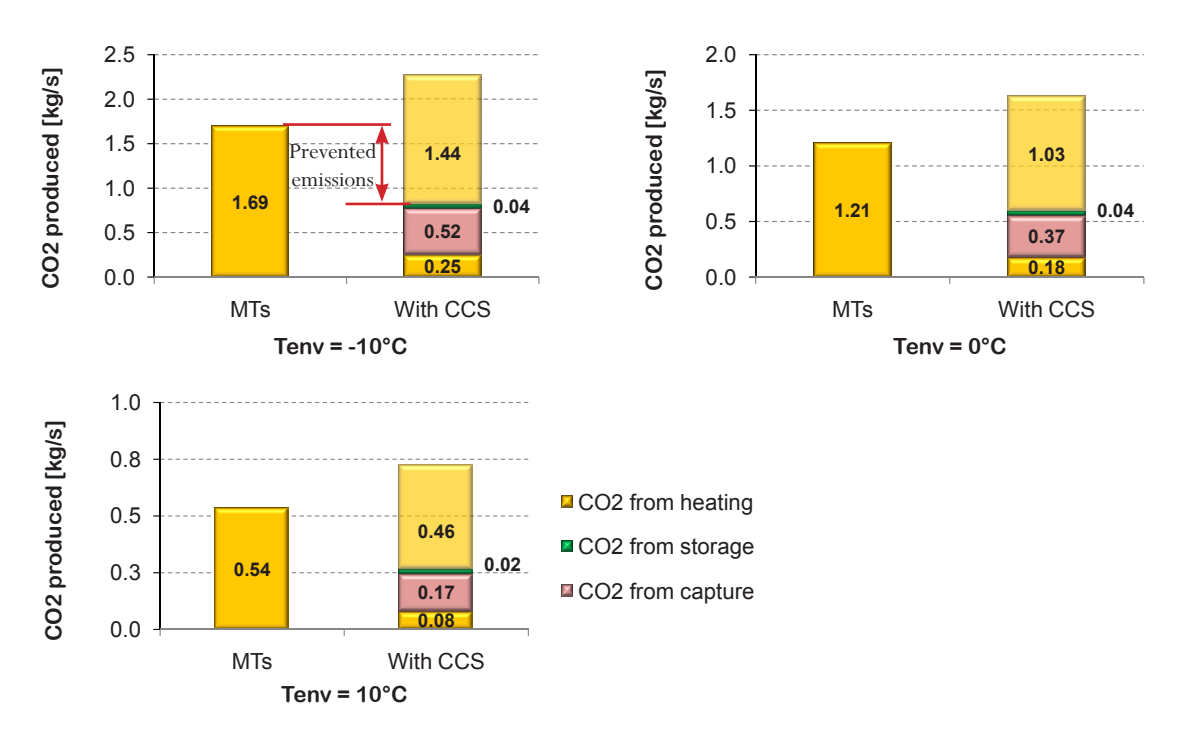


Figure 6.1. Prevented CO<sub>2</sub> emissions with carbon capture and storage (CCS) in the new heating system.

### CONCLUSIONS AND RECOMMENDATIONS

This study evaluates the performance of a new district heating system with geothermal energy for the campus of TU Delft.

Exergy analyses were performed on the present and the new heating systems, which helped to quantify the costs and benefits of the transition. The study is focused on the technical aspects of energy and exergy, avoiding deliberately the restrictions and speculation of financial variables.

The systems were simulated using Cycle-Tempo, a software that facilitates the quantification of exergy under steady state operation. Three load scenarios were simulated, based on the environment temperature at which they occur: -10°C, 0°C and 10°C.

The analysis of the present heating system includes the ongoing transition from a 3-way to a 2-way valve system in the heat exchange equipment, and compares the performance of both configurations.

For the new heating system, three configurations of the network were devised and studied based on the renovation plans of the university: a parallel configuration, a cascade configuration with small MT consumers and a cascade configuration with large MT consumers. One configuration was selected and compared to the present system.

Additionally, the possibility to include carbon capture and storage in the new system was discussed.

#### 7.1 Conclusions

In the present heating system, the transition from a 3-way to a 2-way valve system does not constitute a significant improvement by itself on the exergy efficiency within the system boundaries. However, operating with a 2-way valve system presents an opportunity to implement geothermal energy: lower return temperatures from the network (e.g.  $50^{\circ}$ C at  $T_{env} = 10^{\circ}$ C) allow utilisation of the geothermal resource (75.7°C at the production well). Additionally, the 2-way valve system is expected to have electricity generation at very low partial loads, as opposed to the 3-way system.

The 2-way system presents hourly savings of power required for pumping up to 180 kW. In a broader context, this electricity is supplied by a 44% efficient grid in The Netherlands and is substituted by gas in the local plant with 80% efficiency. Overall, the primary energy supply can decrease by 36%.

In the new heating system, the parallel configuration falls short on geothermal energy utilisation during high heat demand, 1.7 MW vs. 5.9 MW by the cascade configurations.

The medium temperature buildings of a cascade configuration require new heat exchangers. When oversized to 200% of the peak load, the new heat exchangers may still be utilised in a LT system.

In the cascade configuration at partial loads, the outlet of HT buildings with 2-way valves has a temperature lower than the required by the MT buildings (47°C vs. 64°C at  $T_{env} = 10$ °C). The solution proposed is to continue with a 3-way valve system in the, which will compensate the deficit.

However, when the MT building is larger in demand than the preceding HT consumer, the bypass becomes too large, and the exergy destruction due to mixing increases, constituting up to 39% of the exergy losses in the network at low partial loads. Therefore, in cascade systems, it is suggested to avoid connecting large MT consumers in series after small HT consumers.

If small buildings are selected for MT operation, the exergy efficiency is not negatively affected by changes in the demand and it is possible to argue that the minimum geothermal utilisation of 70,000 GJ/yr can be met. Therefore, it is suggested to **renovate the small buildings in campus**. The buildings proposed for renovation are: Aula and Bibliotheek in block N1, 3mE/IO in block N2, and LR, Fellowship (and TNW zuid) in Z2.

Compared to the present system, the selected configuration presents an exergy efficiency 2-14% higher. The primary energy consumption, taking into account the grid efficiency, decreases by 18-47%, along with the associated  $CO_2$  emission.

Therefore, the research objective has been met. A network configuration was devised for the new heating system, which results in an improved exergy efficiency.

Carbon capture and sequestration can reduce the emissions by 51%. However, capture by amine absorption requires additional combustion of fossil fuels. In this way, reducing the impact on climate change does not contribute to the adequate management of scarce fossil fuels.

The contribution of geothermal energy to the heat delivered to the buildings varies with the demand from 20% at  $-10^{\circ}$  C to 51% at  $10^{\circ}$  C. Thus, it is not possible to guarantee that the new heating system will meet the TU Delt goal for 50% share of renewable energy.

The reduction in the gas supply per unit of heat delivered may contribute significantly to the MJA3 goal. In terms of gross floor area, an average 25% reduction in the gas supply can reach 400 MJ/m<sup>2</sup> out of the expected reduction from 519 MJ/m<sup>2</sup> to 364 MJ/m<sup>2</sup> (2005-2020).

### 7.2 Recommendations for future work

The suggested configuration is in line with the ongoing plans of FMVG, last discussed in November 2013. Therefore, it is recommended to proceed with the design process by means of a dynamic model of the district heating system.

The dynamic model and its application for a control strategy should take into account:

- 1) Fouling in the heat exchangers.
- 2) The operation temperatures of the mixing vessel in the boilers, where the exergy destruction can increase with small variations in temperature.
- 3) The difference or ratio between the demands of HT and MT consumers in series, where the bypass or other additional stream required may cause exergy destruction due to mixing.
- 4) The actual operation temperatures of the secondary circuit in each set of heat exchangers (determined depending on the temperature of the building facade that they supply).

Once the renovation plans have been defined by FMVG, it is recommended to include the exergy costs of the renovations and new infrastructure in the buildings as well as an accurate design of the new heat exchangers. The dynamic model will allow for an estimation of the exergy payback time for the system.

Additional applications for geothermal energy when there is no heat demand should be devised and studied, such as providing hot tap water for the buildings.

Alternative methods for  $\mathrm{CO}_2$  capture with lower fossil fuel utilisation should be evaluated, such as absorption solvents other than MEA working on lower temperatures. These systems may work on mainly on geothermal energy. An exergy analysis can help integrating the results of prevented emissions and exergy efficiency of the system.

# **R**EFERENCES

CATO-2. (2013). CO<sub>2</sub> Capture, Transport and Storage in The Netherlands.

Retrieved October, 2013, from http://www.co2-cato.org/cato-2/about-ccs/what-is-ccs

Cornelissen, R.L., & Hirs, G.G. (1997). Exergetic optimisation of a heat exchanger. Energy Conversion and Management, 38(15-17), 1567-1576.

Damen, Kay. (2007). Reforming Fossil Fule Use. The Merits, Costs and Risks of Carbon Dioxide Capture and Storage. (Doctorate), Utrecht University, Utrecht, The Netherlands.

DAP. (2013). Delft Aardwarmte Project.

Retrieved April, 2013, from http://www.delftaardwarmteproject.nl/home/

Day, A.R., Ratcliffe, M.S., & Shepherd, K.J. (2003). Heating Systems. Plant and control: Blackwell Publishing.

De Mooij, J.W.C. (2010). Exergy analysis of the use of geothermal energy and carbon capture, transportation and storage in underground aquifers. (Masterof Science), Delft University of Technology.

Den Boer, Chris, Salimi, Hamidreza, & Wolf, Karl-Heinz. (2012). Integration of Delft Geothermal Project (DAP) and Carbon Sequestration Paper presented at the 8th CATO day, Utrecht, The Netherlands.

DHC;. (2012). Strategic research agenda.

Duan, Z., Sun, R., Zhu, C., & Ming, I.M. (2006). An improved model for the calculation of CO<sub>2</sub> solubility in aqueous solutions containing Na+, K+, Ca2+, Mg2+, Cl-, and SO42-. Marine Chemistry (98), 131-139.

European Commission. (2012). Renewable Energy, Targets by 2020.

Retrieved 16 April, 2013, from http://ec.europa.eu/energy/renewables/targets\_en.htm

Directive 2009/28/EC of the European Parliament and of the Council of 23 April 2009 on the promotion of the use of energy from renewable sources (2009).

Goldstein, B., Hiriart, G., Bertani, R., Bromley, C., Gutiérrez-Negrín, L., Huenges, E., Zui, V. (2011). Geothermal Energy. In IPCC Special Report on Renewable Energy Sources and Climate Change Mitigation.

Harmelink, M., Bosselaar, L., Gerdes, J., Seigers, R., & Verdonk, M. (2012). Berekening van de  $CO_2$ -emissies, het primair fossiel energiegebruik en het rendement van elektriciteit in Nederland.

Hepbasli, Arif. (2010). A review on energetic, exergetic and exergoeconomic aspects of geothermal district heating systems (GDHSs). Energy Conversion and Management, 51(10), 2041-2061.

IEA. (2013). Electricity/Heat in World in 2009.

Retrieved September, 2013, from http://www.iea.org/stats/electricitydata.asp?COUNTRY\_CODE=29

IGA. (2013, 25 April 2013). International Geothermal Association.

Retrieved May, 2013, from http://www.geothermal-energy.org/index.html

IPCC. (2005). Special Report on Carbon Dioxide Capture and Storage.

Kakac, S., & Liu, H. (2002). Heat exchangers. Selection, rating and thermal design (Second ed.): CRC Press.

Lokkhorst, A., & Wong, T. E. (2007). Geothermal energy Geology of the Netherlands: Royal Netherlands Academy of Arts and Sciences.

Macedo Costa, M., Schaeffer, R., & Worrell, E. (2001). Exergy accounting of energy and materials flows in steel production systems. Energy(26), 363-384.

Matsumura, M. H. (2012). Feasibility Study for Renewable Heat Integration into the TU Delft District Heating System. (Master of Science), Delft University of Technology.

Meckler, Milton, & Hyman, Lucas B. (2010). Sustainable On-Site CHP Systems. Design, Construction and Operations: McGraw-Hill.

Ministerie van Economische, Landbouw en Innovatie. (2011). Handreiking Monitoring MJA3 (pp. 72).

Moran, Michael J., & Shapiro, Howard N. (2010). Fundamentals of Engineering Thermodynamics, SI Version (6th ed.): Wiley.

Native Dynamics. (2012). Absolute roughness of pipe material.

Retrieved June, 2013, from http://neutrium.net/fluid\_flow/absolute-roughness/

Pardo, N., Moya, J.A., & Vatopoulos, K. (2012). Prospective Scenarios on Energy Efficiency and  $CO_2$  Emissions in the EU Iron & Steel Industry: JRC.

Platform Geothermie. (2013). Projecten.

Retrieved June, 2013, from http://geothermie.nl/geothermie/projecten/

Rockwool. (2010). Product catalogue. Technical and industrial insulation (pp. 5): Lapinus.

Salimi, H., Groenenberg, R., & Wolf, K.H. (2011). Compositional flow simulations of mixed  $\rm CO_2$ -water injection into geothermal reservoirs: Geothermal energy combined with CO2 storage. Paper presented at the Thirty-Sixth Workshop on Geothermal Reservoir Engineering, Stanford, California.

Saylor. (2013). Standard pipe sizes.

Retrieved June, 2013, from http://www.saylor.org/site/wp-content/uploads/2011/07/ME303-4.1.1.pdf

Schmidt, A.C. (2004). Comparative life cycle assessment of three insulation materials: dk - Teknik Energy & Environment.

Sciubba, Enrico. (2004). Exergoeconomics Encyclopedia of energy (Vol. 2): Elsevier.

Sinnot, R.K. (2003). Coulson and Richardson's Chemical Engineering (Vol. 6): Butterworth Heinemann.

Szargut, J., & Morris, R.D. (1987). Cumulative exergy consumption and cumulative degree of perfection of chemical processes. Energy Research, 11, 245-261.

Taylor, P, Lavagne, D.O., Trudeau, N., & Francoeur, M. (2008). Energy efficiency indicators for public electricity production from fossil fuels: OECD/IEA.

TU Delft. (2013). Energy on the campus.

Retrieved April 16, 2013, from http://tudelft.nl/en/research/energy/energy-on-the-campus/

Undrum, Henriette, Bolland, Olav, & Aarebrot, Eivind. (2000). Economical assessment of natural gas fired combined cycle power plant with CO2 capture and sequestration. Paper presented at the 5th Greenhouse Gas Control Technologies Conference (GHGT5), Cairns, Australia.

Wolf, Karl-Heinz. (2009). An Integrated Approach for the Development of Geothermal Energy Systems: TU Delft.

**APPENDICES** 

# Appendix A Assumptions and inputs for the model of the network

#### **ASSUMPTIONS**

### Pressure and heat losses in the pipes

The pipes are assumed to be horizontal. Therefore, the pressure drop is calculated based only on friction losses.

A roughness  $\varepsilon = 0.35$  mm is calculated for block N1. This value is assumed for the other blocks in the network (moderately corroded steel).

The soil temperature is assumed constant throughout the year,  $T_S = 5^{\circ}$  C.

### Heat exchangers

Heat losses to the environment are neglected due to the relatively low temperatures of operation. This is verified on the field by the cold external surfaces of the heat exchangers.

The pressure drop is determined on the field. Therefore, the effect of fouling on pressure drop is taken into account. It is assumed to change linearly with respect to the environment temperature. These empirical values are also used for the models of the new heat exchangers.

The effect of fouling on heat transfer is neglected. This is an important limitation of the present study, because fouling has a bigger effect on heat transfer than on pressure drop in liquids.

### Operation conditions, present system

The design temperatures for the circuit are  $130/80^{\circ}$ C (inlet/outlet). For the secondary circuits the values are  $70/90^{\circ}$ C.

For partial loads, the temperatures in the primary circuit are determined from averages of the monitoring system at WKC.

The supply temperature to the secondary circuits depends on the facade to which the heat is delivered. Average values from field measurements are used for all the network, without specific differences between buildings or branches. The return temperature is calculated based on literature.

Average values of pressure drop are also assumed for all the heat exchangers based on field measurements. A linear behaviour in  $\Delta P = f(T_{env})$  is assumed to perform a regression.

#### Primary circuit

A polynomial regression (n = 2) from the field data is performed to find the supply and return temperatures.

The values measured for  $T_{supply}$  from the CHP plant are lower than the supply function ( $T_{supply} = 1.73T_{env} + 70 + 42.7$ ). The difference can be explained as follows: For the supply water from the CHP plant, both  $\phi$  and  $T_{supply}$  are controlled variables. There are different heating loads for the same  $T_{env}$ . At a given  $T_{env}$ , high demands are covered by the supply function, and times of low demand are covered by lower  $\phi$  or lower  $T_{supply}$ . Therefore, the average of  $T_{supply}$  for a given  $T_{env}$  is lower than the supply function.

#### Secondary circuits

The temperatures are determined based on the method described in Day et. al. (2003).

The design value in the secondary circuit is  $T_{supply} = 90^{\circ}$  C at  $T_{env} = -10^{\circ}$  C. Assuming that  $T_{supply,min} = 40^{\circ}$  C at  $T_{env} = 20^{\circ}$  C, the temperature of the secondary circuit can be described by the linear equation:  $T_{supply} = -1.667T_{env} + 90$ .

The return temperature is calculated from the following relation:

$$T_{return} = T_{\text{supply}} - \frac{T_{\text{room}} - T_{\text{env}}}{\left(T_{\text{room}} - T_{\text{env}}\right)_{des}} \left(T_{\text{supply}} - T_{return}\right)_{des}$$

Where 
$$T_{room} = T_{room,des} = 20^{\circ}$$
 C,  $T_{env,des} = -10^{\circ}$  C,  $T_{supply,des} = 90^{\circ}$  C and  $T_{return,des} = 70^{\circ}$  C.

It is important to point out that this non-linear temperature profile represents an ideal schedule. Common control strategies use linear schedules with temperatures higher than the ideal for partial loads.

### Operation conditions, new system

The pressure drops in heat exchangers are assumed to be the same as in the present system.

 $T_{supply}$  from the CHP plant is first decreased 10°C. Due to the MT consumers at partial loads, a large bypass requirement causes high velocities in the pipelines.  $T_{supply}$  is then decreased to maintain v < 2 m/s.

#### **MODEL INPUTS**

The variables follows the nomenclature used in Cycle-Tempo. The reference state is the Baehr environment, changing only the environment temperature with the different scenarios.

**Table A.1.** General inputs for the network model

Component	Variable
Heat exchangers	UA, DSMAS1 HT design: 130/80°C and 70/90°C MT design: 80/40°C and 35/75°C. EEQCOD = 1
Valves	(3 way) flow = determined from energy balance (2 way) flow = actual flow to HX (result of 3 way models) DELP = calculated separately
Splitters	DELP = calculated separately
Pipes	DELP, DELH = calculated separately

**Table A.2.** Scenario dependent variables for the present system.

37 1.1 -		Scenarios	
Variable	-10° C	0° C	10° C
Primary circuit			
Source			
POUT [bar]*	13	12	11
TOUT [°C]	130	104.8	85.3
Heat exchangers			
DELP1, DELP2 [bar]	0.5	0.375	0.25
TOUT1 [°C]	90	73.3	56.7
Secondary circuits			
Source			
POUT [bar]*	3	3	3
TOUT [°C]	70	60	50

POUT are gauge pressures.  $P_{\text{atm}} = 1.01325 \ \text{bar}$  must be added for the model.

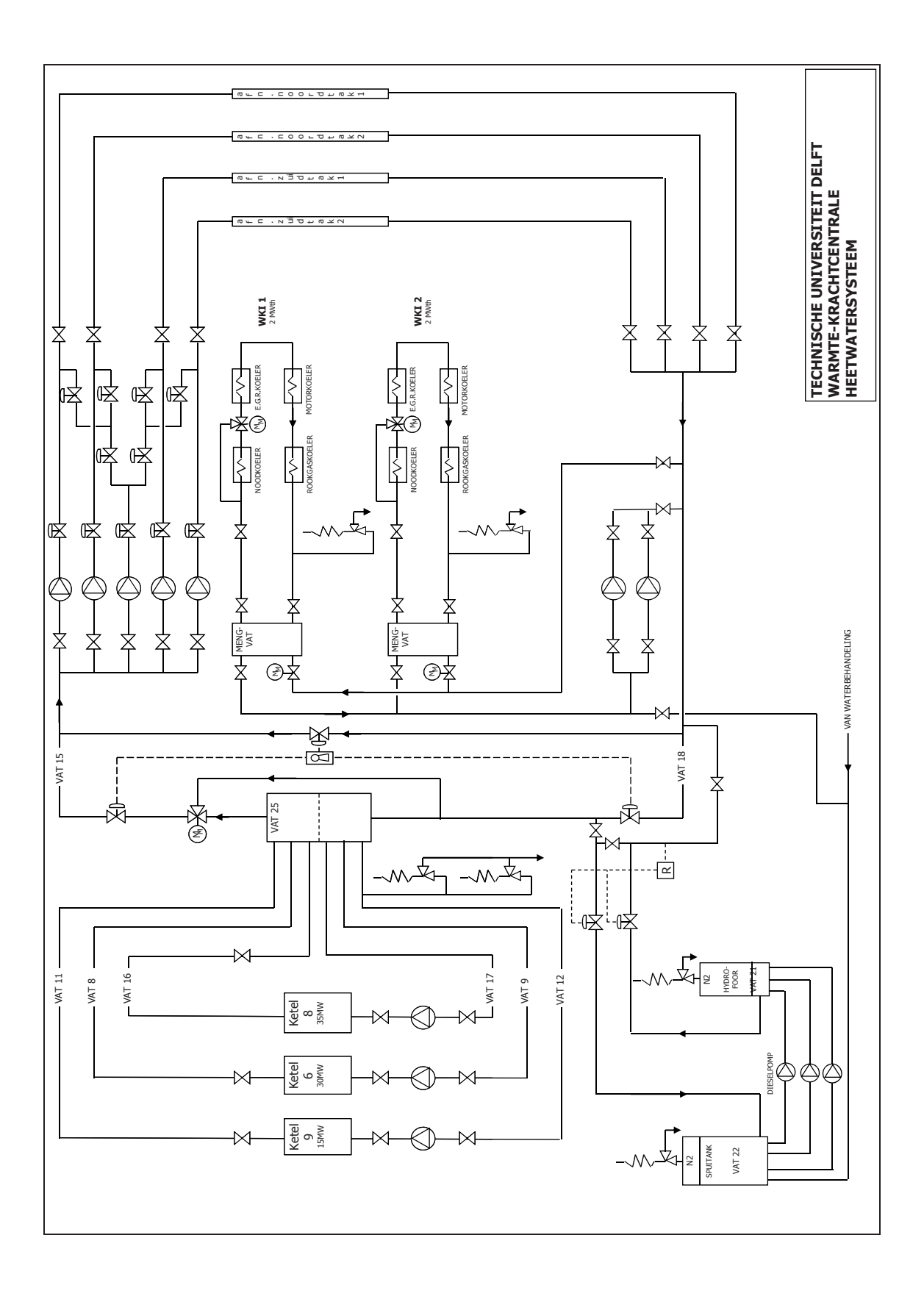
 $\label{thm:continuous} \textbf{Table A.3.} \ \ \textbf{Scenario dependent variables for the new system.}$ 

37 * 11	Sc	enarios I	НТ	Sc	<b>Scenarios MT</b>		
Variable	-10° C	0° C	10° C	-10° C	0° C	10° C	
Primary circuit							
Source							
POUT [bar]	12	11.5	11	11	10.5	10	
TOUT [°C]	130	104.8	85.3	70	70	70	
Heat exchangers							
DELP1, DELP2 [bar]	0.5	0.375	0.25	0.5	0.375	0.25	
TOUT1 [°C]	90	73.3	56.7	65	63	61	
Secondary circuits							
Source							
POUT [bar]	3	3	3	3	3	3	
TOUT [°C]	70	60	50	35	37	39	

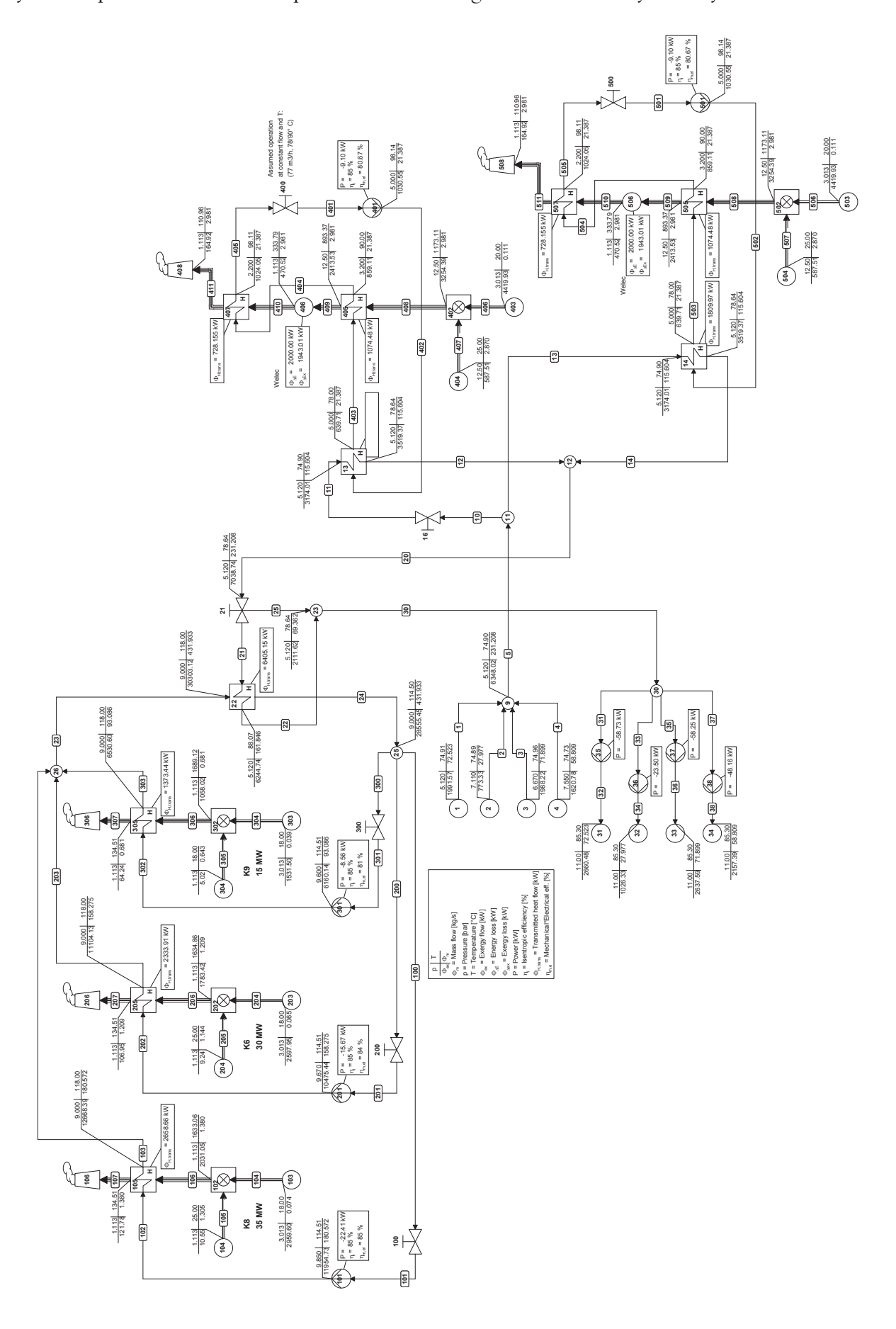
POUT are gauge pressures.  $P_{atm} = 1.01325 \ bar \ must be added for the model.$ 

Appendix B Assumptions and inputs for the model of the CHP plant

Diagram of the CHP plant provided by FMVG.



Cycle-Tempo model of the CHP plant. Current configuration with 3 way valve system at  $10^{\circ}$  C.



#### **ASSUMPTIONS**

The reference state is the Baehr environment, changing only the environment temperature with the different scenarios.

The effect of the expansion tank is simulated as a zero pressure change due to heating and friction/heat loss in the CHP plant. The isentropic efficiency of all the pumps is assumed to be  $\eta_{is} = 85\%$ . The product of the mechanical and electrical efficiencies of the pumps ( $\eta_{mec} \eta_{el}$ ) is interpolated by Cycle-Tempo from the values shown in the figure below.

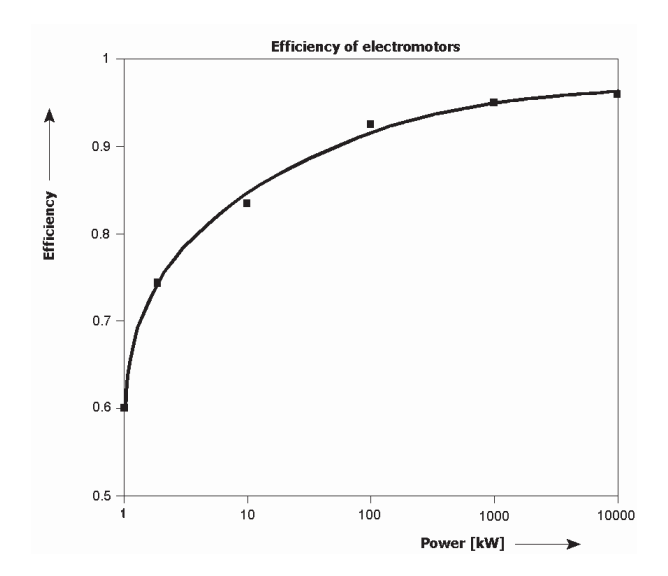


**Figure B.1.** Efficiency of electromotors. Taken from the Cycle-Tempo documentation.

#### Gas engines

It is assumed that the optional heat recovery from flue gas is operational. A pressure drop of 1 bar is assumed for this component.

There is an additional thermal recovery from a secondary cooling system. However, this only represents 6% of the first heat recovery (125/1948 kW) and it requires water below  $44^{\circ}$  C, which is not available in the return water for the scenarios studied. Therefore, the recovery from the secondary cooling system is neglected.

The gas engines can operate at full load in all the scenarios studied. The model simulates accurately the output of the engines in full load. However, the model results deviate from the design data sheet for partial loads.

The data obtained from the technical data sheet provided by FMVG is summarised below.

Electrical output  $W_{el} = 1948$  kW, mechanical output  $W_{mech} = 2000$  kW, gas supply  $\phi_{gas} = 467.1$  nm<sup>3</sup>/h, cooling system temperatures =  $78/90^{\circ}$  C (in/out), thermal recovery of cooling system Q = 1078 kW, cooling water flow rate  $\phi = 77$  nm<sup>3</sup>/h, pressure drop  $\Delta P = 1.8$  bar, radiation loss  $Q_{loss} = 136$  kW, air supply  $\phi_{air} = 7697$  nm<sup>3</sup>/h, maximum temperature of cooling system  $T_{max} = 95^{\circ}$ C.

The equivalence ratio is calculated from the design  $f_{gas}$  and  $f_{air}$ . The result is  $\lambda = 1.9687$ .

#### **Boilers**

A constant flow rate of water circulating between the boilers and the mixing vessel is assumed.

The water temperature delivered by the boilers  $T_{L,boiler}$  changes with  $T_{env}$ . It is calculated based on the design data sheet and monitoring data provided by FMVG. The results of a linear regression are given below. For the new system, a decrease of 10° C in the operation temperature is possible.

It is assumed that the 3-way valve of the boilers is 100% open towards the mixing vessel (no bypass).

**Table B.1.** Calculated temperature delivered by the boilers. A linear behaviour with respect to  $T_{\rm env}$  is assumed for the regression.

Variable		Scenario	
Variable -	-10° C	0° C	10° C
TL,boiler present system [°C]	170	144	118
TL,boiler new system [°C]	160	134	108

The information obtained from the design data sheet provided by FMVG is summarised below.

**Table B.2.** Design data of the boilers. Provided by FMVG.

v · 11	Boiler			
Variable	K8	К6	К9	
Size [MW]	35	30	15	
Water flow rate, $\phi$ [m <sup>3</sup> /h]	752	645	322	
Gas supply at 2 bar(g) and 18° C, $\phi_{gas}$ [nm <sup>3</sup> /h]	4,200	3,612	1,800	
Air supply at 0.1 bar(g), fair [nm³/h]	47,000	40,000	19,000	
Tair [°C]	25	25	18	
$\lambda$ (calculated from fair and fgas)	1.337	1.335	1.272	
Pump flow rate, φ [m <sup>3</sup> /h]	570	650	335	
Pump head [m]	20	25.5	18	
Pressure drop in cooling system [bar]	1.7	1.3	1.2	

The pressure drop is calculated assuming that the pumps are sized to 150%.

# MODEL INPUTS

The general input variables and those depending on each scenario are listed in the tables below.

**Table B.3.** General inputs for the CHP plant model.

Component	Variable	Component	Variable
Gas engines		Boilers	
Source (air)	$POUT = 11 \text{ bar, } TOUT = 25^{\circ}C$	Valve 1	Flow = $0.1806 \text{ nm}^3/\text{s}$
Source (gas)	$POUT = 2 bar(g), TOUT = 20^{\circ}C$	Valve 2	Flow = $0.1583 \text{ nm}^3/\text{s}$
Combustor	EEQCOD = 2, $POUT = 11$ bar,	Valve 3	Flow = $0.0931 \text{ nm}^3/\text{s}$
	DELE = 136  kW, LAMBDA = 1.9687	Pumps	ETHAI = 0.85
Pressure drop	POUT = 1 bar(g), DELE = 2000 kW	Source (air) 1	$POUT = 1 bar(g), TOUT = 25^{\circ}C$
Heat exchanger 1	EEQCOD = 1, $DELP = 1.8$ bar,	Source (air) 2	$POUT = 1 bar(g), TOUT = 25^{\circ}C$
	$TOUT1 = 90^{\circ}C$ , $DELP2 = 0$ bar	Source (air) 3	$POUT = 1 bar(g), TOUT = 18^{\circ}C$
Heat exchanger 2	DELP1 = 1  bar, DELP2 = 0  bar	Sources (gas)	POUT 2 bar(g), TOUT = $18^{\circ}$ C
Valve	Flow = $0.02139 \text{ nm}3/\text{s}$	HXs	EEQCOD = 1, POUT1 = 9 bar
Pump	POUT = 5  bar,  ETHAI = 0.85		DELP1=0.85(1), 0.67(2), 0.6 bar(3)
Mix vessel (HX)	$TOUT2 = 78^{\circ}C$		POUT1 = 9 bar
Sources	POUT, TOUT, DELM		UA and DSMAS1 calculated on design
(from network)	results from network model	Mix vessel (HX)	DELP1 = DELP2 = 0 bar

**Table B.4.** Scenario dependent variables for the CHP plant model.

Vaniables		Scenario	
Variables	-10°C	0°C	10°C
Boilers			
TOUT (present system) [°C]	170	144	118
TOUT (new system) [°C]	160	134	108

# Appendix C Assumptions and inputs for the geothermal plant

#### **ASSUMPTIONS**

The conditions at the reservoir are considered constant. A production of 150 m<sup>3</sup>/h at 75.7° C is assumed. This is assumed constant in order to estimate the maximum network water flow rate that is possible to heat, trying to match the minimum required by the geothermal plant, 70,000 GJ/yr (average 2213.6 kW hourly).

The geothermal plant expects to deliver 73°C. The temperature is assumed to be 70° C for all the scenarios, accounting for a safety margin.

The injection pressure in Amerlaan is 21 bar. However, Matsumura (2012) calculates a pressure drop above 24 bar (including 1 bar in the heat exchangers). A pressure drop of 26 bar is assumed for this study to account for a safety margin (including 1 bar in the heat exchangers). The assumed injection pressure is **30 bar** and the production pressure is **5 bar** (both absolute pressures and at the surface level).

The heat exchangers are oversize to 150% of the heat transfer at the expected production.

#### **MODEL INPUTS**

The reference state is the Baehr environment, changing only the environment temperature with the different scenarios.

The inputs for the model of the geothermal plant are listed below. They are the same for all scenarios.

Component	Variable	Component	Variable
<b>Primary side</b>		Secondary side	(reservoir)
Sources	POUT, TOUT, DELM	Source	POUT = $5 \text{ bar}$ , TOUT = $75.7^{\circ}$ C
	Results from network model		DELM = -40.646  kg/s
	(selecting flows with the lower T)	Sink	PIN = 30 bar
Sinks	PIN = min P from sources	Pump	ETHAI = 0.85
HX	EEQCOD = 1, $DELP1 = DELP2 = 1$ bar		
	UA, DSMAS1 calculated on design		

**Table C.1.** General inputs for the geothermal plant model.

# Appendix D Demand of the DHS in TU Delft

 $\textbf{Table D.1.} \ \text{Average hourly demand measured by Van Beek.}$  Data for 2012 per scenario of  $T_{env}$ , including estimations for the buildings not yet monitored.

				Deman	ıd [kW]	
Block	Van Beek meter	Building	Peak (-11.8° C)	-10° C	0° C	10° C
N1		WKC <sup>[1]</sup>	82.5	157.5	102.0	45.0
	31 TBM-1	TBM-1	110.0	210.0	136.0	60.0
	30 OCP IO OTB	OTB	200.0	200.0	154.0	68.0
	30A O en S	OTB/O&S	200.0	165.0	108.0	43.0
	12TNW Scheikunde	ChemE	2430.0	2445.0	1863.0	895.0
	08 Bouwkunde	BK	3010.0	2730.0	2224.0	1000.0
	20 Aula	Aula	1090.0	1130.0	634.0	271.0
	21 Bibliotheek	Bibliotheek	300.0	340.0	344.0	275.0
	22TNW F-20	TNW	1750.0	1600.0	1146.0	477.0
N2	34 Complex - 4 Sleeptank	3mE-Sleeptank	200.0	165.0	98.0	43.0
	31 TBM-2	TBM-2	550.0	475.0	272.0	105.0
	32 Complex - IO 10b	IO-10b	1340.0	1250.0	900.0	355.0
	32 Complex - IO 10a	IO-10a	470.0	400.0	259.0	111.0
	34 Complex - 8a	3mE-8a	320.0	275.0	209.0	86.0
	34 Complex - 8b	3mE-8b	440.0	385.0	291.0	133.0
	34 Complex - 6 EMC	3mE-6	200.0	200.0	131.0	73.0
	34 Complex - 3 EMC	3mE-3	490.0	470.0	403.0	136.0
	34 Complex - 8c	3mE-8c	380.0	250.0	221.0	98.0
	34 Complex - 8d	3mE-8d	250.0	155.0	164.0	69.0

<sup>[1]</sup> The demand in the power plant building (WKC) is assumed as 75% of the demand in TBM of block N1, based on the installed capacity of the heat exchangers.

Table D.1 (Cont.) Average hourly demand measured by Van Beek. Data for 2012 per scenario of  $T_{env}$ , including estimations for the buildings not yet monitored.

				Deman	ıd [kW]	
Block	Van Beek meter	Building	Peak (-11.8° C)	-10° C	0° C	10° C
<b>Z</b> 1		G44-Aerohydro <sup>[2]</sup>	385.0	359.0	257.0	116.0
	34 Complex - 4	3mE-4	730.0	695.0	520.0	186.0
	36 EWI - 2 College zalen	EWI-2	280.0	250.0	183.0	86.0
	35 Corn. Drebbelweg 5	G35	470.0	365.0	266.0	90.0
	22TNW+TNO-TPD F-98	TNW-F98	549.0	507.0	462.0	157.0
	22 TNW E-18	TNW-E18	561.0	518.0	160.0	195.0
		G104TNO <sup>[3]</sup>	2302.0	2151.0	1537.0	695.0
	23 CiTG Onderwijs	CiTG-Onderwijs	3200.0	3275.0	2227.0	1022.0
		G116-Deltares <sup>[3]</sup>	1052.0	983.0	703.0	318.0
	23 CiTG Stevin I	CiTG-St1	360.0	320.0	217.0	101.0
	23 TNO Stevin 4	CiTG-St4	200.0	200.0	183.0	141.0
<b>Z</b> 2	45 LR LS Windtunnel	LR-G45	200.0	160.0	126.5	62.3
	46 WBMT API	G46-P&E	480.0	400.0	141.0	116.5
	47 DUWO woningen	DUWO	320.0	280.0	203.0	100.7
	36 EWI - 4 Hoogsp. Hal	EWI-4	480.0	470.0	350.0	150.8
	23 CiTG Stevin 3	CiTG-St3	460.0	370.0	349.5	140.5
	23 CiTG Stevin 2	CiTG-St2	780.0	530.0	427.5	160.9
	36 EWI - 3 Laagbouw	EWI-3	1020.0	925.0	621.0	287.9
	36 EWI - 1 Hoogbouw	EWI-1	2210.0	2100.0	1378.5	634.4
	37 Sportcentrum	SC	420.0	350.0	259.3	122.7
	66 Onderwijsgebouw	G66-Fellowship	280.0	285.0	160.5	65.2
	61 LR Vliegtuighal	LR-G61	470.0	495.0	322.5	125.0
	65 DTC gebouw	FMVG	990.0	875.0	680.5	280.9
	64 LR Windtunnel	LR-G64	180.0	175.0	119.3	57.9
	62 LR Hoofdgebouw	LR-G62	850.0	910.0	594.5	235.5

<sup>[2]</sup> The demand of building 44 (G44, Aerohydrodynamica) is calculated from monthly data, based on the average ratio hourly/monthly of all the monitored buildings.

<sup>[3]</sup> The demand from building 104 (G104-TNO) and building 116 (G116-Deltares) is calculated distributing the yearly heating delivered to third parties, provided by FMVG, in those two buildings based on the installed capacity of heat exchangers. The average hourly demand is calculated from the yearly figures based on the average ratio hourly/monthly of all the monitored buildings.

		Installed HX	нх		Deman	ıd [kW]	
Block	Branch	capacity [kW]	qty	Peak (-11.8° C)	-10° C	0° C	10° C
N1	WKC	250	1	82.5	157.5	102.0	45.0
	TBM-1 340	340	1	110.0	210.0	136.0	60.0
	OTB	1280	2	200.0	200.0	154.0	68.0
	OTB/O&S	1280	2	200.0	165.0	108.0	43.0
	ChemE	5068	2	2430.0	2445.0	1863.0	895.0
	BK 70	70	1	18.5	16.7	13.6	6.1
	BK 419	419	1	110.5	100.2	81.6	36.7
	BK 184	184	1	48.5	44.0	35.9	16.1
	BK 4650	4650	2	1226.3	1112.2	906.0	407.4
	BK 220	220	1	58.0	52.6	42.9	19.3
	BK 4650/640/581	4650	2	1226.3	1112.2	906.0	407.4
	BK 4650/640/581	640	1	168.8	153.1	124.7	56.1
	BK 4650/640/581	581	1	153.2	139.0	113.2	50.9
	Aula	2326	2	930.1	964.2	541.0	231.2
	Aula	400	1	159.9	165.8	93.0	39.8
	Bibliotheek	1600	2	300.0	340.0	344.0	275.0
	TNW 2400	2400	2	1039.6	950.5	680.8	283.4
	TNW 1640	1640	2	710.4	649.5	465.2	193.6
N2	3mE-Sleeptank 950	950	1	200.0	165.0	98.0	43.0
	TBM-2 1120	1120	2	550.0	475.0	272.0	105.0
	IO-10b 3315	3315	3	1340.0	1250.0	900.0	355.0
	IO-10a 1745	1745	2	470.0	400.0	259.0	111.0
	3mE-8a 1518	1518	2	320.0	275.0	209.0	86.0
	3mE-8b 1628	1628	2	440.0	385.0	291.0	133.0
	3mE-6 450	450	1	200.0	200.0	131.0	73.0
	3mE-3 523	523	2	490.0	470.0	403.0	136.0
	3mE-8c 1628b	1628	2	380.0	250.0	221.0	98.0
	3mE-8d 525/523	525	1	125.0	77.6	82.2	34.6
	3mE-8d 525/523	523	1	125.0	77.4	81.8	34.4

 ${\it Table D.2.} \ ({\it Cont.}) \ {\it Average hourly demand per branch}.$  Data for 2012 per  $T_{\it env}$  scenario, calculated based on Van Beek measurements and installed HX capacity.

		Installed HX	нх		Deman	d [kW]	
Block	Branch	cap. [kW]	qty	Peak (-11.8° C)	-10° C	0° C	10° C
<b>Z</b> 1	G44 Aerohydro	1512	2	385.0	359.0	257.0	116.0
	3mE-4 1349	1349	2	730.0	695.0	520.0	186.0
	EWI-2 698	698	2	280.0	250.0	183.0	86.0
	G35-930	930	1	268.6	208.3	151.8	51.3
	G35-700	700	1	201.4	156.7	114.2	38.7
	TNW-F98 1360	1360	2	549.0	507.0	462.0	157.0
	TNW-E18 1296/92	1296	2	514.3	483.7	149.4	182.1
	TNW-E18 1296/92	92	1	46.8	34.3	10.6	12.9
	G104TNO	5250	3	2302.0	2151.0	1537.0	695.0
	CiTG-Ondewijs 349	349	1	124.7	131.0	89.1	40.9
	CiTG-Onderwijs 8374	8374	4	3075.3	3144.0	2137.9	981.1
	G116 Deltares	2400	1	1052.0	983.0	703.0	318.0
	CiTG-St1 698/267	698	1	270.0	231.5	157.0	73.1
	CiTG-St1 698/267	267	1	90.0	88.5	60.0	27.9
	CiTG-St4 1163	1163	2	200.0	200.0	183.0	141.0
<b>Z</b> 2	LR G45	837	2	200.0	160.0	126.5	62.3
	G46 P&E	1047	2	480.0	400.0	141.0	116.5
	DUWO	450	1	320.0	280.0	203.0	100.7
	EWI-4 1745	1745	2	480.0	470.0	350.0	150.8
	CiTG-St3 1163	1163	2	460.0	370.0	349.5	140.5
	CiTG-St2 1396	1396	2	780.0	530.0	427.5	160.9
	EWI-3 3900	3900	2	1020.0	925.0	621.0	287.9
	EWI-1 4187/698	4187	2	1883.9	1799.9	1181.5	543.7
	EWI-1 4187/698	698	2	326.1	300.1	197.0	90.6
	SC	940	2	420.0	350.0	259.3	122.7
	G66 Fellowship	643	1	280.0	285.0	160.5	65.2
	LR-G61 907	907	1	470.0	495.0	322.5	125.0
	FMVG	2000	2	990.0	875.0	680.5	280.9
	LR-G64 407	407	2	180.0	175.0	119.3	57.9
	LR-G62 2100	2100	2	850.0	910.0	594.5	235.5

# **Appendix E Simulation results**

# **Present heating system**

Figure E.1. Simulation results of the present heating system.

Wasialala	T <sub>env</sub> =	-10°C	T <sub>env</sub> =	= 0°C	T <sub>env</sub> =	10°C
Variable	3-way	2-way	3-way	2-way	3-way	2-way
Network						
$\phi_T [kg/s]$	146.9	136.6	208.5	126.5	231.2	68.8
φ N1 [kg/s]	42.5	39.5	63.3	38.4	63.3	21.6
φ N2 [kg/s]	19.4	18.0	27.8	16.9	27.8	8.3
φ Z1 [kg/s]	45.6	42.3	63.3	38.3	63.3	21.3
φ Z2 [kg/s]	39.4	36.9	54.1	33.0	54.1	17.6
$\Delta$ P N1 [bar]	2.4	2.1	4.7	2.0	5.9	0.7
$\Delta$ P N2 [bar]	1.9	1.7	3.1	1.1	3.9	0.6
$\Delta$ P Z1 [bar]	2.1	1.9	3.4	1.5	4.3	0.6
$\Delta$ P Z2 [bar]	2.0	1.8	3.3	1.5	3.4	0.5
$T_L N1 [°C]$	79.6	75.7	79.4	62.7	74.9	50.0
$T_L N2 [^{\circ}C]$	79.7	75.6	79.4	62.7	74.9	49.9
$T_L Z1 [^{\circ}C]$	79.8	75.8	79.5	62.8	75.0	50.1
T <sub>L</sub> Z2 [°C]	79.4	75.9	79.2	62.7	74.7	49.8
CHP plant						
$T_{E}$ [°C]	79.6	75.8	79.4	62.8	74.9	49.9
$\phi_{gas} [kg/s]$	1.004	1.014	0.748	0.751	0.400	0.405
Q [kW]	31244	31253	22216	22318	10025	10187
W <sub>el,in</sub> [kW]	120.2	110.7	208.1	104.0	255.3	75.5
φ <sub>CO2</sub> [kg/s]	2.140	2.162	1.597	1.599	0.851	0.864
Gas engines						
$\phi_{gas} [kg/s]$	0.224	0.222	0.224	0.222	0.222	0.222
Q [kW]	3672	3609	3664	3609	3620	3608
$W_{el,in}$ [kW]	18.2	18.2	18.2	18.2	18.2	18.2
W <sub>el,out</sub> [kW]	3881	3881	3874	3876	3886	3872
$T_L$ [°C]	85.6	82.1	83.6	69.6	78.6	62.5
$\phi_{\rm CO2}  [{\rm kg/s}]$	0.479	0.474	0.479	0.474	0.474	0.474
Boilers						
φ <sub>gas</sub> [kg/s]	0.780	0.792	0.524	0.529	0.178	0.183
Q [kW]	27572	27645	18552	18710	6405	6578
W <sub>el,in</sub> [kW]	48.5	48.5	48.5	48.5	48.5	48.5
φ <sub>CO2</sub> [kg/s]	1.662	1.688	1.119	1.125	0.377	0.390
Distribution pumps						
W <sub>el,in</sub> [°C]	53.5	44.1	141.4	37.4	188.6	8.8

# New heating system

**Table E.2.** Simulation results of the new system.

	Te	nv = -1(	)°C	Te	$e_{nv} = 0^{\circ}$	C	Te	$Tenv = 10^{\circ}C$			
Variable	N HT	MTs	MTb	N HT	MTs	MTb	N HT	MTs	MTb		
Network				,			,				
Q delivered [kW]	30950	29435	31258	22108	20989	22334	9991	9453	10079		
φ <sub>E</sub> total [kg/s]	136.6	120.8	104.3	138.6	122.0	117.7	60.1	57.3	95.3		
φ <sub>E</sub> NT1 [kg/s]	39.5	24.8	26.6	42.0	29.8	29.4	18.8	17.7	35.7		
$\phi_E$ NT2 [kg/s]	17.7	29.3	17.7	18.4	23.9	18.4	7.2	0.0	7.2		
$\phi_E ZT1 [kg/s]$	42.4	42.4	37.3	42.0	42.0	47.6	18.6	18.6	40.4		
$\phi_E ZT2 [kg/s]$	37.0	24.4	22.7	36.1	26.4	22.2	15.4	21.0	11.9		
ΔP N1 [bar]	2.0	1.9	1.8	2.2	2.2	1.8	0.6	1.1	1.7		
$\Delta$ P N2 [bar]	1.7	3.5	1.7	1.5	2.3	1.5	0.5	0.7	0.5		
$\Delta$ P Z1 [bar]	1.8	1.8	2.4	1.7	1.7	2.6	0.5	0.5	2.2		
$\Delta$ P Z2 [bar]	2.0	2.1	2.1	1.9	2.0	1.9	0.5	1.7	0.8		
T <sub>L</sub> N1 [°C]	65.7	43.7	39.2	56.9	47.1	40.5	46.7	49.6	65.8		
T <sub>L</sub> N2 [°C]	65.6	37.1	65.6	56.9	38.4	56.9	46.6	39.0	46.6		
$T_L Z1 [°C]$	65.8	65.8	50.6	56.9	56.9	57.2	46.7	46.7	66.2		
T <sub>L</sub> Z2 [°C]	65.9	42.3	41.2	56.9	48.0	41.1	46.5	50.3	40.8		
Geothermal plant											
φ Low T [kg/s]	136.6	78.5	49.3	138.6	80.1	51.6	60.1	57.3	61.4		
$T_{E}$ [°C]	65.8	40.8	40.1	56.9	44.8	40.7	46.6	47.1	58.7		
φ <sub>E</sub> plant [kg/s]	96.0	47.8	47.6	58.5	49.3	47.8	50.1	50.3	61.3		
φ bypass [kg/s]	40.6	30.7	1.8	80.1	30.8	3.8	9.9	6.9	0.0		
Q [kW]	1666	5820	5932	3186	5179	5836	4891	4815	2895		
$T_L$ [ ${}^{\circ}C$ ]	68.8	51.8	68.9	62.4	56.2	67.8	66.1	67.2	70.0		
φ to N2 [kg/s]	0.0	29.3	0.0	0.0	23.9	0.0	0.0	0.0	0.0		
φ to WKC [kg/s]	136.6	49.2	49.3	138.6	56.2	51.6	60.1	57.3	61.4		
W <sub>el</sub> pump to plant [kW]	60.1	14.7	10.2	38.08	15.2	10.5	12.1	15.6	10.9		
W <sub>el</sub> well pump [kW]	136.2	134.6	134.6	135.58	134.9	134.6	135.0	135.0	135.7		

Table E.2. (Cont.). Simulation results of the new heating system.

	Te	nv = -10	)°C	Te	$env = 0^{\circ}$	C	Te	nv = 10	°C
Variable	NHT	MTs	MTb	N HT	MTs	MTb	N HT	MTs	MTb
CHP plant									
$T_{E}$ [°C]	68.8	58.3	61.8	62.4	56.5	61.8	66.1	67.2	68.6
$\phi_{gas}[kg/s]$	0.958	0.796	0.847	0.656	0.568	0.583	0.267	0.253	0.325
W <sub>el,in</sub> [kW]	114	146	124	111	124	105	79	82	97
$\phi_{\rm CO2}  [kg/s]$	2.038	1.693	1.804	1.397	1.209	1.241	0.568	0.536	0.692
Q [kW]	29443	23718	25512	19025	15898	16464	5248	4742	7334
Gas engines									
$\phi_{gas} [kg/s]$	0.222	0.222	0.222	0.222	0.222	0.222	0.222	0.222	0.222
Q [kW]	3609	3609	3609	3609	3609	3609	3613	3608	3608
W <sub>el,in</sub> [kW]	18	18	18	18	18	18	18	18	18
W <sub>el,out</sub> [kW]	3881	3881	3881	3876	3876	3876	3895	3872	3872
$T_L$ [°C]	75.1	67.8	70.1	68.7	65.3	69.1	80.5	82.3	77.7
$\varphi_{\rm CO2}  [kg/s]$	0.474	0.474	0.474	0.474	0.474	0.474	0.474	0.474	0.474
Boilers									
φ <sub>gas</sub> [kg/s]	0.736	0.574	0.625	0.434	0.346	0.361	0.045	0.031	0.103
Q [kW]	25834	20110	21903	15417	12289	12855	1636	1133	3725
$W_{el,in}[kW]$	48	48	48	48	48	47	48	48	48
$\phi_{\rm CO2}  [kg/s]$	1.564	1.219	1.330	0.923	0.735	0.767	0.094	0.062	0.218
Distribution pumps									
W <sub>el,in</sub> [kW]	48	80	58	44	58	45	13	16	31

# Appendix F Exergy cost of the new network infrastructure

#### Heat exchangers

A preliminary evaluation of the performance of a given heat exchanger under new temperatures of operation can be done based on the heat transfer equation, assuming a constant value of *UA*.

$$Q = UA\Delta T_{lm} = UA \frac{\left(T_{E1} - T_{L1}\right) - \left(T_{L2} - T_{E1}\right)}{\ln\left(\frac{T_{E2} - T_{L1}}{T_{T2} - T_{E1}}\right)}$$

For the present system the design temperatures are  $130/80^{\circ}$  C and  $70/90^{\circ}$  C ( $T_{E2}/T_{L2}$  and  $T_{E1}/T_{L1}$ ). This is equivalent to  $\Delta T_{lm} = 21.64$  K. For the MT consumers, the operation temperatures will be  $70/40^{\circ}$  C and  $35/65^{\circ}$  C, equivalent to a  $\Delta T_{lm} = 5$  K. The expected heat transfer under the at MT conditions is calculated for the current size  $\emph{UA}$  and the new  $\Delta T_{lm}$ . The majority of the current heat exchangers cannot operate under MT conditions (Table F.2).

The design of new heat exchangers is performed based on the Kern method with the objective of estimating the exergy cost. The construction parameters are listed below. The main results are the number of tubes (Nt), the length (L) and the diameter of the shell (Ds) (Table F.2).

<b>Table F.1.</b> Construction parameters for the heat exchanges using the Kern method.
Based on (Kakac. 2002).

Parameter	Description	Value	Unit
N <sub>tp</sub>	Number of tube passes	2	-
$N_{sp}$	Number of tube passes	2	-
$d_i$	Pipe internal diameter	0.015	m
$d_o$	Pipe external diamater	0.021	m
$L_{max}$	Maximum length of HX	3.5	m
CL	Tube layout constant for 60° arrangement	0.87	-
CTP	Tube count calculation constant for two tube passes	0.9	-
PR	Tube pitch ratio (PT/ $d_o$ )	1.4	-
Rft	Total fouling resistance	0.002	$m^2/W\ K$

For the mechanical design (Sinnot, 2003), the thickness of the shell is calculated as:

$$th_S = P_S D_S/(2 stress - P_S),$$

where the design pressure of the shell  $P_S = 25$  bar, and the stress for steel at 150°C is 156 MPa.

Flat ends are assumed for the shell, with a thickness

$$th_e = CP D \sqrt{(P_S/stress)},$$

where the design constant for bolted cover CP = 0.4 and  $D = D_S + 0.08$  m.

Once the size of the heat exchangers is determined, the mass of steel is calculated assuming a density  $\rho_{steel} = 7800 \text{ kg/m}^3$ . The exergy for the production is based on the figures reported by Szargut (1987):

- Tubes. Exergy cost for manufacturing steel tubes, 58.77 MJ/kg.
- Shell. Exergy cost for manufacturing cold rolled steel products, 47.62 MJ/kg.
- Flat ends. Exergy cost for manufacturing general steel products, 45.9 MJ/kg.

#### **Pipeline segments**

The exergy for steel is calculated based on the value for tubes shown above.

The exergy for the production of stone wool is assumed equal to the energy utilised for its production,  $17.5 \, \text{MJ/kg}$  (Schmidt, 2004), since its raw materials are basalt rock and slag recycled from steel industry. Its density is taken as an average  $120 \, \text{kg/m}^3$  (Rockwool, 2010).

**Table F.2.** Current (HT) and new heat exchangers (MT). The results in red show the heat transfer at MT conditions that the HT HX cannot meet...

Building	Bl.	qty	Q <sub>des</sub>	UA [m²K/W]	Q <sub>max,2012</sub> [kW]	Q <sub>MT</sub> [kW]	New qty	New Q <sub>des,MT</sub> [kW]	D <sub>s</sub> [m]	L [m]	N <sub>t</sub>
WKC	N1	1	250	11.552	187.5	57.8	2	187.5	0.80	2.7	594
TBM	N1	1	340	15.711	250.0	78.6	2	250.0	0.87	2.9	707
OTB	N1	2	1280	29.574	195.0	147.9	3	260.0	0.86	3.0	696
OTB/O&S	N1	2	1280	29.574	145.0	147.9	3	193.3	0.81	2.7	613
ChT	N1	2	5068	117.096	1340.0	585.5	4	1340.0	1.95	3.0	3588
BK 70	N1	1	70	3.235	20.6	16.2	1	41.2	0.52	1.8	250
BK 419/184	N1	1	419	19.362	123.3	96.8	1	246.7	0.86	2.9	697
BK 419/184	N1	1	184	8.503	54.2	42.5	1	108.3	0.69	2.3	444
BK 4650	N1	2	4650	107.438	684.4	537.2	4	684.4	1.40	3.0	1833
BK 220	N1	1	220	10.166	64.8	50.8	1	129.5	0.70	2.5	464
BK end	N1	2	4650	107.438	684.4	537.2	4	684.4	1.40	3.0	1833
BK end	N1	1	640	29.574	188.4	147.9	2	188.4	0.80	2.7	597
BK end	N1	1	581	26.848	171.0	134.2	2	171.0	0.76	2.7	542
Aula	N1	2	2326	53.742	499.2	268.7	4	499.2	1.19	3.0	1337
Aula	N1	1	400	18.484	171.7	92.4	2	171.7	0.76	2.7	544
Bibliotheek	N1	2	1600	36.968	240.0	184.8	4	240.0	0.85	2.9	678
TNW 2400	N1	2	2400	55.452	582.2	277.3	4	582.2	1.29	3.0	1559
TNW 1640	N1	2	1640	37.892	397.8	189.5	4	397.8	1.06	3.0	1065
3mE 950	N2	1	950	43.899	210.0	219.5	2	210.0	0.82	2.8	628
TBM	N2	2	1120	25.877	320.0	129.4	4	320.0	0.95	3.0	857
IO 3315	N2	3	3315	51.062	446.7	255.3	6	446.7	1.13	3.0	1196
IO 1745	N2	2	1745	40.318	305.0	201.6	4	305.0	0.93	3.0	817
3mE 1518	N2	2	1518	35.073	185.0	175.4	3	246.7	0.86	2.9	697
3mE 1628a	N2	2	1628	37.615	220.0	188.1	4	220.0	0.84	2.8	658
3mE 450	N2	1	450	20.794	230.0	104.0	2	230.0	0.83	2.9	650
3mE 523	N2	2	523	12.084	315.0	60.4	4	315.0	0.95	3.0	843
3mE 1628b	N2	2	1628	37.615	205.0	188.1	3	273.3	0.88	3.0	732
3mE 525/523	N2	1	525	24.260	125.2	121.3	1	250.5	0.87	2.9	708
3mE 525/523	N2	1	523	24.168	124.8	120.8	1	249.5	0.87	2.9	705

 $\label{eq:Table F.2 (Cont.) Current (HT) and new heat exchangers (MT).}$  The results in red show the heat transfer at MT conditions that the HT HX cannot meet.

Building	Bl.	qty	Q <sub>des</sub>	UA [m²K/W]	$\begin{array}{c} Q_{max,2012} \\ [kW] \end{array}$	Q <sub>MT</sub> [kW]	New qty	$\begin{aligned} &\text{New} \\ &\text{Q}_{\text{des},\text{MT}} \\ &\text{[kW]} \end{aligned}$	D <sub>s</sub> [m]	L [m]	$N_{_{\mathrm{t}}}$
G44 Aerohydro	Z1	2	1512	34.935	179.5	174.7	3	239.3	0.85	2.90	677
3mE	<b>Z</b> 1	2	1349	31.169	395.0	155.8	4	395.0	1.06	3.00	1058
EWI	<b>Z</b> 1	2	698	16.127	165.0	80.6	3	220.0	0.84	2.80	658
G35-930	<b>Z</b> 1	1	930	42.975	336.6	214.9	2	336.6	0.98	3.00	901
G35-700	<b>Z</b> 1	1	700	32.347	253.4	161.7	2	253.4	0.85	3.00	678
TNW-1360	Z1	2	1360	31.423	780.0	157.1	4	780.0	1.49	3.00	2088
TNW1296	<b>Z</b> 1	2	1296	29.944	574.2	149.7	4	574.2	1.28	3.00	1538
TNW92	<b>Z</b> 1	1	92	4.251	81.5	21.3	1	163.1	0.76	2.60	549
TNO	<b>Z</b> 1	3	5250	80.867	717.0	404.3	6	717.0	1.43	3.00	1920
CiTG-349	<b>Z</b> 1	1	349	16.127	131.6	80.6	1	263.3	0.87	3.00	705
CiTG-8374	<b>Z</b> 1	4	8374	96.740	789.6	483.7	8	789.6	1.60	3.00	2416
G116 Deltares	<b>Z</b> 1	1	2400	110.904	983.0	554.5	2	983.0	1.67	3.00	2632
CiTG 698/267	<b>Z</b> 1	1	698	32.254	260.4	161.3	2	260.4	0.86	3.00	697
CiTG 698/267	Z1	1	267	12.338	99.6	61.7	1	199.2	0.80	2.80	596
CiTG1163	Z1	2	1163	26.871	200.0	134.4	3	266.7	0.87	3.00	714
G45 LR	Z2	2	837	19.339	110.0	96.7	2	220.0	0.84	2.80	658
G46 P&E	Z2	2	1047	24.191	245.0	121.0	4	245.0	0.86	2.90	693
DUWO	Z2	1	450	20.794	340.0	104.0	2	340.0	0.98	3.00	910
EWI 1745	Z2	2	1745	40.318	240.0	201.6	4	240.0	0.85	2.90	678
CiTG 1163	Z2	2	1163	26.871	385.0	134.4	4	385.0	1.05	3.00	1031
CiTG 1396	Z2	2	1396	32.254	395.0	161.3	4	395.0	1.06	3.00	1058
EWI 3900	Z2	2	3900	90.109	565.0	450.5	4	565.0	1.27	3.00	1513
EWI 4187/698	Z2	2	4187	96.740	947.1	483.7	4	947.1	1.64	3.00	2536
EWI 4187/698	Z2	2	698	16.127	157.9	80.6	3	210.5	0.82	2.80	629
SC	Z2	2	940	21.719	220.0	108.6	4	220.0	0.84	2.80	658
Fellowship	Z2	1	643	29.713	290.0	148.6	2	290.0	0.91	3.00	776
G61 LR 907	Z2	1	907	41.912	610.0	209.6	2	610.0	1.32	3.00	1633
FMVG	Z2	2	2000	46.210	535.0	231.0	4	535.0	1.23	3.00	1432
G64 LR 407	Z2	2	407	9.404	105.0	47.0	2	210.0	0.82	2.80	628
G62 LR 2100	Z2	2	2100	48.520	460.0	242.6	4	460.0	1.14	3.00	1232
New from BK	N2						4	840.0	1.55	3.00	2249
New from G35	<b>Z</b> 1						3	250.0	0.87	2.90	707
New in TNW zuid	Z2						4	247.5	0.86	2.90	700

# Appendix G Exergy cost of the geothermal plant infrastructure

### **Heat exchangers**

The heat exchangers are sized for  $40/73^{\circ}C$  and  $75.7/42.7^{\circ}C$  ( $T_{E1}/T_{L1}$  and  $T_{E2}/T_{L2}$ ) and a geothermal flow rate of  $150 \text{ m}^3/\text{h}$  ( $\phi_2 = 40.655 \text{ kg/s}$ ).

The design is based on the Kern method, with the parameters listed in Appendix F. Different parameters are used for:

pipe diameter,  $d_i = 0.0209$  m and  $d_o = 0.0267$  m, maximum length  $L_{max} = 6$  m tube pitch ratio PR = 1.45.

This parameters are used to reach a tube velocity of 0.1 m/s, in order to prevent fouling.

### **Pipelines**

A distance of 500 m is assumed between the CHP plant and the geothermal plant. Therefore, a total of 1000 m of pipe are required to transport the working fluid between plants. The exergy cost is calculated with the parameters described in Appendix F.

#### Wells

De Mooij estimates the exergy cost of the wells based on a steel-concrete construction. The depth of the production well is 3300 m. The injection well is 1850 m deep. Both wells are divided in sections. A reproduction of the main parameters and results is shown in Table G.1 and Table G.2.

For the production of steel, an exergy cost of 60 MJ/kg is assumed. The estimated exergy for the production of concrete is 2.95 MJ/kg. Both figures are slightly different than those reported by Szargut (1987) (5.35 MJ/kg and 58.77 MJ/kg).

<b>Table G.1.</b> Parameters for the construction of the	geothermal doublet (steel).
--	-----------------------------

Interval [m]	Casing Do [in]	Casing Di [in]	Casing length [m]	Steel Volume [m³]	Casing Weight [kg]					
0 - 60	13 3/8	12.459	60	1.10	8,930					
60 - 700	10 3/4	9.794	640	12.21	99,415					
700 - 1790	7	6.331	1290	17.22	140,227					
1790 - 1850	5 4/5	4.767	60							
Total for inje	ction well:			30.52	248,572					
0 - 60	13 3/8	12.459	60	1.10	8,910					
60 - 1200	10 3/4	9.794	1140	21.74	177,083					
1200 - 3100	7	6.331	1900	25.36	206,535					
3100 - 3300	5.812	4.767	200							
Total for pro	Total for production well: 48.20 392,549									

 $\textbf{Table G.2.} \ \textbf{Parameters for the construction of the geothermal doublet (concrete)}.$ 

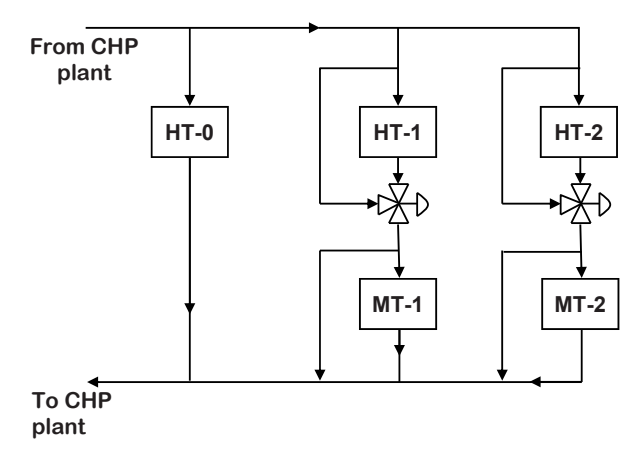
Interval [m]	Hole D [in]	Casing Do [in]	Casing length [m]	Cement Volume [m³]	Cement Weight [kg]			
0 - 60	16	13 3/8	60	3.14	4,524			
60 - 700	12 1/4	10 3/4	640	19.15	22,578			
700 - 1790	8 1/2	7	1290	38.60	55,586			
Total for injec	ction well:			60.89	87,688			
0 - 60	16.000	13 3/8	60	3.14	4,524			
60 - 1200	12.250	10 3/4	1140	34.11	49,123			
1200 - 3100	8.500	7	1900	56.85	81,871			
Total for production well: 94.11 135,								

### Appendix H New network configurations

The new pipeline segments are based on the existing infrastructure. The diameter is taken from the widest adjacent pipe and the thickness of the insulation is assumed to be  $th_{ins} = 0.1$  m.

This appendix is addressed to readers that have some familiarity with the heating network at TU Delft.

### N1 Renovating small buildings (MTs)



- HT-0: WKC, TBM, OTB, OTB/O&S.
- HT-1: BK (all its branches).
- MT-1: Potential new buildings (WBED)
- HT-2:TNW 1800 and TNW 1640.
- MT-2: Bibliotheek and Aula.

### New pipe segments required:

- 25 m (D = 0.125 m) to connect outlet of Bibliotheek to outlet of Aula.
- 10 m (D = 0.125 m) to connect a bypass from the outlet of TNW to the joint outlet Bibliotheek/Aula.

#### Remarks:

• This configuration relies on the availability of new MT buildings connected in series to BK, with a demand  $Q = 0.5 Q_{BK}$ .

### N1 Renovating large buildings (MTb)

Same schematic as MTs

- HT-0: WKC, TBM, OTB, OTB/O&S.
- HT-1: ChemE.
- MT-1: BK.
- HT-2: Bibliotheek and Aula.
- MT-2: TNW 1800 and TNW 1640.

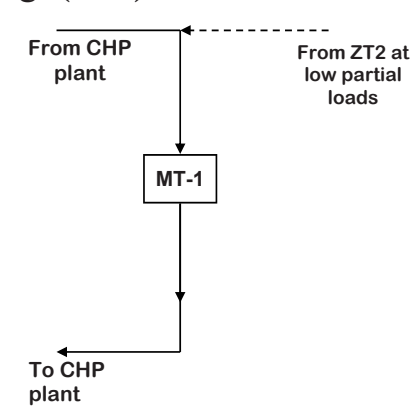
New pipe segments required:

- 25 m (D = 0.125 m) to connect outlet of Bibliotheek to outlet of Aula.
- 10 m (D = 0.125 m) to connect a bypass from the joint outlet of Bibliotheek/Aula to the outlet of TNW.

#### Remarks:

• The demand of the MT consumers is considerably larger than the HT buildings. A large 3-way bypass is thus required in the HT buildings.

### N2 Renovating small buildings (MTs)

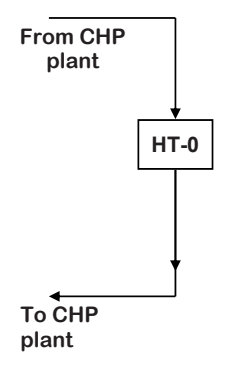


• MT-1: All branches in the block (TBM-2 1120, IO and 3mE) connected in parallel.

#### Remarks:

- The section of TBM operating at MT in this block must be insulated from the section operated at HT in N1.
- Connection pipeline with Z2 is specified in that block.

#### N2 Renovating large buildings (MTb)

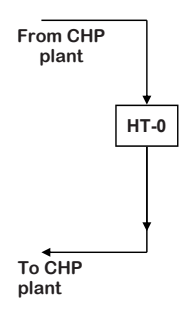


• HT-0: All branches in the block (TBM-2 1120, IO and 3mE) connected in parallel.

#### Remarks:

• This configuration for N2 is the same as New HT (no renovations in the block)

#### Z1 Renovating small buildings (MTs)

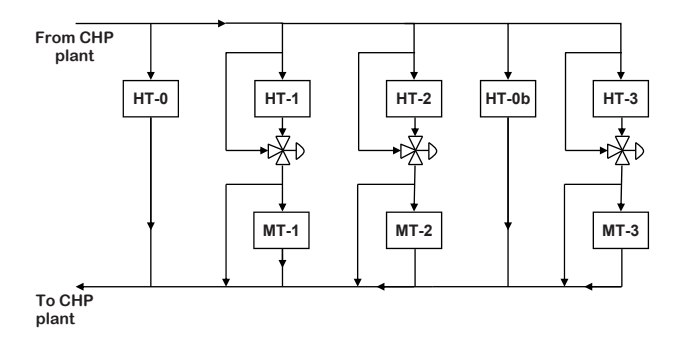


• HT-0: All branches in the block (Geb44, 3mE, Geb35, EWI, TNW and CiTG) connected in parallel.

#### Remarks:

- This configuration for Z1 is the same as New HT (no renovations in the block)
- It might be possible to add the new connections of DUWO as MT consumers in series with EWI/Geb35, as long as the MT outlet is transported to the return line of Z2 (the simulations are recommended for future work).

#### Z1 Renovating large buildings (MTb)



- HT-0: Geb44 Aerohydrodynamica, 3mE-4 1349.
- HT-1: EWI-2 698, Geb35 930 and G35 700.
- MT-1: Potential for new MT building (DUWO).
- HT-2: Geb 104 TNO, TNW 1296/92
- MT-2: Geb 116 Deltares, TNW 1360
- HT-0b: CiTG 349 (small education building)
- HT-3: CiTG-StIV 1163, CiTG-StI 698/267. Additionally, CiTG-StII 1396 and CiTG StIII 1163 from Z2.
- MT-3: CiTG 8374 (main education building)

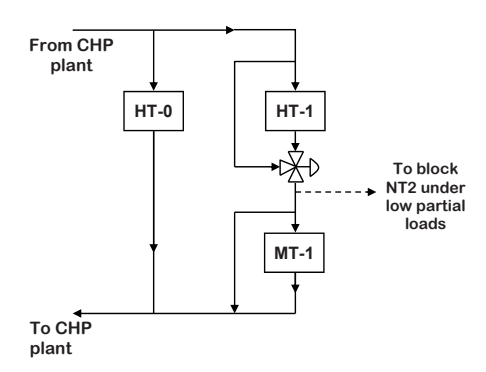
New pipe segments required:

- 100 m + 20 m (D = 0.15 m) to connect the outlet of TNW HT to Deltares MT.
- 31 m (D = 0.2 m) to connect the outlet of EWI/Geb35 to possible new DUWO MT consumer.
- 50 m of assumed branching line to possible new connection from DUWO.
- 125 m (D = 0.2 m) to connect the outlet of TNO/TNW (HT) to TNW (MT).
- 40 m to connect the outlet of CiTG 8374 (MT) to the outlet of CiTG 349 (HT).

#### Remarks:

- It is possible to have a new connection to a DUWO MT consumer fed from the outlet of EWI/Geb 35 with demand Q = 0.5  $Q_{EWI/Geb35}$
- This configuration requires several new connections to prevent excessively large bypass in 3-way valves.
- The building of Deltares is connected to TNW (instead of CiTG as today).
- The buildings Stevin II and Stevin III are included in this block (presently fed in Z2).
- An important bottleneck in finding a more simple configuration arises from the small educational building in CiTG kept as HT consumer.
- This configuration relies on the possibility to connect new DUWO MT consumers to EWI/Geb35.

### Z2 Renovating small buildings (MTs)



- HT-0: Geb 45, Geb 46 API, DUWO.
- HT-1: EWI, CiTG (all branches in the present block).
- MT-1: SC, FelS, LR (all branches), potential for new building such as TNW zuid (instead of FMVG today).

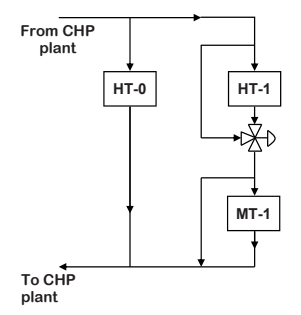
New pipe segments required:

- 50 m (D = 0.2 m)to connect the outlet of EWI 1745 to the return stream of the MT consumers (LR area).
- 50 m (D = 0.2 m) for a bypass on the previous connection.
- 90 m to connect the outlet of EWI 3900 and 4187/698 to block N2.

#### Remarks:

- It is possible to connect a new building with ca. 10% of the demand of the other MT consumers in the block, i.e.  $Q = 0.1 (Q_{MT-1} Q)$  (replacing FMVG).
- At low partial loads (scenario  $T_{env} = 10^{\circ}$  C) the outlet of the HT buildingsis much larger than the required demand. This excess energy can supply the entire block N2.

### **Z2** Renovating large buildings (MTb)



- HT-0: Geb 45, Geb 46 API, DUWO.
- HT-1: SC, FelS, LR (all branches), FMVG.
- MT-1: EWI (branches of the present block.

#### New pipe segments required:

• 50 m (D = 0.2 m) to connect a bypass from the return strema of the HT consumers (LR area) to the outlet of the MT building (EWI).

#### Remarks:

• The branches of CiTG in this block are connected to Z1 under this configuration.

### **Appendix I** Error analysis

Several variables used in the models can introduce error in the simulations. These variations can be classified by 1) individual model and 2) model connection.

#### Error from individual models

The error introduced by the following variables is determined:

- Reference temperature. The temperature of the dead state is selected according to the simulated scenarios, but the demand and operation conditions are determined within an interval of  $\pm 1^{\circ}$ C.
- Temperature average. The temperature of operation for the heat exchangers in the network is averaged from field and design data.
- Pressure average. The pressure drop of the heat exchangers is averaged from field data.
- Electricity from gas engines: The simulation of the gas engines is performed using a simplified model for the gas engines. Variations in the electricity production with respect to the design values are observed in the results.

These variables are simulated for different values in individual components, based on design criteria and the observed minimum/maximum. The variations are reported in the table below. The error for individual components can add up to 2.2%.

Parameter	Parameter variation	Reference	Value		Result variation		ror
$T_{\text{env}}$	10 ± 1°C	Ex <sub>D,HX</sub> [kW]	5.64	5.62	5.66	-0.4%	0.4%
T operation HX	$50/56.7 \& 85.3/75 \pm 2$ °C	$Ex_{D,HX}[kW]$	5.64	5.61	5.66	-0.5%	0.4%
P operation HX	$0.25 \pm 0.15  \mathrm{bar}$	$\operatorname{Ex}_{\operatorname{D,HX}}\left[\operatorname{kW}\right]$	5.64	5.6	5.67	-0.7%	0.5%
W <sub>el</sub> engines	$W_{el}$	W <sub>el,des</sub> [kW]	1948	1936	-	-0.6%	

**Table I.1.** Error derived from variables for individual models.

#### Error from model connection

The simulation results of one module are manually introduced in the next module. This is done by rounding the results do a practical decimal digit. The errors from the connection of modules are listed in the table below. The error can add up to 1.6%.

Parameter	Parameter variation	Reference	Value	Result variation		Error	
φ	± 0.001 kg/s	Ex <sub>D,HX</sub> [kW]	5.64	5.64	5.64	0.0%	0.0%
T	± 0.01°C	$\mathrm{Ex}_{\mathrm{D,HX}}\left[\mathrm{kW}\right]$	5.64	5.61	5.66	-0.5%	0.4%
P	$\pm$ 0.1 bar	Ex <sub>D,HX</sub> [kW]	5.64	5.64	5.64	0.0%	0.0%

**Table I.2.** Error derived from rounding results when connecting modules.

The combined cases explained above can lead to a **total error up to 3.8%**.